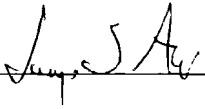


AN ABSTRACT OF THE THESIS OF

William Russell Jacobson Jr. for the Master of Science in Physical Sciences

presented on Dec. 2, 2004

Title: Glaciotectonic Structural Analysis of Devils Lake, North Dakota

Abstract approved:  _____

The ice-shoved terrain south of Devils Lake was formed by the last advance of the Late Wisconsinan glaciers approximately 12,000 years ago. Two series of ice-shoved ridges and associated source depressions (lake basins) formed during this event. Many of these features formed as a result of proglacial and subglacial thrusting processes. Ice-thrusting was facilitated by high pore-water pressures in the underlying Spiritwood Aquifer. Permafrost conditions may have contributed to overpressurizing the aquifer.

Two study sites in the Devils Lake area revealed a kame deposit at the head of the Big Coulee Spillway Valley and an ice-shoved hill that was overridden (Devils Lake Mountain). This study has demonstrated that till micromorphology can be utilized to discriminate between subglacial and gravity-driven deformation processes. Field and microstructural evidence of the Devils Lake Mountain suggest that the sediments were subjected to high finite shear strains within a subglacial environment. Microstructural observations in this study also indicate that subglacial till can be identified by pressure shadow artifacts and highly crushed quartz grains. In addition, a consistent

southeastward directional trend was revealed in both macro and microscopic deformation structures.

The flow tills in a kame at Sullys Hill suggest sediment deformation under low confining pressures. This was documented by the lack of pressure shadows and crushed quartz grains. Similar deformation microstructures were identified in both glaciogenic deposits indicating formational processes under disparate glacial environments.

Microstructural evidence in the flow till suggests that the sediment behaved in fluid-like manner during till redeposition. Characteristic microstructures in both glaciogenic deposits included: discrete shears, till pebble fabrics, galaxy or turbate structures, clast haloes, pressure shadows, crushed quartz grains, clay and iron translocations, boudins, and plasma fabrics.

GLACIOTECTONIC STRUCTURAL ANALYSIS OF DEVILS
LAKE, NORTH DAKOTA

A Thesis

Presented to

The Departments of Physical Sciences

EMPORIA STATE UNIVERSITY

In Partial Fulfillment

of the Requirements for the Degree

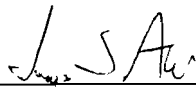
Master of Science in Physical Sciences

by

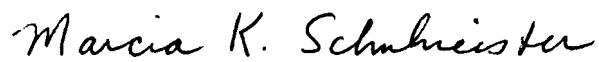
William Russell Jacobson, Jr.

December 2004

Thesis
2004
J



Approved by Dr. James Aber, Committee Chairman



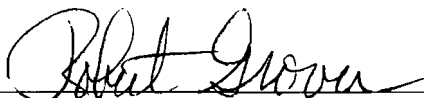
Approved by Dr. Marcia Schulmeister, Committee Member



Approved by Dr. Jorge Ballester, Committee Member



Approved by the Department Chair



Approved by the Dean of Graduate Studies and Research

© 2004

William Russell Jacobson Jr.

ALL RIGHTS RESERVED

TABLE OF CONTENTS

TABLE OF CONTENTS.....	iv
LIST OF FIGURES.....	vi
LIST OF TABLES.....	x
ACKNOWLEDGEMENTS.....	xi

CHAPTER

1 Background.....	1
Geology of Devils Lake.....	3
Study Site Areas.....	9
Previous Work.....	11
Glaciotectonic Deformation.....	15
Ice Thrusting Process.....	18
Definition of Till.....	20
Melt-out Till.....	25
Lodgement Till.....	26
Deformation Till.....	30
Subglacial Glaciotectonic Deformation.....	32
Progressive Simple Shear.....	34
Strain and Deformational Styles.....	37
Till Properties and the Onset of Deformation.....	39
Glacial Micromorphology.....	41
Microstructures within Glacigenic Sediments.....	42
2 Methodology.....	44

Till Sampling and Preparation.....	44
Kite and Blimp Aerial Photography.....	46
Clast Fabric Analysis.....	50
Image Processing.....	53
3 Results: Data and Analysis.....	54
Site 1: Devils Lake Mountain.....	54
Site 2: Sullys Hill.....	61
Till Clast Fabrics.....	61
Microstructure Descriptions.....	70
Site 1: Devils Lake Mountain.....	72
Site 2: Sullys Hill.....	88
Computer Modeling and Remote Sensing.....	96
4 Interpretations.....	108
Microstructure Interpretations.....	108
Field Interpretations.....	111
5 Conclusions.....	115
References.....	117

LIST OF FIGURES

Figure 1. Glaciation of North America.....	4
Figure 2. Glaciation of North Dakota.....	5
Figure 3. Physiographic regions of North Dakota.....	6
Figure 4. Geologic map of Devils Lake, ND.....	8
Figure 5. Geologic map of Devils Lake, ND.....	10
Figure 6. Photograph of Devils Lake Mountain (DLM).....	12
Figure 7. Photograph of gravel pit.....	13
Figure 8. Photograph of glaciotectonic fold.....	14
Figure 9. Photograph of glaciotectonic fold within Falkirk Coal Mine.....	16
Figure 10. Diagram of subglacial thrusting process.....	19
Figure 11. Diagram of till classification.....	22
Figure 12. Diagram of the lodgement process.....	27
Figure 13. Photograph of glacier sole.....	29
Figure 14. Diagram of till deposition through time.....	33
Figure 15. Diagram of strain ellipse.....	36
Figure 16. Diagram of stress ellipse.....	36
Figure 17. Diagram of subglacial shear zone with strain ellipse.....	38
Figure 18. Diagram of microfabrics and microstructures within glacial sediments.....	43
Figure 19. Three-dimensional block model of glacigenic sediment.....	45
Figure 20. Photograph of blimp assembly.....	47
Figure 21. Photograph of rokkaku kite.....	48
Figure 22. Photograph of kite rig.....	49

Figure 23. Photograph of till fabric process at DLM.....	51
Figure 24. Photograph of till fabric process at Sullys Hill.....	52
Figure 25. Topographic map of DLM.....	55
Figure 26. Photograph of glacial stratigraphy at DLM.....	57
Figure 27. Photograph of till interface a DLM.....	58
Figure 28. Photograph of till interface at DLM.....	59
Figure 29. Photograph of till interface at DLM.....	60
Figure 30. Topographic map of Sullys Hill.....	62
Figure 31. Photograph of kame.....	63
Figure 32. Photograph of kame deposits.....	64
Figure 33. Photograph of kame deposits.....	64
Figure 34. Photograph of glacial striations.....	65
Figure 35. Photograph of flow till.....	66
Figure 36. Photograph of symmetric fold.....	67
Figure 37. Diagram of Schmidt equal-area stereonet.....	68
Figure 38. Photomicrograph of till (DLM) 10-02-01.....	74
Figure 39. Photomicrograph of till (DLM) 10-02-01.....	76
Figure 40. Photomicrograph of till (DLM) 10-02-01.....	77
Figure 41. Photomicrograph of till (DLM) 10-02-02.....	78
Figure 42. Photomicrograph of till (DLM) 10-02-01.....	79
Figure 43. Photomicrograph of till (DLM) 10-02-02.....	80
Figure 44. Photomicrograph of till (DLM) 10-02-01.....	81
Figure 45. Photomicrograph of till (DLM) 10-02-01.....	82

Figure 46. Photomicrograph of till (DLM) 10-02-02..... 83

Figure 47. Photomicrograph of till (DLM) 10-06-02..... 84

Figure 48. Pressure shadow diagram..... 85

Figure 49. Photomicrograph of till (DLM) 10-02-01..... 86

Figure 50. Photomicrograph of till (DLM) 10-02-01..... 87

Figure 51. Photomicrograph of till (DLM) 10-06-01..... 89

Figure 52. Photomicrograph of till (DLM) 10-02-01..... 90

Figure 53. Photomicrograph of till (DLM) 10-02-01..... 91

Figure 54. Photomicrograph of till Sullys Hill..... 92

Figure 55. Photomicrograph of till Sullys Hill..... 93

Figure 56. Photomicrograph of till Sullys Hill..... 94

Figure 57. Photomicrograph of till Sullys Hill..... 95

Figure 58. Photomicrograph of till Sullys Hill..... 97

Figure 59. Photomicrograph of till Sullys Hill..... 98

Figure 60. Photomicrograph of till Sullys Hill..... 99

Figure 61. Photomicrograph of till Sullys Hill..... 100

Figure 62. Three-dimensional color orthophoto of DLM..... 101

Figure 63. Three-dimensional color orthophoto of DLM..... 102

Figure 64. Three-dimensional color orthophoto of fault lineament DLM..... 103

Figure 65. Three-dimensional color orthophoto of Sullys Hill..... 104

Figure 66. Three-dimensional color orthophoto of Sullys Hill..... 105

Figure 67. Aerial photograph of DLM..... 106

Figure 68. Satellite image of Devils Lake, ND..... 107

Figure 69. Particle mobility till diagram.....	109
Figure 70. Till deformation profile.....	113

LIST OF TABLES

Table 1. Genetic classification of till.....	21
Table 2. Definitions and terminology.....	35
Table 3. Till clast fabric criteria.....	69
Table 4. Glacial micromorphological terms.....	71
Table 5. Glacial microstructure comparison.....	73
Table 6. Evidence of subglacial deformation from modern glaciers.....	112

ACKNOWLEDGEMENTS

I would like to express my thanks to Dr. James Aber for his helpful suggestions and field assistance during the completion of this thesis. This project was primarily supported through the NASA EPSCoR Grant. Thank you to Rod Bassler at the North Dakota State Water Commission for providing color orthophotos of the Devils Lake area. I would also like to thank the committee members Dr. Marcia Schulmeister and Dr. Jorge Ballester for critically reading the thesis and providing helpful comments. Thanks are due to Lorraine Manz at the North Dakota Geological Survey for supplying research materials during thesis preparation. For field assistance and computer modeling of the Devils Lake area, I thank Shawn Salley. Best wishes go to Brain and Kandi Burnham at Burnham petrographics in Rathdrum, Idaho. Their expertise and craftsmanship in thin-section development is highly valued. Final thanks go Dr. Richard Sleezer for helpful discussions and comments throughout the thesis.

Chapter 1. Background

Glaciotectonic deformation structures and ice-shoved hills have been widely recognized in North Dakota (Bluemle, 1966; Bluemle, 1970; Clayton and Moran, 1974; Moran et al., 1980; Bluemle and Clayton, 1984; Aber, 1988; Aber et al., 1989, 1997; Bluemle, 2000; Colgan et al., 2003). It has been established that many of these ice-shoved features have formed either entirely, or in part, by the subglacial thrusting mechanism (Bluemle and Clayton 1984). Our current knowledge of these processes at the subglacial interface and within the subglacial materials is deficient (Menzies, 1981). Although, the distribution of ice shoved features and glaciotectonic structures have been located and recognized in the Devils Lake vicinity, little emphasis has been focused on the kinematics of deformation and till genesis. A comprehensive study of the southern Laurentide Ice Sheet is provided by Mickelson and Colgan (2003).

The aim of this study is to analyze both micro- and macroscale deformational structures of Wisconsinan tills from the Sullys Hill and Devils Lake Mountain areas of North Dakota. Structural evidence is utilized to reconstruct the deformational histories and paleoenvironments. Samples of oriented till were collected because limited evidence of macroscopic structures exists in the literature. This thesis is the first investigation of till micromorphology within the Devils Lake area. Kite aerial photography and three-dimensional, color, orthophoto models are used to document the glacial bedform morphologies.

Glacial environments can pose many opportunities for deformation of weakly consolidated rock to unconsolidated sediments (van der Wateren, 1995). Glacial deformation can occur in various settings: in the front of the glacier, beneath the ice margin, or under the center of a thick ice sheet (Aber et al., 1989). Deformational structures that develop within the sediment can provide invaluable information about the environment of formation (McCarroll and Rijdsdijk, 2003). By analyzing the geometries of the structures and the deformational styles of the glacial deposits it is possible to reconstruct the paleostress fields that formed them (McCarroll and Rijdsdijk, 2003). Many paleostress fields are related to local glacial ice movements. However, paleostress fields may also be produced by other nonglacial processes, such as the effects of slumping and gravitational processes.

Glacigenic deposits often are difficult to interpret because they form in a wide variety of depositional environments and by an array of processes (Evans, 2003). This has prompted many glacial specialists to combine multiple approaches when analyzing glacigenic sediments. The analysis of glacigenic sediments at the micro-scale has been conducted in recent studies (van der Meer et al., 1983, 1992; van der Meer, 1987, 1990, 1993; Menzies and Maltman, 1992; Menzies, 2000; Lachniet et al., 2001; Hiemstra, 2001; Carr, 2001). This relatively new approach has been used most frequently to infer the importance of subglacial shear in till genesis (Khatwa and Tulaczyk, 2001). This technique has been especially applied to glacigenic sediments largely because of the homogenous nature of till and the lack of macroscale deformation structures. Analyzing

glacigenic sediments at the micro-scale in conjunction with other field observations can provide a better understanding of the formational processes of the deposits.

Geology of Devils Lake

The most recent phase of glaciation that affected the Devils Lake region was the Late Wisconsinan Glaciation. This pulse of glaciation occurred approximately 26,000 years ago and ended about 10,000 years ago (Bluemle, 2000). The last ice dome to form in North America was the Laurentide Ice Sheet (LIS). The LIS formed west of Hudson Bay and advanced southward from the Keewatin center (Fig. 1). Numerous glacier lobes of LIS advanced southward into North Dakota. Former glacier margin positions of eastern North Dakota have been documented by Clayton et al. (1980). Ice margin positions are based largely on boulder abundances, till lithology and constructional landform evidence (Fig. 2). The Late Wisconsinan glaciers eventually advanced and covered all northeastern North Dakota (Bluemle, 2000). Many remnant glaciotectionic landforms of northeastern North Dakota were emplaced by the Late Wisconsinan glaciers.

The Devils Lake region is situated within the Glaciated Plains of the Central Lowland Province (Fig. 3). The Devils Lake area is characterized by an undulating to rolling terrain which is underlain by Pleistocene (ice age) (Hobbs and Bluemle, 1987).

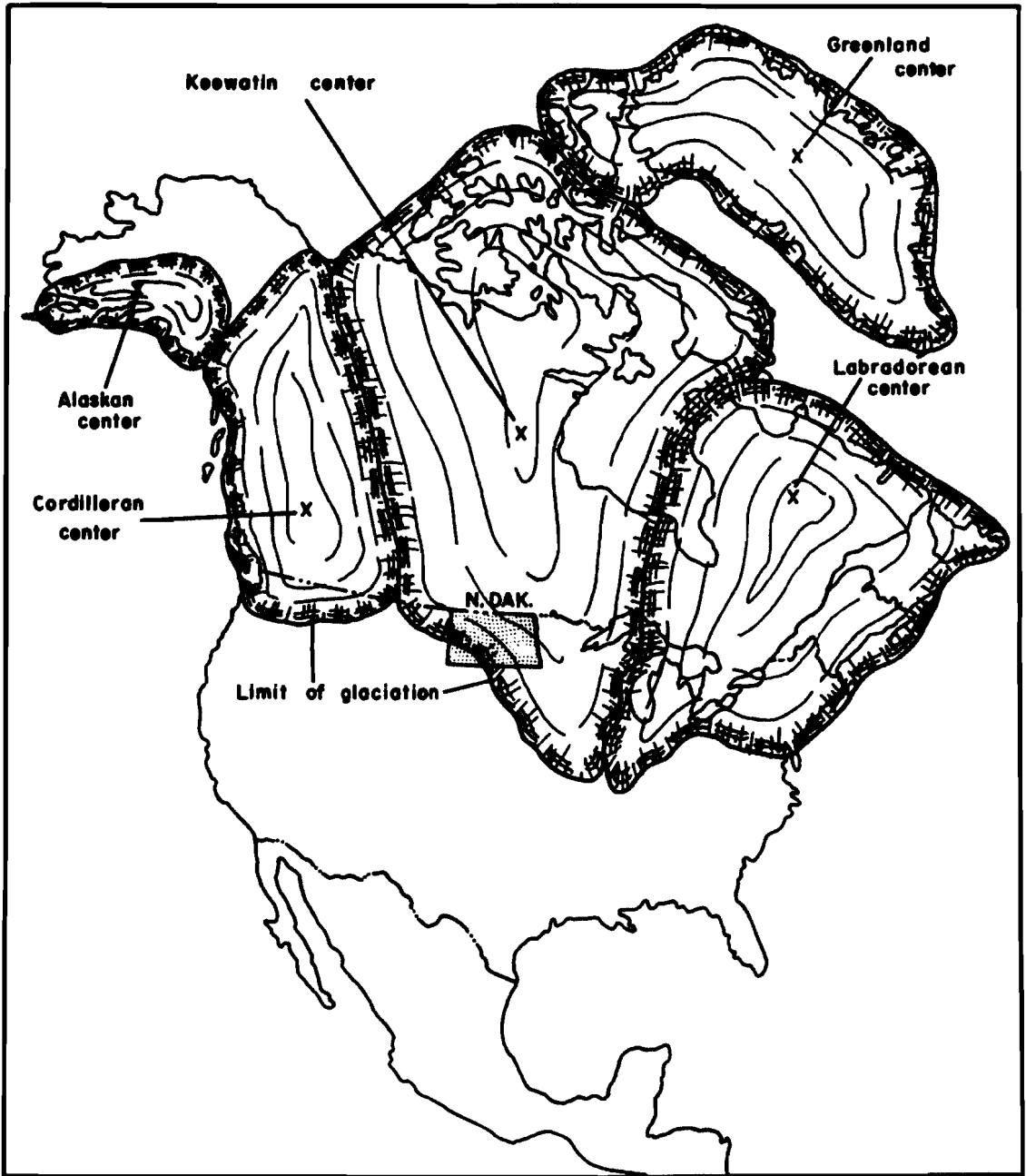


Figure 1. Map of North America showing the maximum Wisconsin limit of continental glaciation. Note the main centers of snow accumulation from which the ice advanced. North Dakota was glaciated by ice derived from the Keewatin center.

Diagram adapted from Bluemle, 1974.

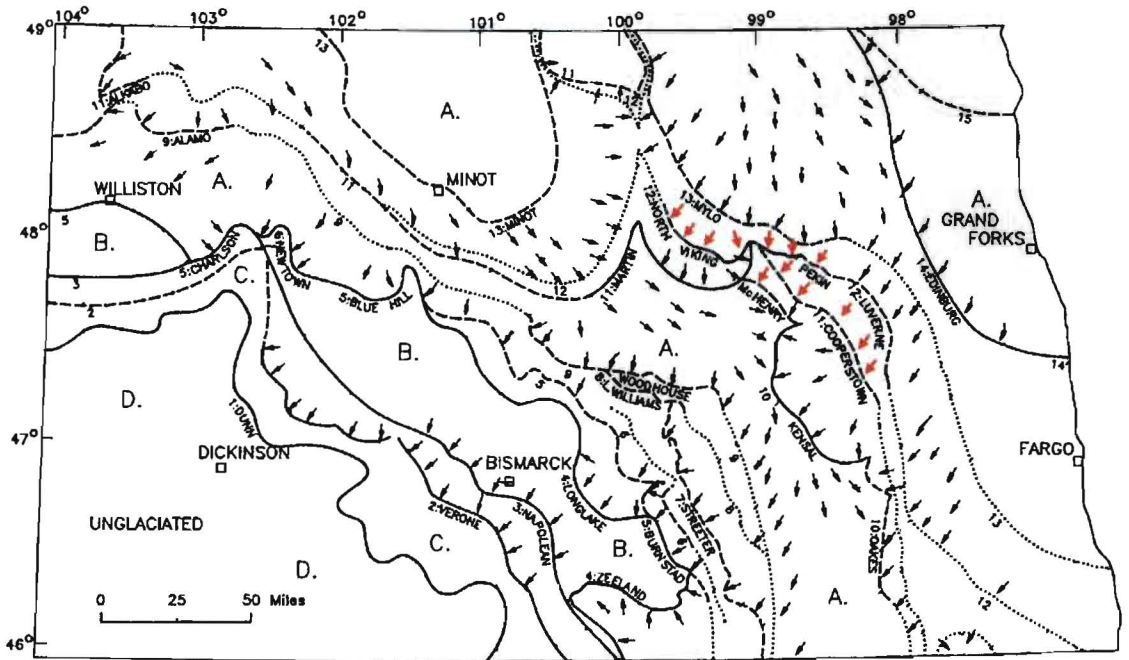


Figure 2. Map of North Dakota showing local ice-movements (arrows) and maximum glacial margin positions. Red arrows indicate ice-movements in the Devils Lake vicinity. Oldest ice margin positions are labeled with the lowest numbers; and the younger ice margins have progressively higher numbers. Modified after Clayton et al., (1980, Fig. 32).

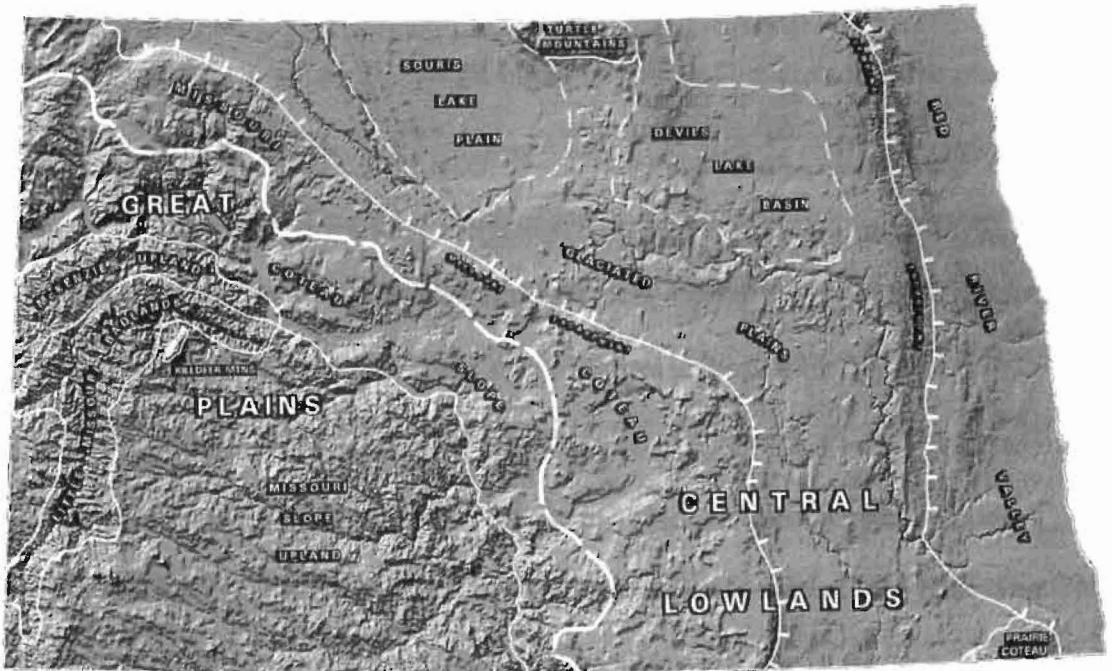


Figure 3. Physiographic regions of North Dakota. Note Devils Lake Basin area and the Glaciated Plains. Map acquired from Bluemle, 2000.

Glacial deposits range in thickness from a few meters to several tens of meters in Ramsey and Benson Counties. The underlying bedrock consists of Cretaceous shale. This rock unit is referred to as the Pierre Formation. The local relief in this area is generally less than 30 meters, but ranges up to 90 meters in some places (Bluemle, 2000).

The ice-shoved complex south of Devils Lake Main Bay was formed by the last advance of the Late Wisconsinan glaciers approximately 12,000 years ago (Bluemle, 2000). Two series of ice-shoved ridges and associated source depressions (lake basins) formed during this event (Aber et al., 1997). Sullys Hill represents the point of convergence between the two series of ice-shoved ridges (Fig. 4). One series extends in a southwest orientation towards Crow Hill. The other series trends in a southeast direction, past Devils Heart Butte, to near Horseshoe Lake. These two series of ice-shoved ridges correspond with the North Viking and Cooperstown ice margins. The two trends of ice-shoved ridges may have formed at the margins of two converging ice lobes (Aber et al., 1997).

The Spiritwood aquifer exists underneath the Devils Lake depressions within the buried preglacial Cannonball valley (Fig. 4). The Spiritwood aquifer is comprised of gravel and sand which was deposited by glacial meltwater from an earlier pre-Wisconsin Glaciation (Hobbs and Bluemle, 1987). High groundwater pressures in the Spiritwood aquifer are likely to have facilitated major glaciotectionic thrusting (Bluemle and Clayton, 1984).

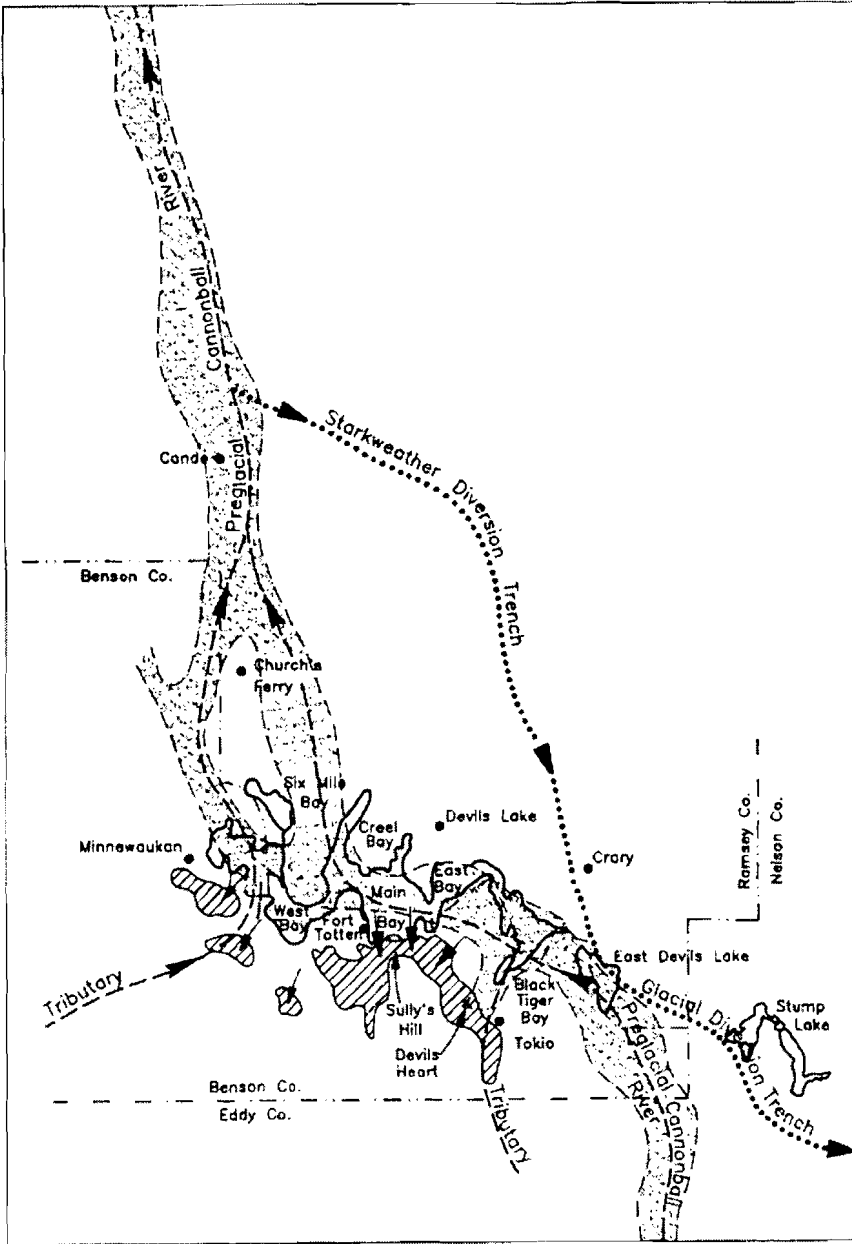


Figure 4. Map of the Devils Lake area demonstrating main geologic relationships. Note ice-shoved topography (lined pattern) south of Main Bay. Ice-shoved material derived from Devils Lake source depressions. The stippled pattern denotes the Spiritwood Aquifer. High confining pressures in the aquifer probably facilitated major subglacial thrusting. Diagram adapted from Bluemle, 2000.

Study Site Areas

The Devils Lake region is located in northeastern North Dakota in Ramsey and Benson Counties (Fig. 5). The Devils Lake area consists of several poorly connected depressions (West Bay, Main Bay, and East Bay) that were formed by glacial ice-shoving (Aber et al., 1997). The ice-shoved terrain south of Devils Lake is built of materials that were scooped out of Devils Lake depressions. This type of glaciotectionic landform is referred to as a hill-hole pair (Aber, 1988). Generally, the ice-shoved hill is paired with a source depression of similar size up-glacier (Colgan et al., 2003). These ice-shoved hills may appear arcuate in shape and may range up to 1 kilometer across and a few meters to a few tens of meters high. Much of the material in the ice-shoved hill is derived from the up-glacier source depression. These anomalous hill-hole pairs generally form within 1 or 2 kilometers of the glacier terminus (Colgan et al., 2003). Many of the source depressions are now occupied by lakes, sloughs, or bogs.

The Sullys Hill-Devils Lake thrust complex, located south of the Devils Lake Main Bay, covers approximately 780 km² and is composed of deformed glacial materials and Cretaceous shale blocks (Aber et al., 1997). These shale blocks have been interpreted by Bluemle and Clayton (1984) and Moran et al. (1980) as the products of subglacial thrusting. The total relief between the bottom of Devils Lake basin and Sullys Hill exceeds approximately 200 m (Hobbs and Bluemle, 1987). The ice-scooped depressions and ice-shoved hills are among the largest and best-developed glacial landforms of this type in the United States (Bluemle and Clayton, 1984).

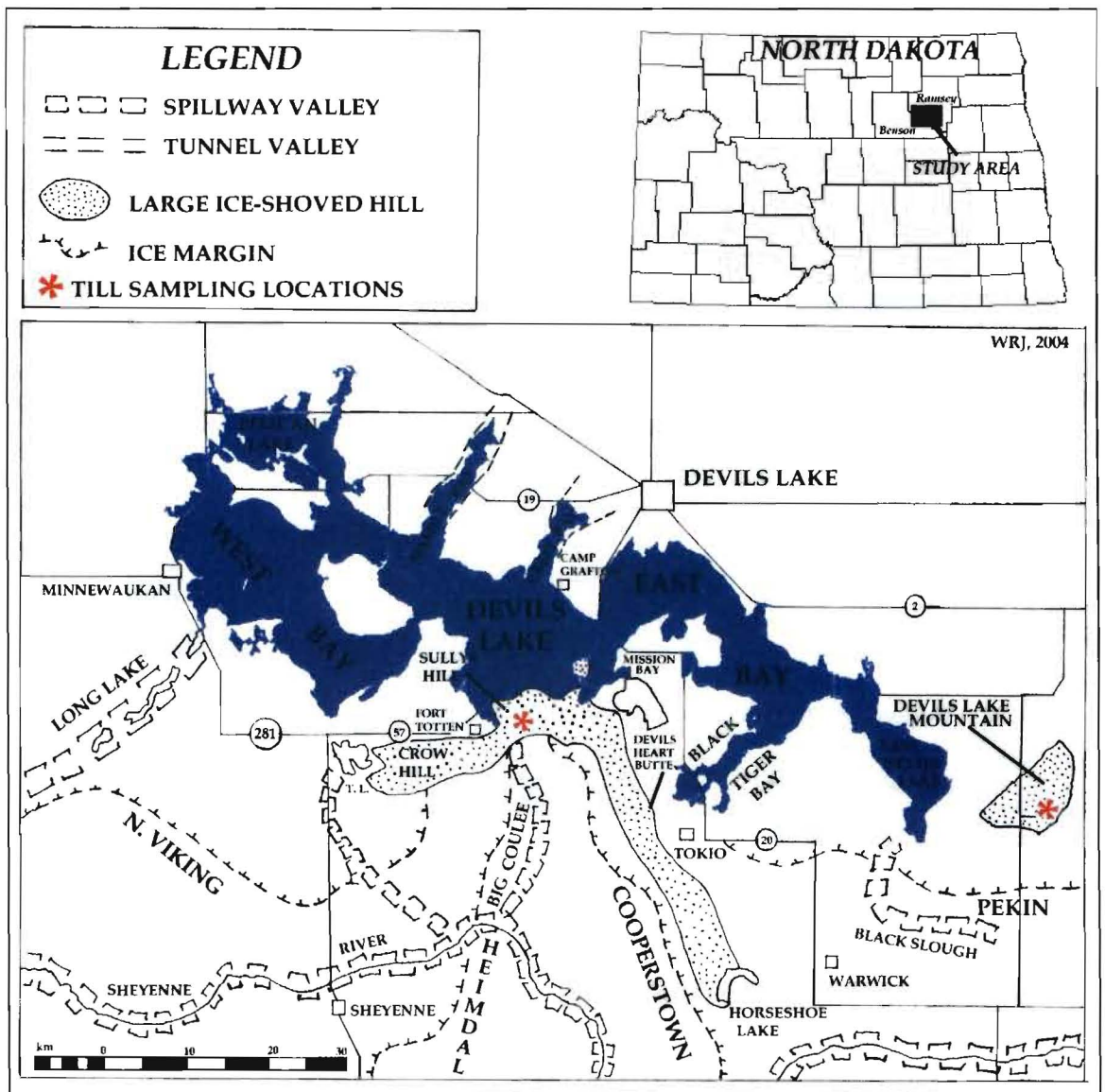


Figure 5. Location map of Devils Lake, northeastern North Dakota. Note the ice-shoved complex and the associated Devils Lake source depressions. The red asterisks represent till sampling locations. Ice margin positions based on Clayton, Moran, and Bluemele (1980, Fig. 32). Diagram modified after Aber et al., 1997.

Two sites of opportunity were discovered during field reconnaissance, one of these sites is an overridden ice-shoved hill and the other site is a proglacial feature located on the southern side of Sullys Hill. Samples of oriented till were collected southeast of Sullys Hill National Game Preserve.

Another ice-shoved hill that was examined is Devils Lake Mountain, located in southern Ramsey County (Fig. 6). A well-developed source depression is located northwest of Devils Lake Mountain. Samples of oriented till were also collected southeast of Devils Lake Mountain within a gravel pit (Fig. 7).

Previous Work

Early reports of glacial ice-thrusting in North Dakota include those by Bluemle (1966, 1970, 1979). He described an ice-thrust bedrock feature near Hannah in northwest Cavalier County, North Dakota. This site exposure was one of the 165 excavations for ICBM Minuteman Missile installations which were constructed in 1964 in northeastern North Dakota (Hobbs and Bluemle, 1987). During the missile excavations, Bluemle visited and described the geology at all 165 site areas. In addition to the ice-thrust bedrock feature in Cavalier County, Bluemle also documented glacially deformed lake sediments in western Steele County (Bluemle, 2000). These sediments were folded into complex, contorted configurations as a result of glacial ice movement (Fig. 8). Evidence for thrusting by glacial ice was noted in nearly half of the 165 excavations (Bluemle, 2000).

Hobbs and Bluemle (1987) published a report on the geology and glacial stratigraphy of Ramsey County. Hobbs analyzed data from approximately 250

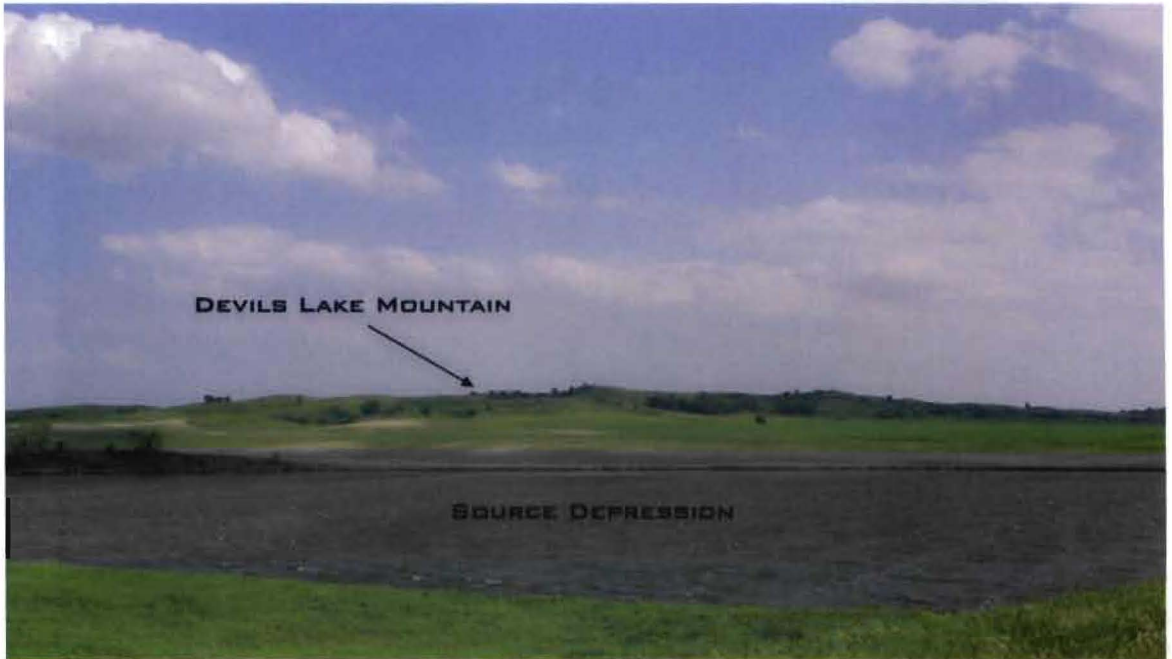


Figure 6. Photograph of Devils Lake Mountain, North Dakota. Note the source depression in the foreground and associated ice-shoved hill in the background. View toward the southeast.



Figure 7. Gravel pit exposure southeast of Devils Lake Mountain. Note the conical gravel piles in background. The till samples described in the text were obtained from this pit. View toward the southeast.



Figure 8. A glaciotectionic fold in western Steele County. Photograph was taken during the installation of nuclear missile silos in 1964. Glacier movement was interpreted by Bluemle as occurring from left to right. Photograph taken from Bluemle (2000, Fig. 38).

test holes throughout Ramsey County. Sediment cores were sampled by using a truck-mounted soil probe. Hobbs also gathered lithologic data from local road cuts during his summer field season in 1976. Bluemle and Clayton (1984) discussed the importance of subglacial thrusting and its role with confined aquifers. Glaciotectonic evidence was also revealed in December of 2002 at the Falkirk Coal Mine, North Dakota. The mine workers uncovered a spectacular glaciotectonic fold on the northwestern edge of the mine (Fig. 9).

Glaciotectonic Deformation

Glaciotectonic deformation is the study of structural disturbances of the underlying substratum caused by glacial stresses (van der Wateren, 1995). Glaciotectonic stresses are produced as a result of direct glacial-ice movement or ice loading (Aber et al., 1989). A glacier or ice sheet exerts two kinds of stress on its bed: (1) vertical stress due to static weight of the ice column ($\sigma_x =$ glaciostatic pressure) and (2) drag or shear stress due to movement of the ice over its bed ($\tau_{ice} =$ glaciodynamnic pressure) (Aber et al., 1989). The vertical stress generated by the ice column produces a lateral pressure gradient on the substratum regardless of any ice movement. The lateral pressure gradient at the glacier sole is produced because of variations in ice thicknesses that occur near the glacier margin (Aber et al., 1989). These pressure gradients at the glacier sole will vary in magnitude depending on the changes of ice column thicknesses and ice surface gradients near the ice margin.

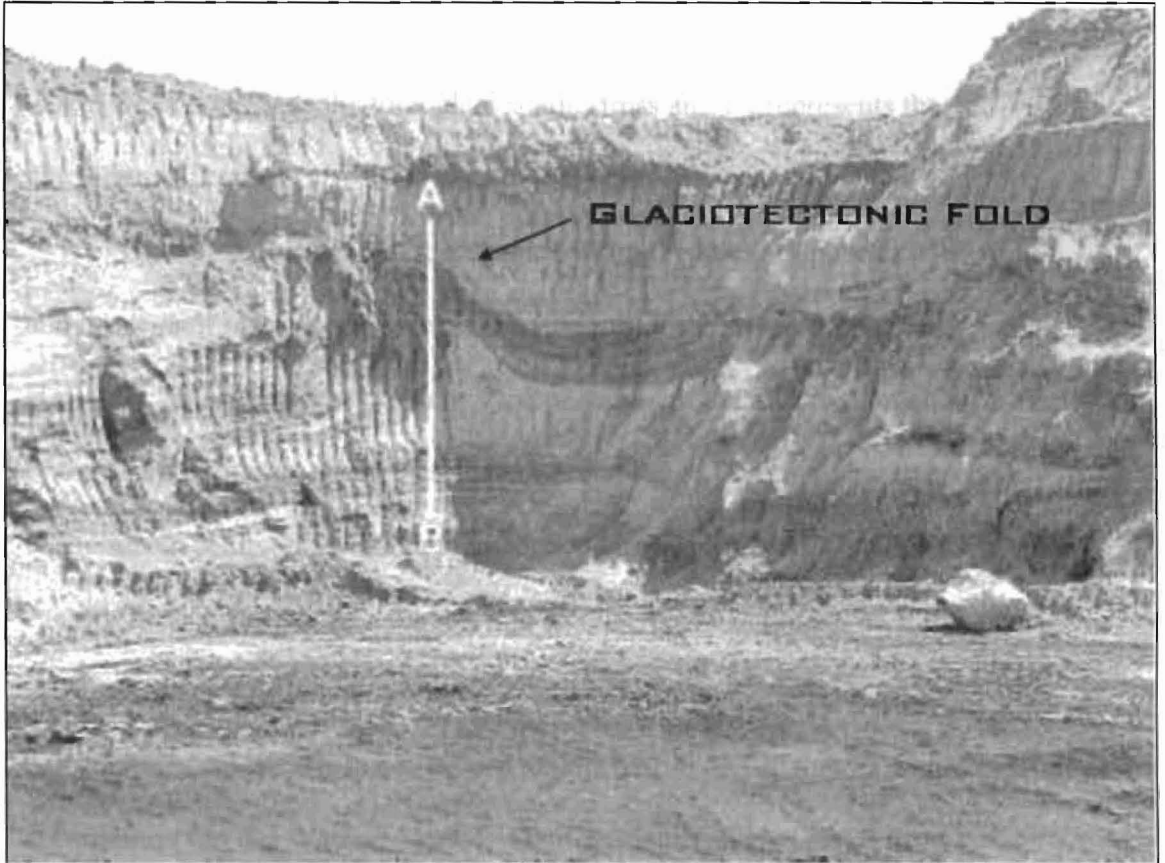


Figure 9. Glaciotectionic fold exposed in overburden of the Falkirk Coal Mine in Washburn, North Dakota. View is from the east. Total height of line AB in photograph is approximately 8 m. Photograph taken by Len Friedt. Image acquired from (Manz, 2002).

The combination of glaciodynamic stress and glaciostatic stress generates shear stress within the substratum. The total glaciotectonic stress (σ_{gt}) exerted horizontally on the substratum is expressed as the sum of these:

$$\sigma_{gt} = \Sigma \sigma_x + \tau_{ice} \quad (1.1)$$

where $\Sigma \sigma_x$ represents the total glaciostatic stress and τ_{ice} represents the glaciodynamic stress.

Glaciotectonic deformation occurs when the stress imposed by the weight and movement of a glacier exceeds the strength of the stressed material (Aber et al., 1989), and can operate on any type of sediment mass or rock in either frozen or thawed conditions. Deformed materials can range from moderately to poorly consolidated sedimentary strata to unconsolidated sediments. Glacial deformation can originate either beneath the ice, in a subglacial environment, or at the glacier margins, in a proglacial environment (Hart and Boulton, 1991). Glaciotectonic deformation typically does not exceed depths of 200 or 300 meters within the substratum (van der Wateren, 1995). Deformations can also result from gravitational instabilities associated with stagnant ice masses (Hart and Boulton, 1991). This process typically occurs near the outer margins (proglacial area) of an ablating ice sheet or glacier. Supraglacial melt-out tills (flow tills) and ice-collapse structures are commonly found in this area.

The definition of glaciotectonics and its limitations have been discussed thoroughly by Aber et al. (1989). This term does not involve structures within glacial ice nor structures resulting from primary depositional processes (such as till fabrics and structures produced during initial till deposition) (Maltman et al.,

2000). Other deformational processes such as the effects of freeze/thaw, iceberg groundings, and lithospheric adjustments due to ice loadings are excluded (Maltman et al., 2000).

Ice Thrusting Process

The landscape terrain of northeastern North Dakota has been influenced strongly by the ice thrusting process. Glacial thrusting was an important process by which the glacier transported large amounts of debris beneath the ice (Bluemle, 1979). Glacier scooping from a source depression is one means by which a glacier could entrain and transport large amounts of debris downglacier (Aber, 1985). The source area of the ice-shoved material was left as a deep depression. The process of glacier thrusting is illustrated in Figure 10.

Ice-thrust features have been known to exist above aquifers. The subglacial thrusting process has been suggested to be coupled to geohydrological processes (Bluemle, 1979). The ice-thrusting process takes place where a glacier advances over a pressurized aquifer system. The layers of sediment beneath the glacier contain beds of permeable material confined in between less permeable materials. This situation allows for high pore-water pressures to build up within the less permeable beds. The overlying weight of the glacier also contributes to increasing the pore water pressures. As a final result, the layers of rock and sediment above the zone of high pressure are shoved upward into the path of the advancing glacier. The escaping pressurized water helps lubricate the surface thus reducing the frictional forces between the materials. This makes it easier for the glacier to shove the material a short distance (Bluemle, 1979).

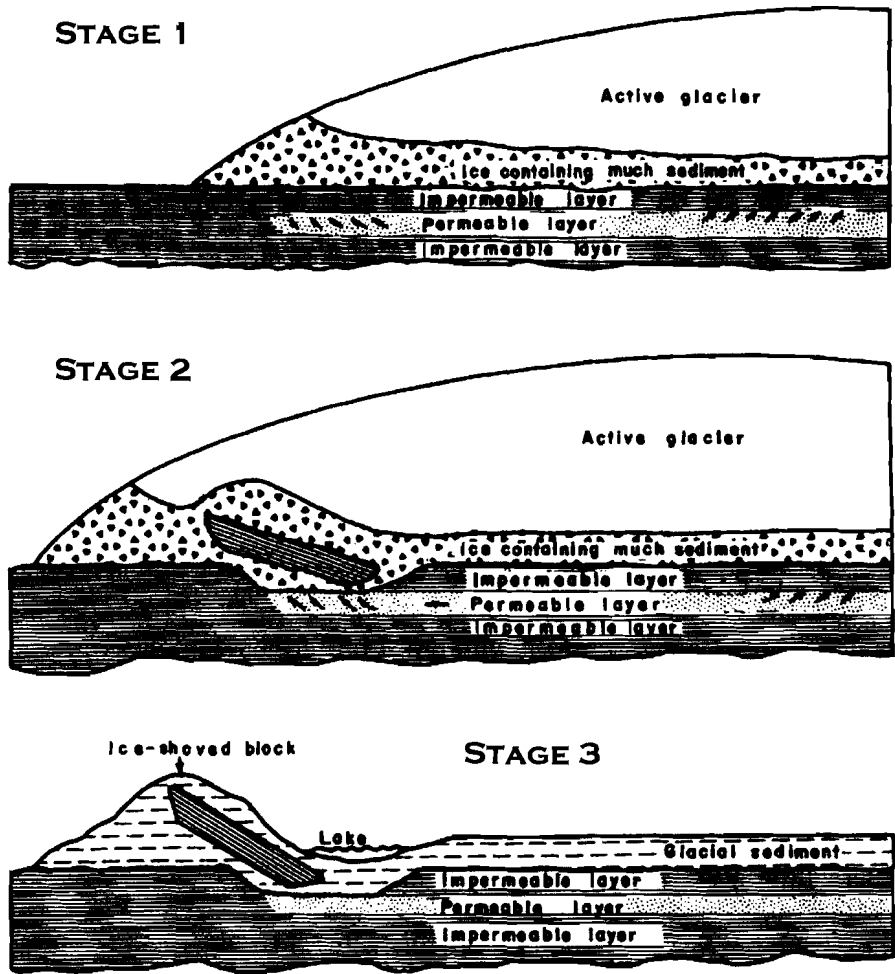


Figure 10. Subglacial thrusting process and its progressive stages. The top diagram shows a confined groundwater system (stage 1). At stage 2, the ice overburden pressures cause the groundwater to migrate toward zones of decreased pressure. If the pressurized groundwater comes in contact with a weak substratum, materials may be forced upward into the path of the advancing glacier. The final result is a large block that has been shoved upward. The resultant depression, from which the block was moved, may become a lake, slough, or marsh. Diagram was adapted from Bluemle (2000, Fig. 34).

Definition of Till

“Till is more variable than any other sediment known by a single name” (Flint 1971, p. 154). This high variability can be attributed to the diversity of materials that are present in the till, and from different processes involved in the formation and deposition of till (Dreimanis and Schüchter, 1985). The complex nature of till has caused many glacial investigators to interpret and select their own criteria in distinguishing the different varieties of tills. This has led to much confusion in literature and with till classification schemes. An agreement however, has been achieved by the International Union for Quaternary Research (INQUA), Commission on Genesis and Lithology of Quaternary Deposits. The INQUA till classification has developed a set of criteria which subsequently has satisfied the majority of the INQUA correspondents (Dreimanis, 1989). The till criteria of the INQUA classification are based on the following: formational and depositional processes, the general environment of deposition, and the position in relation to glacial ice (Hambrey, 1994) (Table 1). The genetic till classification consists of two main categories: primary and secondary tills. Primary tills are formed by the direct release of debris from a glacier and are deposited by primary glacial processes, such as melt-out, lodgement, or during deformation induced by glacier ice action (Hambrey, 1994). The till classification scheme is represented by a tetrahedron (Fig. 11).

Secondary tills result from resedimentation of glacial debris which has already been deposited by the glacier, with little or no sorting by meltwater

RELEASE OF GLACIAL DEBRIS AND ITS DEPOSITION OR REDEPOSITION			DEPOSITIONAL GENETIC VARIETIES OF TILL		
I. ENVIRONMENT	II. POSITION	III. PROCESS	IV. BY ENVIRONMENT	V. BY POSITION	VI. BY PROCESS
GLACIO- TERRESTRIAL	ICE-MARGINAL: -FRONTAL -LATERAL	A. PRIMARY MELTING OUT SUBLIMATION LODGE MENT SQUEEZE FLOW SUBSOLE DRAG	TERRESTRIAL NONAQUATIC TILL	ICE-MARGINAL TILL SUPRAGLACIAL TILL	A. PRIMARY TILL MELT-OUT TILL -SUBLIMATION TILL LODGE MENT TILL
GLACIOAQUATIC	SUPRAGLACIAL SUBGLACIAL SUBSTRATUM	B. SECONDARY: -GRAVITY FLOW SLUMPING SLIDING AND ROLLING FREE FALL	SUBAQUATIC OR WATERLAIN TILL	SUBGLACIAL TILL	DEFORMATION TILL OR GLACITECTONITE SQUEEZE FLOWTILL B. SECONDARY TILL FLOWTILL -GRAVITY FLOWTILL

NOTE: EACH VERTICAL COLUMN IS INDEPENDENT FROM THE OTHER FIVE, AND NO CORRELATION HORIZONTALLY IS IMPLIED. ONLY SOME COMBINATIONS ARE FEASIBLE.

Table 1. Genetic classification of till in a terrestrial setting. (Table adapted from Dreimanis, 1989, Table 11).

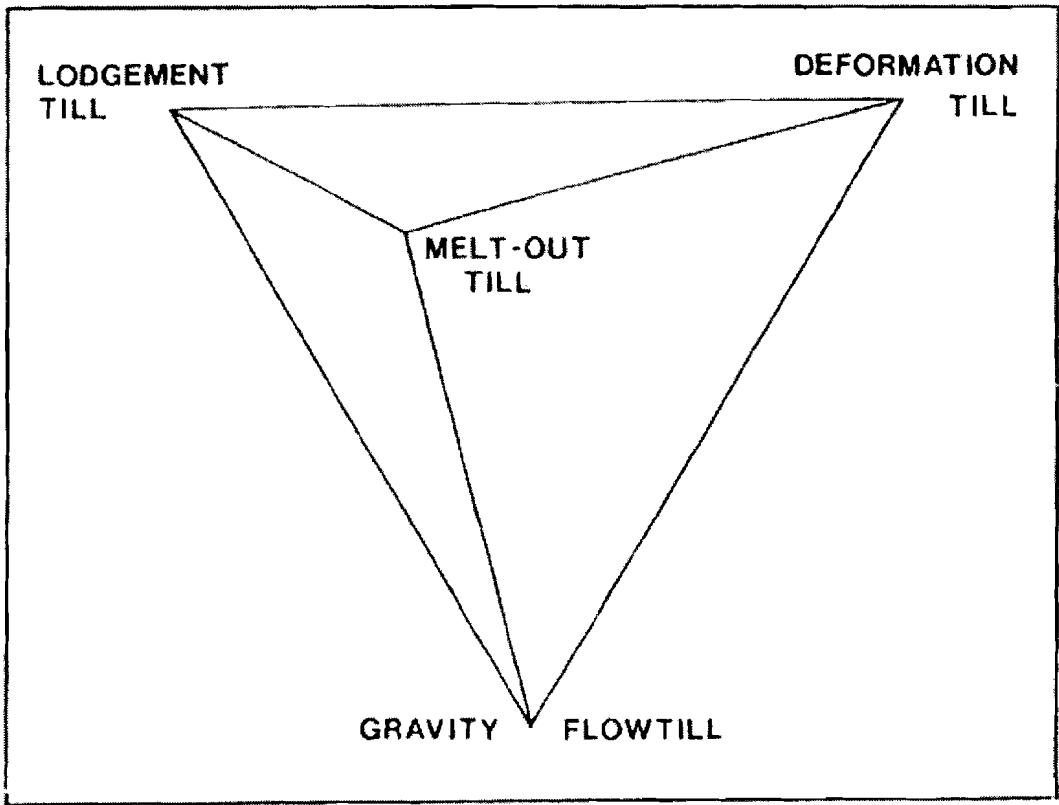


Figure 11. Genetic depositional classification of till. End members are situated at the apices of the tetrahedron. Tills are typically a mixture of various end members Dreimanis (1989, Fig. 1).

(Hambrey, 1994). The primary glacial depositional processes are often intricately coupled to each other (Dreimanis, 1990). This close interrelationship between processes has made it arduous to draw a boundary between primary and secondary deposition (Dreimanis, 1989). The till definitions used in this report follow the INQUA classification scheme.

The INQUA definition of till includes: “any poorly sorted sediment that has been transported and subsequently deposited by or from glacial ice, with little or no sorting by water” (Dreimanis et al., 1985).

The deposition of till may be by or from glacier ice. The phrase, “by glacier ice” indicates that deposition is related to moving glacier ice. The “from glacier ice” part of the expression may be interpreted in various ways. This has permitted the definition of till to be understood either in a narrow or broad sense. The narrow meaning of till generally implies that deposition occurs in direct contact with glacial ice only, by passive melting-out or sublimation (Dreimanis, 1989). This definition however, still includes discrepancies because till may also contain resedimented debris, which was pointed out by Dreimanis (1983) and Lawson (1979, 1981) at the Matanuska glacier. The broad definition “from glacial ice” would include some resedimentation products, after the glacial debris has been initially released from the ice, but “with little or no sorting by water,” as the definition implies (Dreimanis, 1989). The phrase “with little or no sorting by water,” excludes water transport that produces sediment size sorting, but other transport mechanisms “from glacier ice” such as gravity flow, sliding, squeeze flow and slumping are permitted (Dreimanis, 1989).

Dreimanis and Lundqvist (1984) described in detail how glacial debris may evolve into till,

“... the debris is carried by a glacier: in the ice, on the ice, or dragged by the sole of the glacier. Then comes the release of glacial debris from the glacier, usually by melting of glacier ice. This release of debris permits subsidiary geologic agents- meltwater and the force of gravity-to participate in the formation of till, in its modification and final deposition. However, in order to call the resulting sediment “till”, these subsidiary agents shall not dominate the formation and deposition of till, and the deposition of till shall take place in a glacial environment-in contact with glacier ice or in its direct vicinity.” (p. 5)

Dreimanis and Lundqvist (1984) clearly emphasized the glacier as the main formative agent during till genesis. The participation of meltwater and gravity in till genesis can not be disregarded, as nearly all till-forming processes involve meltwater and gravity to minimal degrees. They required that the following three specifications have to be met, in order to call sediment till:

- (1) till consists of debris that has been transported by a glacier;
- (2) close spatial relationship exists to a glacier: till is deposited by a glacier, or it is deposited from a glacier;
- (3) sorting by water is absent or minimal during the formation of till.

Recognition of just one or two of these criteria listed above is not sufficient to call sediment “till” (Dreimanis and Lundqvist, 1984). The

wide range of till-forming processes has made it difficult to develop a classification scheme that would apply to all situations (Dreimanis, 1989).

The following section describes the formational and depositional processes of both primary and secondary tills.

Melt-out Till

INQUA stated that: “Melt-out till is deposited by a slow release of glacial debris from ice that is not sliding or deforming internally” (Dreimanis 1989, p. 45). Melt-out tills may either form on the ice surface or at the base of the ice (Boulton, 1971). The melt-out process may be associated with either a stagnant glacier or a stagnant zone underneath a moving glacier (Dreimanis, 1989). Melt-out till is commonly deposited in unstable situations, and is thus prone to flowage (Hambrey, 1994). Melt-out tills that originate on the ice surface are generally described as supraglacial melt-out tills, which form as a result of downmelting of the glacier ice surface. Temporal changes in ice surface gradients through time can cause supraglacial melt-out till and other supraglacial debris to become resedimented and transformed into flowtill (Dreimanis, 1989). Flowtills are usually considered to be secondary tills (Dreimanis, 1989). The INQUA definition of flowtill states:

“Flowtills (broad meaning) may derive from any glacial debris upon its release from glacier ice or from a freshly deposited till, in direct association with glacier ice. The redeposition is accomplished by gravitational slope processes, mainly by gravity

flow, or by squeeze flow, and it may take place ice-marginally, supraglacially, or subglacially, and subaerially or subaquatically” (Dreimanis, 1989, p. 48).

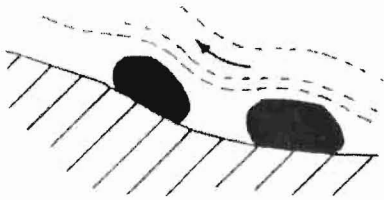
Resedimentation by gravity flow is probably the most common mechanism in flowtill formation. Sediment shear strength is reduced during the resedimentation process as a result of increased pore water pressures (Dreimanis, 1989). Melt-out tills which are derived from the base of the ice are classified as subglacial melt-out tills. Subglacial melt-out tills may also preserve traces of debris-rich ice structures (Dreimanis, 1989).

Lodgement Till

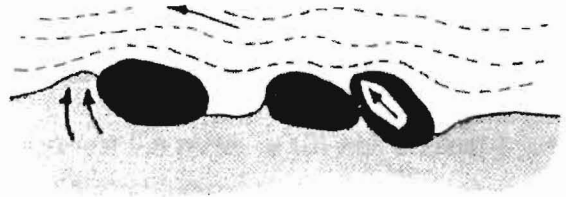
The INQUA definition of lodgement till states that: “Lodgement till is deposited by plastering of glacial debris from the sliding base of a moving glacier by pressure melting and/or other mechanical processes” (Dreimanis, 1989, p. 43).

This process takes place where the frictional drag between the debris and bed is greater than the shear stress imposed by the moving ice. This process may occur for single particles or masses of debris-rich basal ice (Benn and Evans, 1998). Lodgement processes for different situations are described in (Fig. 12). Lodgement tills are commonly characterized by the following properties: (1) overconsolidation due to ice overburden pressures, (2) high bulk density, (3) fissile to jointed structure due to subglacial shearing and dewatering processes, and (4) massive concrete appearance (Benn and Evans, 1998).

(a) Frictional retardation against bed



(b) Prow of soft sediment or clast provides obstacle



(c) Lodgement of debris-rich ice mass

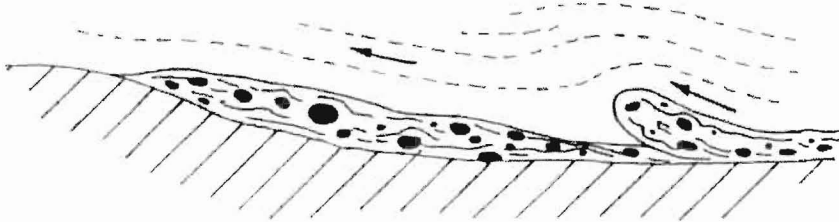


Figure 12. The lodgement process. (a) Particles lodged against a rigid bed by frictional retardation. (b) Clasts embedded in the ice can plough through the soft bed or lodge against other particles or (c) Whole masses of debris rich ice are lodged against the bed, and later melt out *in situ*. Schematic diagram adapted from Benn and Evans (1998, Fig. 5.24).

The lodgement process is often complex because of the combined effect of both glacial-nonglacial interactions. Many of these penecontemporaneous interactions participate in the formation and deposition of subglacial tills (Dreimanis, 1990).

This process has been observed in action by Boulton et al. (1974), Boulton (1979), and Boulton and Hindmarsh (1987) under the snout of the Breidamerkurjökull Glacier in southeastern Iceland. It was shown that subglacial deformation occurred by pervasive shearing rather than by sliding at the glacier-bed interface. They recognized that the uppermost 0.5 meter of till was dilated and contained a high percentage of fined-grained materials. It was suggested the upper till horizon has undergone continuous subglacial shearing. The effect of ice overriding the till has thus produced shear strain and dilation in the till. Evidence of dilation and interparticle crushing are typical of many subglacially deformed tills (Benn and Evans, 1998). Boulton et al. (1974) also examined the contact between the glacier sole and the till bed (Fig. 13). They noticed the lower 10-15 centimeters of glacier ice was concentrated with debris. Much of this debris is incorporated into the basal ice zone as a result of pressure melting and regelation sliding (Hambrey, 1994).

Pressure melting occurs because high pressure actually depresses the temperature at which ice melts. Conversely, a reduction in pressure typically elevates the melting point temperature, causing freezing (Benn and Evans, 1998). As a result of this phenomenon, melting and freezing may coexist simultaneously in different parts of the glacier bed in response to pressure variations. This



Figure 13. Contact between the glacier sole and lodgement till exposed in a subglacial tunnel. Clasts embedded in the basal ice layers may lodge against other clasts or plough through the till matrix. Ice movement is from right to left. Photograph adapted from Boulton et al. (1974, Fig. 2).

process typically occurs when the glacier flows over a bump or obstruction on the glacier bed (Hambrey, 1994). During this process, melt water is produced on the upstream side of a bump and is followed downstream by refreezing of the released meltwater. The ice layers formed by refreezing at the glacier sole are referred to as regelation ice. Any loose debris that accumulates at the base of the glacier is added to the layer of regelation ice. Debris concentrations within the regelation layer may reach up to 50% by volume (Boulton et al., 1974). Clasts that protrude from the glacier sole may also plough through the substrate or collide with other particles already lodged in the substrate.

Whether a glacier deforms its bed, ploughs, or slides over the bed depends on the degree of coupling between the glacier and its bed (Murray, 1997). Temporal changes in effective pressure (ice overburden pressure – porewater pressure) at the ice-sediment interface can either promote coupling or decoupling (Boulton and Hindmarsh, 1987). Because of complications in assessing the base of glacier and observing this slow hidden process, lodgement till mechanisms are still being proposed and debated (Dremanis, 1990).

Deformation Till

Deformation till was first defined by Elson (1961): “Deformation till comprises weak rock or unconsolidated sediment that has been detached from its source, the primary sedimentary structures distorted or destroyed, and some foreign material admixed.” Deformation till is formed at the glacier sole.

Deformation till may incorporate unconsolidated materials such as lake sediments, or weak rocks such as siltstones and shales (Elson, 1989).

In many cases, the lodgement process is similar to the deformation process. Deformation may take place as a result of direct glacial ice action or by plastering and lodging of clasts against the substrate. Sediment deformation takes place when the effective pressure in the sediment is low because of high pore water pressures (Boulton, 1996). The shear stress exerted by the moving ice may be sufficient enough to promote sediment deformation (Boulton et al., 1979). If deformation arises, a change in the grain structure arrangement will occur. Both lodgement and deformation tills may share so many till characteristics that it is often difficult to differentiate them (Dremanis, 1989). In addition, lodgement till may grade into deformation till or deformed till. This makes deformation and lodgement till problematic to identify in the field (Boulton and Hindmarsh 1987; Hart et al., 1991). Deformation tills are best identified by a range of characteristics, none of which may be diagnostic in itself (Benn and Evans, 1998). Further analysis on the microscale is encouraged when trying to genetically classify deformed tills. Dremanis (1990) emphasized the difference between lodgement and deformation process, “The main difference, theoretically, is that lodgement deposits basal debris shortly after its release from the glacier sole, while subsole drag and its stoppage may affect any subsole material, glacial or nonglacial.” Sugden and John (1976, p. 217) as well as Dreimanis (1990, p. 50) also addressed that deformation by stoppage of subsole drag and shearing may actually represent part of the lodgement process. Hindmarsh (1997) also

suggested that it could be related to the rate of subglacial movement compared to the consolidation time. These two processes may overlap in time but the rate of consolidation significantly affects the resultant product (Fig. 14).

Subglacial Glaciotectonic Deformation

The role of sediment deformation beneath glaciers represents one of the most important and actively studied boundaries in glaciology and glacial geology. The effects of sediment deformation and the actual mechanisms that contribute to this phenomenon are still poorly understood. As illustrated by Maltman et al. (2000), this largely results from the difficulty of observing the deformation processes and trying to recreate the boundary conditions of those processes within a laboratory setting. These above constraints have made it difficult to explore this unique boundary. Thus, the nature of sediment deformation beneath glaciers remains somewhat unresolved. Previous investigations by Boulton (1979) and Boulton and Hindmarsh (1987) in Iceland and Alley et al. (1986) in Antarctica concluded that glacier motion, to a high degree, is controlled by deformation of the underlying bed. Boulton (1979) concluded that 88% of the forward movement of the glacier was derived from deformation of the bed rather than by slip at the glacier-bed interface.

It has been suggested (Banham, 1977; Hart and Boulton, 1991; Hicock, 1992) that the subglacial layer of deforming rock and sediment may function as a shear zone. Similar deformational structures from mylonites and cataclastic shear zones have been recognized within glacial tills (Slater, 1926 and Banham, 1977).

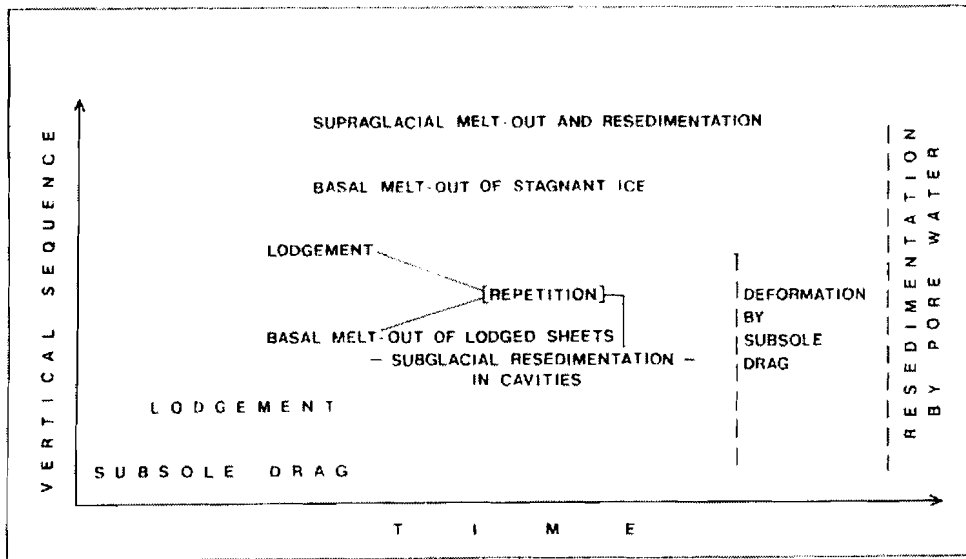


Figure 14. Till deposition at various levels for a continental ice sheet proximal to its margin. Note the effects of the re sedimentation processes in both the vertical and time dimension. Diagram adapted from Dreimanis (1990, Fig. 7).

This shear zone model should also include the lower basal ice layers since the glacier and its substratum are commonly coupled (Benn and Evans, 1996).

In order to understand the dynamic processes that operate in the subglacial environment it is necessary to understand the kinematics (movement history) and stress regimes that prevailed within the bed during deformation. The next section discusses the kinematics of progressive simple shear and structural styles of the resulting fabrics. The geometric principles and terms are defined in Table 2.

Progressive Simple Shear

Deformation by progressive simple shear is modeled by utilizing the strain ellipse (Fig. 15). Two styles of deformation are considered here, pure shear and simple shear. In reality both simple and pure shear act simultaneously (van der Wateren et al., 2000). Pure shear is a type of deformation in which the strain ellipse is flattened (compressed) or stretched (extended) without a rotational component (Fig. 15a) (Benn and Evans, 1996). Identifying the effects of both pure shear and simple shear is to record the orientation of the least and greatest principal stress directions (σ_1, σ_3) (McCarroll and Rijdsdijk, 2003). These axes or principle stress directions are defined by the stress ellipse (Fig 16).

Kinematics	Movement history.
Dynamics	Force distribution.
Fabric	The complete spatial and geometrical configuration of all those components that are contained in a rock, and are penetratively and repeatedly developed throughout the volume of rock at the scale of observation. Includes features such as foliation, lineation, preferred orientation and grain size.
Foliation	Planar fabric consisting of a compositional layering or a preferred orientation of planar discontinuities (fractures, platy minerals).
Bedding	Primary foliation, alternating bands with distinct lithologies.
Cleavage	Secondary foliation defined by a preferred orientation of inequant fabric elements, a penetrative set of discrete fracture surfaces (fracture cleavage; term to be avoided), shear bands (shear band cleavage), or surfaces along which platy minerals are bent (crenulation cleavage).
Stress	Tensorial quantity describing the orientation and magnitude of force vectors acting on planes of any orientation at a specific point in a volume of rock. Force per unit area acting in a given direction on a body at an instant in time.
Normal stress	Stress acting perpendicular to a material plane.
Shear stress	Stress acting parallel to a material plane.
Strain	The change in shape or internal configuration of a body resulting from certain types of displacement; tensorial quantity including features of distortion and rotation. A strained situation is commonly represented by an ellipsoid, compared with the unstrained sphere.
Incremental (infinitesimal) strain	Imaginary, infinitely small strain.
Finite strain	Strain accumulated over a finite period of time.
Coaxial deformation	Material lines that are instantaneously parallel to the incremental stretching axes remain fixed with respect to these axes throughout the deformation history.
Non-coaxial deformation	Material lines that are instantaneously parallel to the incremental stretching axes rotate with respect to these axes.
Style	Embodies all morphological features of a structure or group of structures (e.g. fold shape, presence/absence of foliations).
Brittle deformation	Failure of a stressed body along discrete discontinuous dislocations (cracks and faults), when the elastic limit is exceeded.
Ductile deformation (ductile flow)	In structural geology, usually reserved for deformations that are continuous throughout the rock body, such as crystal lattice deformations, crystal flow, grain boundary diffusion etc. Since these are obviously lacking in deformed unlithified sediments, we use the term ductile, lacking a better term, to denote a permanent deformation without fracturing on the observation scale.
Rheology	The relationship of stress and strain within fluids in motion (in the strict sense). Used here in a wider sense, referring to the mechanical behaviour of materials.

Table 2. Definitions used in this paper (Passchier and Trouw 1996 with modifications by van der Wateren et al., 2000).

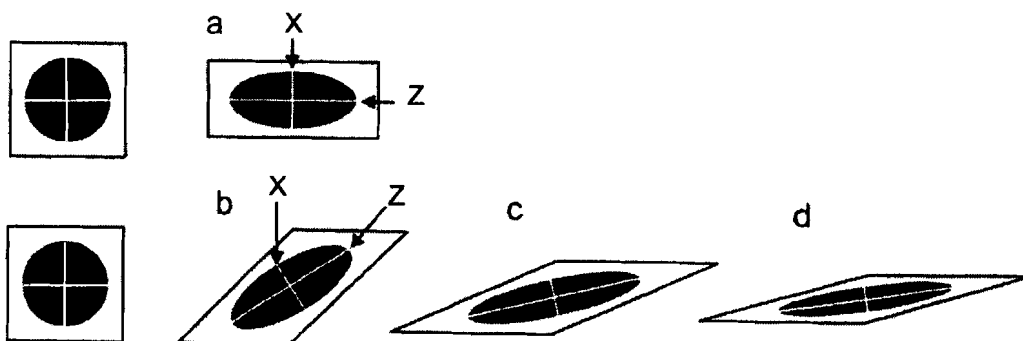


Figure 15. Strain ellipse in accordance with pure and simple shear processes. (a) Pure shear (flattening and extension). (b) Simple shear; no volume loss. (c) Simple + 67% flattening; no volume loss. (d) Simple + flattening + consolidation, 33% loss. Diagram modified after van der Wateren et al. (2000, Fig. 1).

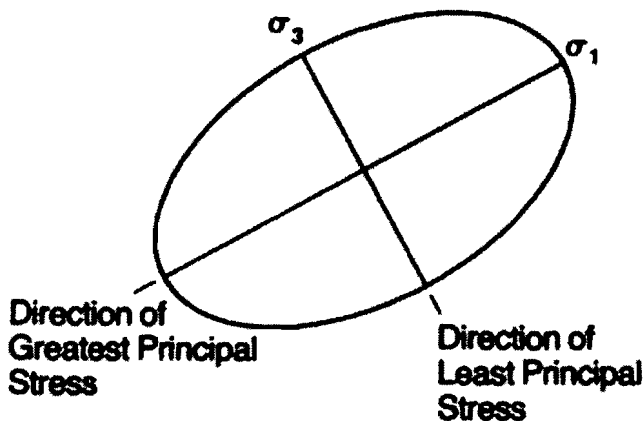


Figure 16. Depicts the stress ellipse in two-dimensions. Note the orientations of the maximum and minimum stress axes. Diagram acquired from Davis and Reynolds (1996, Fig. 3.19).

A flattened vertical principle strain axis (X) and extended horizontal principle strain axis (Z) indicates a loading style regime. Such structures are produced as a result of loading underneath a thick overburden of glacial ice (McCarroll and Rijdsdijk, 2003). However, progressive simple shear includes both changes in shape and orientation of the strain ellipse (Fig. 15b, c, d) (Benn and Evans, 1996). The principal strain axes of the strain ellipse (Z and X) gradually show an elongation in the Z axis and shortening in the X axis during subglacial shearing. The Z axis becomes progressively parallel to the shear zone boundaries (van der Wateren et al., 2000). The resultant strain trajectories within the subglacial shear zone exhibit sigmoidally shaped lines (van der Wateren, 1995) (Fig. 17).

Dilation also takes place during progressive simple shear. Dilatancy causes the sediment to expand and contract (Clarke, 1987). Dilatant sediment layers generally have a high void-to-solid ratio and low density. The resultant fabrics and structures which we observe in the field or in thin-section reflect the total or finite strain that accumulated through numerous incremental strain steps (van der Wateren et al., 2000).

Strain and Deformational Styles

The way in which strain is imprinted on a material is a well developed concept in structural geology (Davis and Reynold, 1996). The deformation history is often analyzed by comparing its present deformed configuration with a previous undeformed configuration (Benn and Evans, 1996). The difference between these two states defines the cumulative strain.

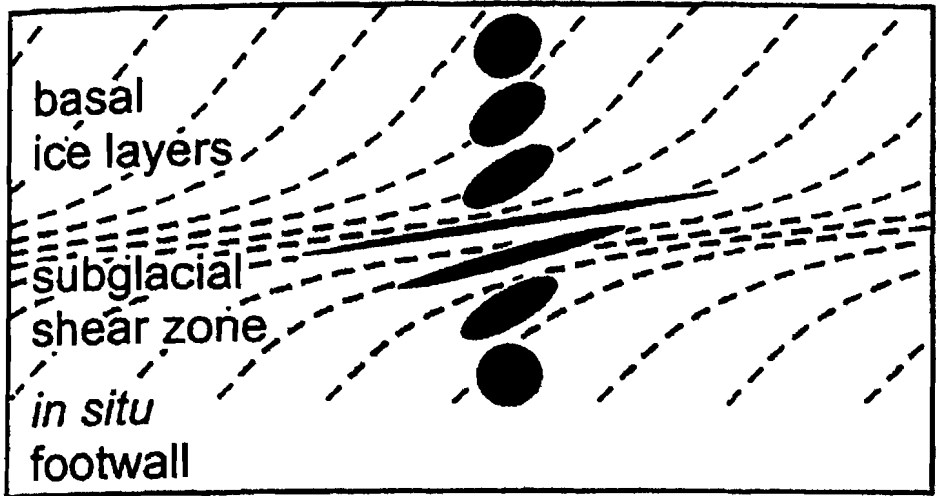


Figure 17. Subglacial shear zone and the finite strain ellipses.

Note the sigmoidally shaped strain trajectories (λ_1) within the shear zone.

Diagram adapted from van der Wateren et al. (2000, Fig. 4).

Primary structures (undeformed configurations) which are preserved within deformed glacial materials can sometimes be utilized to reconstruct the initial undeformed state and also provide information about the cumulative strain (Benn and Evans, 1996). Two basic deformational styles can exist within unlithified sediments: brittle deformation, in which movement is concentrated along discrete failure surfaces, such as cracks or faults, and ductile deformation, in which strain is distributed throughout the entire mass exhibiting permanent deformation without fracturing. Glacial materials consisting of clay tend to show more ductile behavior, while brittle type structures usually form in coarse-grained sediments such as gravels and sands (van der Wateren et al., 2000). Many brittle and ductile deformational structures may be misidentified because of the scale of observation. Macroscopic ductile structures may appear to be smooth but in reality they may represent discrete continuous microfaults (van der Wateren et al., 2000). On the other hand, what appears to be a fault may actually be a narrow shear zone in which the material has been extremely attenuated but has not failed. Glacial materials that have been subjected to high subglacial shear strains are typically macroscopically structureless and homogenized (Hiemstra and van der Meer, 1997).

Till Properties and the Onset of Deformation

Theoretical modeling of subglacial deformation has been undertaken by Boulton (1979), Boulton and Hindmarsh (1987), G.K.C. Clarke (1987), P.U. Clarke (1994), Hindmarsh (1997), Murray (1997), Alley (2000), and Truffer et al. (2001). A major aim of these theoretical studies is to develop rheologic laws to predict the

amount of deformation that will occur under given conditions (Benn and Evans, 1998).

Glaciotectonic deformation occurs where the stress transferred from the glacier exceeds the shear strength of the material. Glacigenic material will not undergo permanent deformation unless subjected to some threshold stress (Benn and Evans, 1998). This threshold stress is known as the yield stress or critical shear stress. Shear strength is controlled by two components: cohesion and intergranular friction. Cohesion refers to both the electrostatic forces and chemical bonds that hold the materials together while intergranular friction refers to the resistance to grain sliding processes and grain crushing. A minimum or equivalent value of yield stress is needed to overcome the shear forces that hold the material together (Benn and Evans, 1998). Subglacial failure conditions may be expressed by employing the Coulomb equation. This equation was first introduced and formulated by a French engineer named Charles Augustin de Coulomb in 1776 (Benn and Evans, 1998). The Coulomb equation states that the total shear strength (τ) is given by the cohesion (c) plus the product of the normal stress (N) multiplied by the angle of internal friction (ϕ_i).

$$\tau = c + N \tan \phi_i \quad (1.2)$$

This equation was later modified because of sediment porosity effects. The presence of water in between the sediment grains will reduce the material shear strength (Benn and Evans, 1998). The effect of porewater pressure on material strength is incorporated into the Coulomb equation:

$$\tau = c + (p_i - p_w) \tan \phi_i \quad (1.3)$$

where (τ) is the shear strength at any point in the material, (c) is the cohesion, (p_i) ice overburden pressure, (p_w) is the porewater pressure, and (ϕ_i) is the angle of internal friction.

Sediment shear strength is dependent upon grain size and sorting, the existence of weak planar boundaries within the substratum, and porewater pressures (Benn and Evans, 1998). Both spatial and temporal changes in sediment shear strength will vary as the stress conditions change beneath the ice.

Glacial Micromorphology

The analysis of glacial sediments at the micro-level has been employed recently in reconstructing till genesis. This technique allows glacial specialists to directly observe and study the interrelationships between sediment particles (van der Meer, 1996). Various micromorphological features in thin-sections of tills are used to characterize the depositional environment (van der Meer, 1985). Glacial deposits often reveal many relict structures that are directly related to glacial processes of till formation (Menzies, 2000). One major aim currently of glacial micromorphology is to identify and differentiate between microstructures of a particular depositional environment (Lachniet et al., 2001). The search continues for diagnostic criteria that would allow more precise differentiation of individual glacial facies (Menzies, 2000). Several authors have attempted to calibrate this technique by examining glacial deposits of known origin (Menzies and Maltman, 1992, et al. 1997; van der Meer, 1987, 1993; Hiemstra, 2001; Khatwa and Tulaczyk, 2001). These proficient studies have increased our understanding of the mechanics of glacial

deposition. The studies have attempted to apply the process-microstructure link to various glaciogenic deposits. In order for ancient glaciogenic deposits to be successfully reconstructed more calibration studies are needed to further establish a better process link. One perpetual problem may be attributed to the natural processes within the glacial environment. Many different sets of glacial processes (e. g. gravity flow versus subglacial processes) often produce similar microstructural features. In many aspects this complicates the differentiation process (Menziés, 2000). The following section introduces microstructural features that have been found currently within glaciogenic sediments.

Microstructures within Glaciogenic Sediments

In describing soils and sediments in thin section, Brewer and Sleeman (1960), following FritzPatrick (1984), distinguished between the plasma or matrix, and particles or skeleton grains. Skeleton grains are analogous to phenocrysts within an igneous rock. Skeleton grains may comprise of any lithic fragment greater in thickness than the thin-section itself (approximately $>25\text{-}30\ \mu\text{m}$) (Menziés, 2000). The plasma or matrix, in contrast, is characterized by clay-sized particles $<25\text{-}30\ \mu\text{m}$ in thickness. The plasma commonly exhibits a distinct birefringence under cross-polarized light. In addition, the plasma will also arrange itself in a specific preferred orientation in response to various stress field conditions. Various microstructural features may be viewed in Figure 18.

Microfabrics and Microstructures within Glacial Sediments

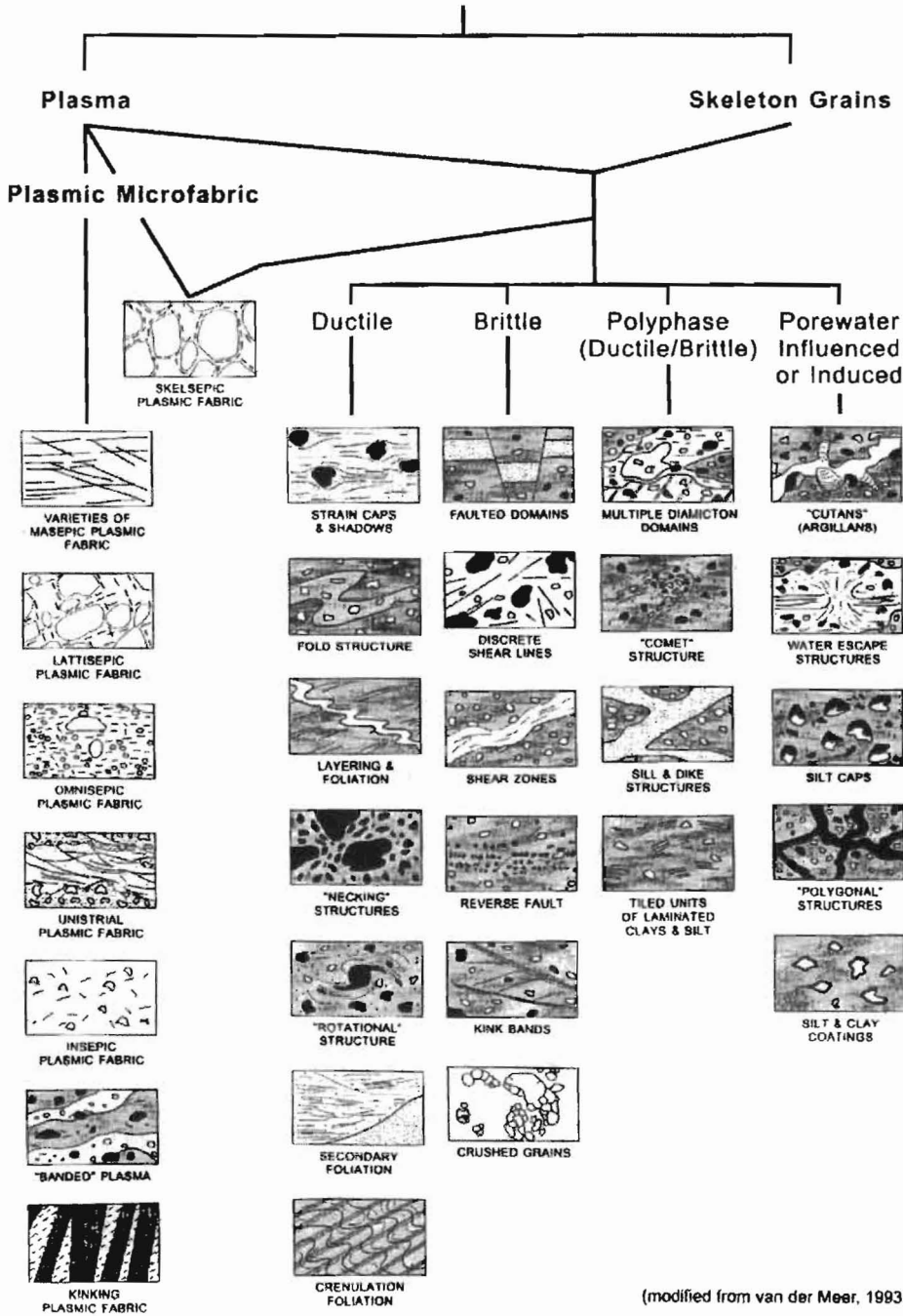


Figure 18. A taxonomy of microfabrics and microstructures. Diagram adapted from Menzies (2000, Fig. 2) modified after van der Meer (1993).

Chapter 2. Methodology

Till Sampling and Preparation

Samples of till were obtained by carefully carving out blocks from the sediment exposures. Samples were gathered from two localities in the Devils Lake area: (Site 1) gravel pit southeast of Devils Lake Mountain and (Site 2) field exposure southeast of Sullys National Game Preserve (situated within Sullys Hill Thrust Complex). Two sediment block samples were retrieved from site 1 and four samples from site 2. These site areas were chosen because of minimal evidence of field exposures elsewhere in the region.

Precautionary measures were taken to prevent disturbance of the structural integrity of the till during sampling (Lachniet et al., 2001). The size of the blocks ranged from 5-10 cm long to 3-5 cm wide. Orientation and sample numbers were properly. The samples were then carefully wrapped in aluminum foil and stored in air-tight plastic containers. Samples were subsequently packed and transported in a larger box to avoid shock damage. Vertically aligned thin-sections were prepared for the microstructural analysis at Burnham Petrographic Laboratory in Rathdrum, ID (Fig. 19). At the laboratory, the samples were air dried and impregnated with Petropoxy 154, a low-viscosity, high-bond-strength epoxy. The resultant thin-sections were prepared from the hardened sediment blocks.

Following the production of the thin-sections, a petrographic microscope was used to examine the physical and structural properties of the sediment (Khatwa and Tulaczyk, 2001). The till samples were examined between 50x and 100x magnification using a Nikon Optiphot2 pol Petrological Microscope under plane and cross-polarized

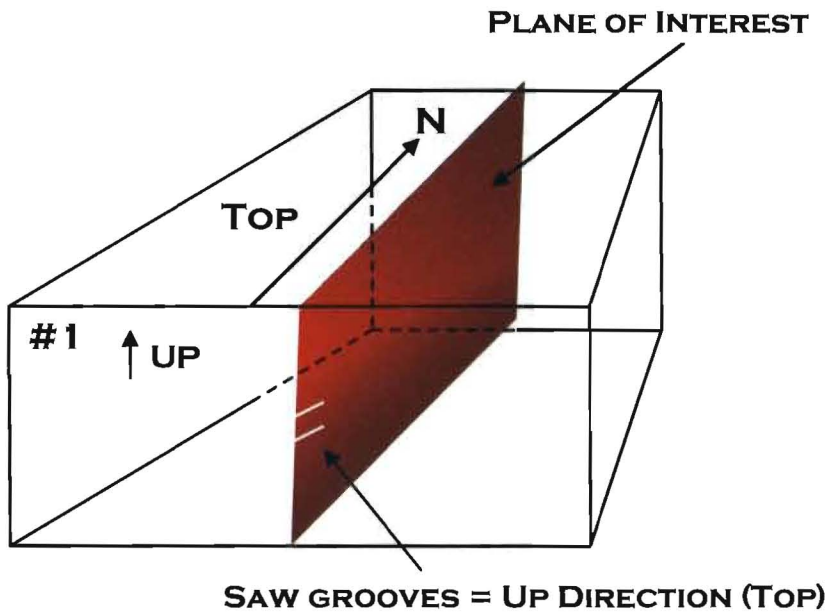


Figure 19. 3-D block model of glacial sediment. The above labels are utilized as orientational indicators. Note the vertical plane cutting through the block.

light. Photomicrographs were taken on 35 mm color film using a Nikon FX-35DX manual camera attached to an automatic shutter/exposure control box. The Nikon FX-35DX camera mount was used to capture the micromorphological data.

Kite and Blimp Aerial Photography

Kite and blimp aerial photography was carried out during the early part of October of 2004 with Dr. James Aber, and Shawn Salley, an undergraduate field assistant. Aerial photographs of glacial features acquired at two sites, Devils Lake Mountain and Devils Heart Butte (Fig. 5). Aerial views were taken with radio-controlled camera rigs. On this particular trip, a small helium blimp and a variety of kites were used (Figs. 20, 21). Three advanced, high resolution camera rigs were employed to harness the different types of cameras sizes. All of the camera rigs were designed and constructed by Brooks Leffler, a camera rig specialist from California.

The first camera rig was designed for the Olympus Stylus Epic point-and-shoot camera. This camera rig was designed and constructed to maximize versatility and minimize weight. The second rig system was constructed for the Canon EOS Rebel X SLR camera. The weight of the rig and camera is just over 1 kg (36 oz.) (Fig. 22). The final rig system was designed to accommodate the micro-size, high resolution digital Elph camera manufactured by Canon. This particular camera and rig system is reliable and is used routinely in the field. The aerial photographs were taken at a height of approximately 100-150 m above the ground surface.



Figure 20. Ground view of author (left) and Shawn Salley (field assistant) holding the helium blimp at Devils Lake Mountain, ND. Helium blimp is 13 ft (4 m) long and lifts the same camera rigs used in kite aerial photography. (Photograph courtesy of James Aber, 2004).



Figure 21. Giant rokkaku kite. This particular kite has a rigid framework with great lifting power. The large surface area allows the kite to operate under light wind conditions. (Photograph from http://www.geospectra.net/kite/equip/g_rok1.jpg)

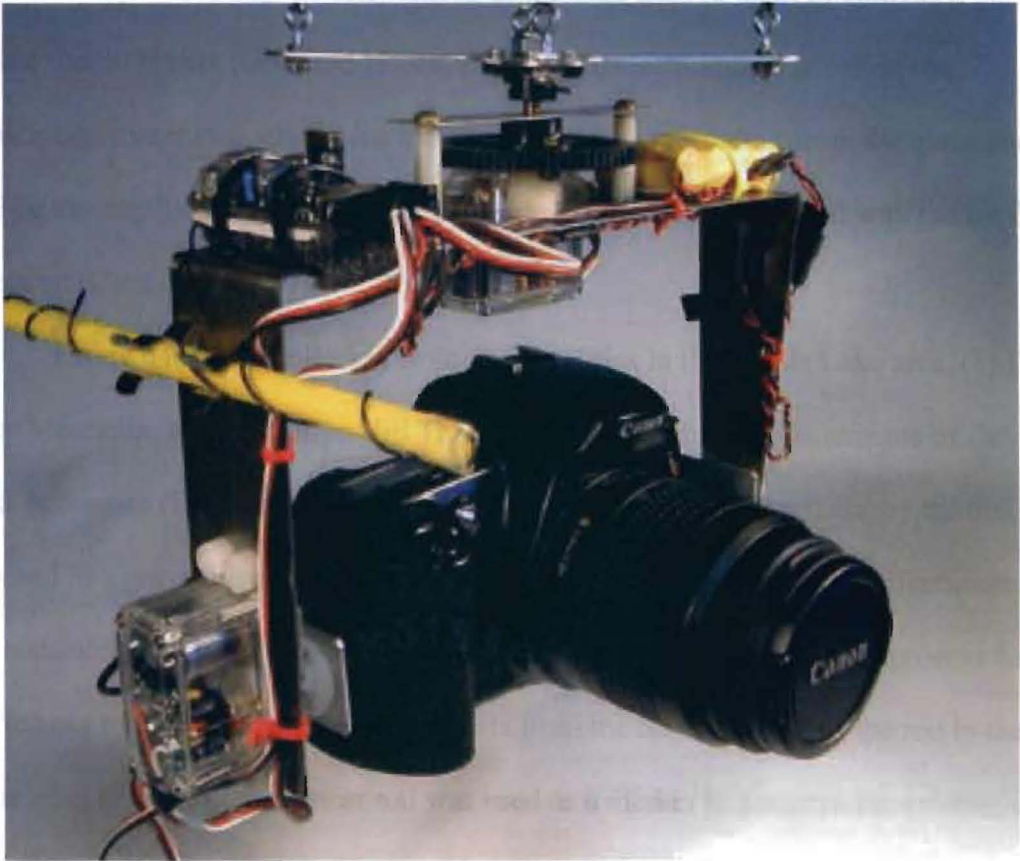


Figure 22. The camera rig and the Canon EOS Rebel X SLR camera. (Image acquired from James Aber, 2000).

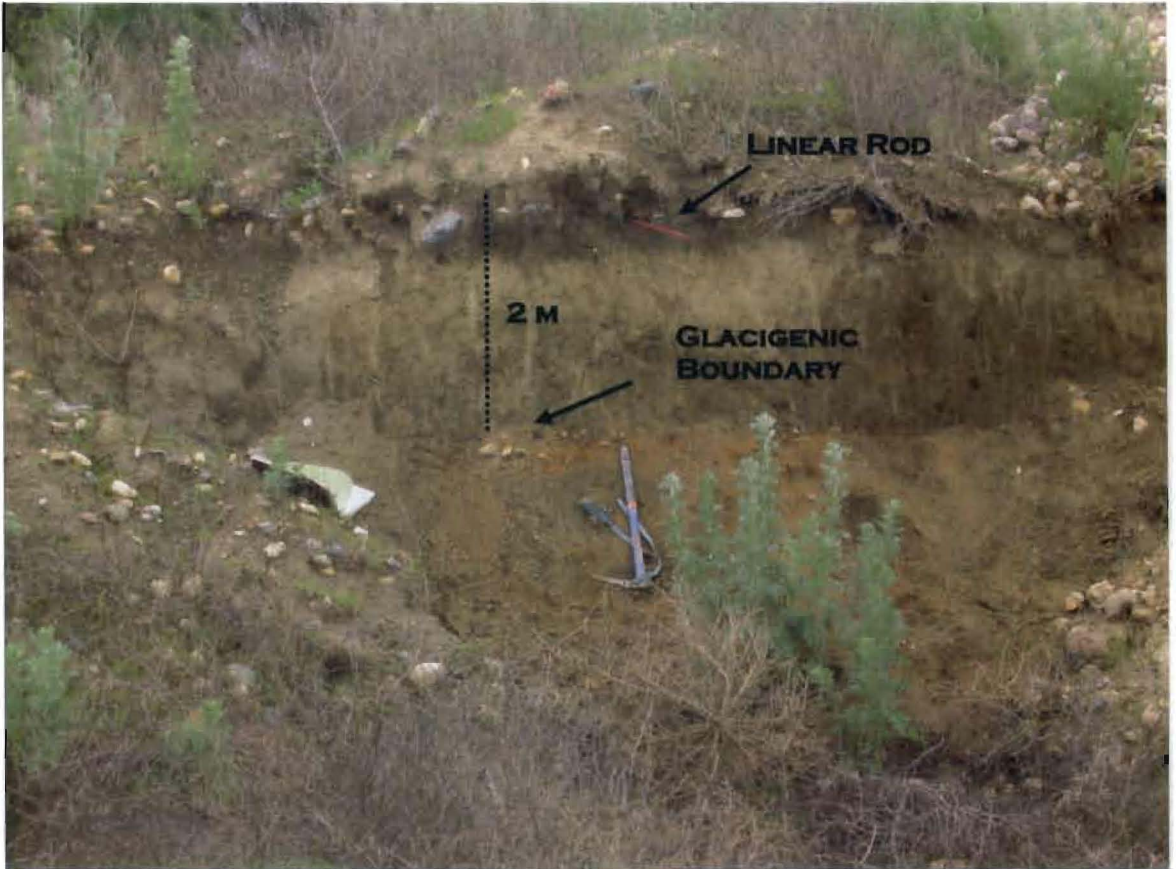


Figure 23. Till fabric process at Devils Lake Mountain. Note the red linear rod (17 cm in length) at the top of the till section. A transitional boundary occurs at the bottom of till section.



Figure 24. Stage 1 (clast removal) of till fabric process at Sullys Hill Thrust Complex.

Image Processing

Image processing was conducted using *Idrisi Kilimanjaro* and *Arcscene*™ software packages. Land surface data were obtained from a variety of government agencies. Satellite imagery (Landsat Thematic Mapper) was obtained from the EROS Data Center at Sioux Falls, North Dakota. Digital orthophotography quarter quadrangles (DOQQ) and digital orthophotography quadrangles (DOQ) were acquired online from the North Dakota Geological Survey (NDGS). Scanned topographic maps (Digital Raster Graphics) were also obtained online from the NDGS. Full-color orthophotography quadrangles were supplied by Dennis James, a GIS technician at the North Dakota State Water Commission. Thirty-minute digital elevation models (DEM) were also utilized in the image analysis. Digital elevation models were acquired from the National Elevation Data Center, United States Geological Survey (USGS).

The digital land-surface data were primarily used to study and interpret the glacial landform assemblages over large synoptic views. False-color composites were developed from the satellite data to emphasize and accentuate the ice-shoved features. Digital elevation data were merged with full color orthophotographs and subsequently draped over the digital elevation models. One major aim of the image data analysis was to evaluate the geometric and kinematic relationships of the ice-shoved terrain in three-dimensions. Specific attention is focused on Devils Lake Mountain area in Ramsey County.

Chapter 3. Results: Data and Analysis

Two sites display clear geomorphic evidence of recent glaciotectonism within the Devils Lake Region (Aber et al., 1989, Bluemle and Clayton, 1984). Site 1, Devils Lake Mountain (DLM), is situated in southern Ramsey County near East Devils Lake. Site 2, Sullys Hill, is situated within the ice-shoved ridge complex located south of Devils Lake Main Bay.

Site 1: Devils Lake Mountain (DLM)

The distinct landscape pattern of DLM is clearly apparent on a contour map (Fig. 25). The landscape configuration depicted in Fig. 25 is characterized by a cluster of well-developed hills. The hills generally trend northeast-southwest and outline a slightly arcuate pattern. The hill complex is slightly concave toward the northwest. DLM reaches a maximum elevation of 550 m (1625 feet), some 54 m (177 feet) above the local source depression, located immediately to the northwest. Steep-sided slopes are depicted on the northeastern side in the downglacier direction. The similar shape of the source depression and the ice-shoved mass suggests a genetic link between these features. Additional evidence for this association is revealed along the southwestern flanks of DLM. The line A-A' denotes a southeast-trending lineament formed by the western edge of the lake depression and the western flank of DLM. This linear feature is essentially the boundary of a tear fault in which the material from the lake depression was shoved into DLM during glaciotectonic thrusting. The DLM lineament is more than 1.5 km long and displays 37 m of total topographic relief. A similar feature has been found within the Wolf Hill Complex, in east-central Alberta (Aber et al., 1989).

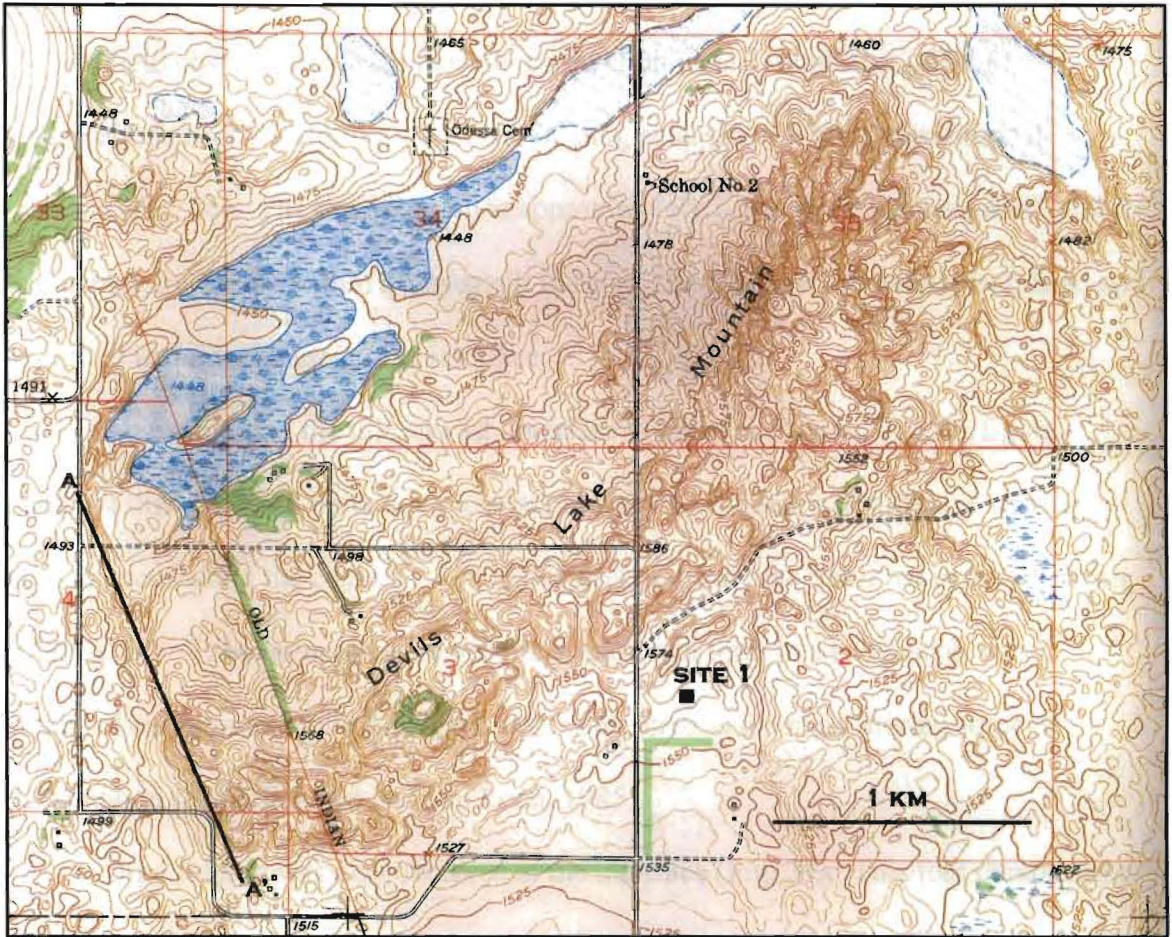


Figure 25. USGS 1:24,000 scale contour map depicting DLM and location of gravel pit (Site 1). Note the slightly arcuate geometry of the ice-shoved feature and the fault lineament towards the southwest (A-A'). Elevations in ft; contour interval = 5 ft. Contour map acquired from United States Geological Survey.

The orientation of the source depression and fault lineament indicates a southeastward ice movement.

Field observations were made in a gravel pit (Site 1) southeast of DLM. Observations near DLM revealed a layer of subglacial till overlying glaciofluvial outwash (Fig. 26). The overlying till is approximately 1-2 m thick and consisted of shale and pebble fragments within a clayey silt matrix. The till appeared overconsolidated and exhibited textural changes at the interface.

An example of the till/outwash interface is given in Figure 27. This figure depicts a disrupted and transitional contact boundary. Evidence of diffusive mixing is seen to occur along the contact. A diapiric structure was also observed in the overlying till (Fig. 28). These structures are generally known to form in a subglacial, water-saturated environment with high pore-water pressures as the main driving force of deformation (Brodzikowski and van Loon, 1985).

Drag folding was also observed at the interface (Fig. 29). This fold demonstrates movement of the base of the till over the underlying sandy sediments. The distinct tails stretching in opposite directions, i.e. down-ice on top and up-ice underneath the clast, clearly indicates a difference in deformation velocities around the clast during lateral movement. The asymmetric geometry indicates a southeastward transport direction.

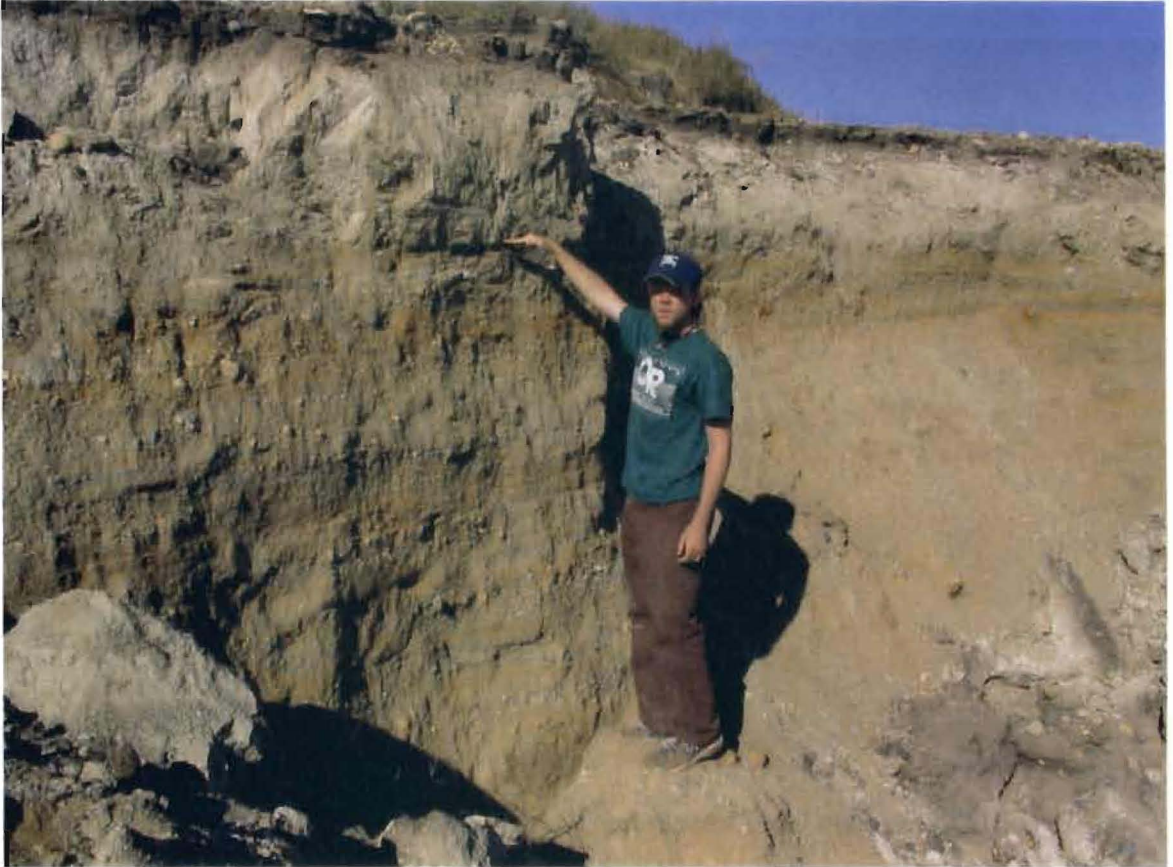


Figure 26. Photograph of glaciofluvial outwash and the overlying till carapace. View toward the northwest. Note the lateral till continuity and irregular contact.

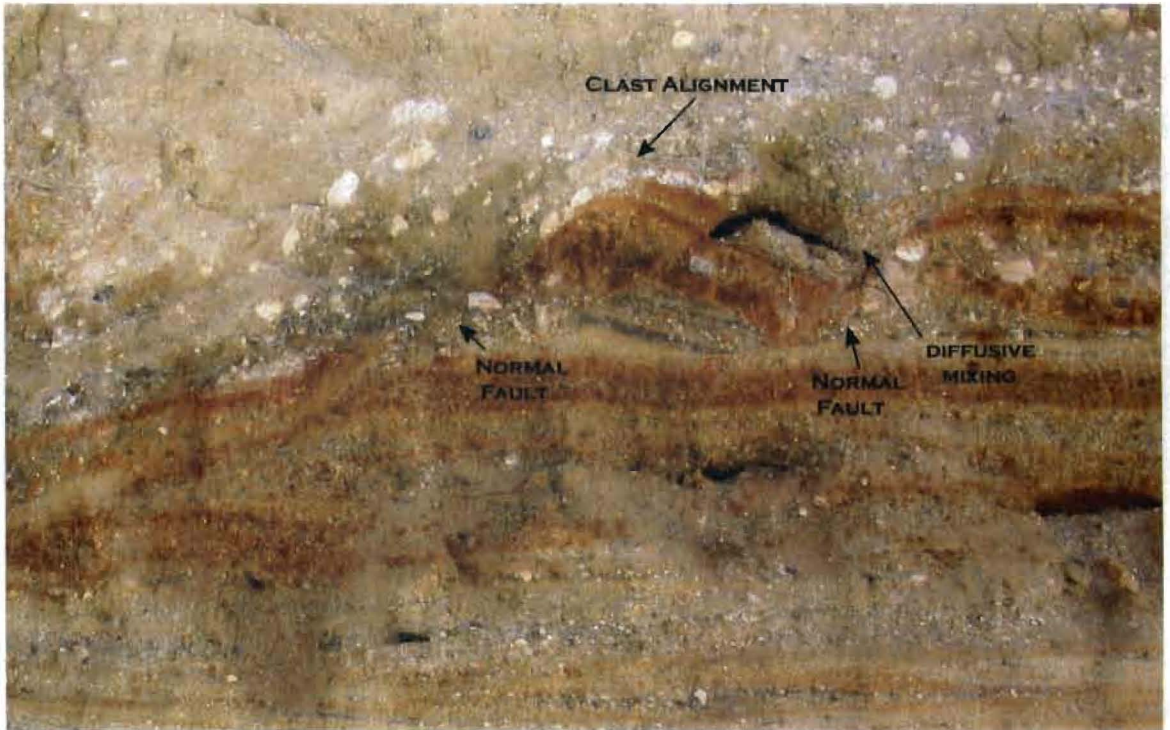


Figure 27. Contact between the overlying till and glaciofluvial outwash. Diffusive mixing has taken place along the interface. Note the convex alignment of clasts along the contact boundary. Rotation of normal fault blocks is depicted near the boulder impression. These faults have been subsequently rotated due to extension.

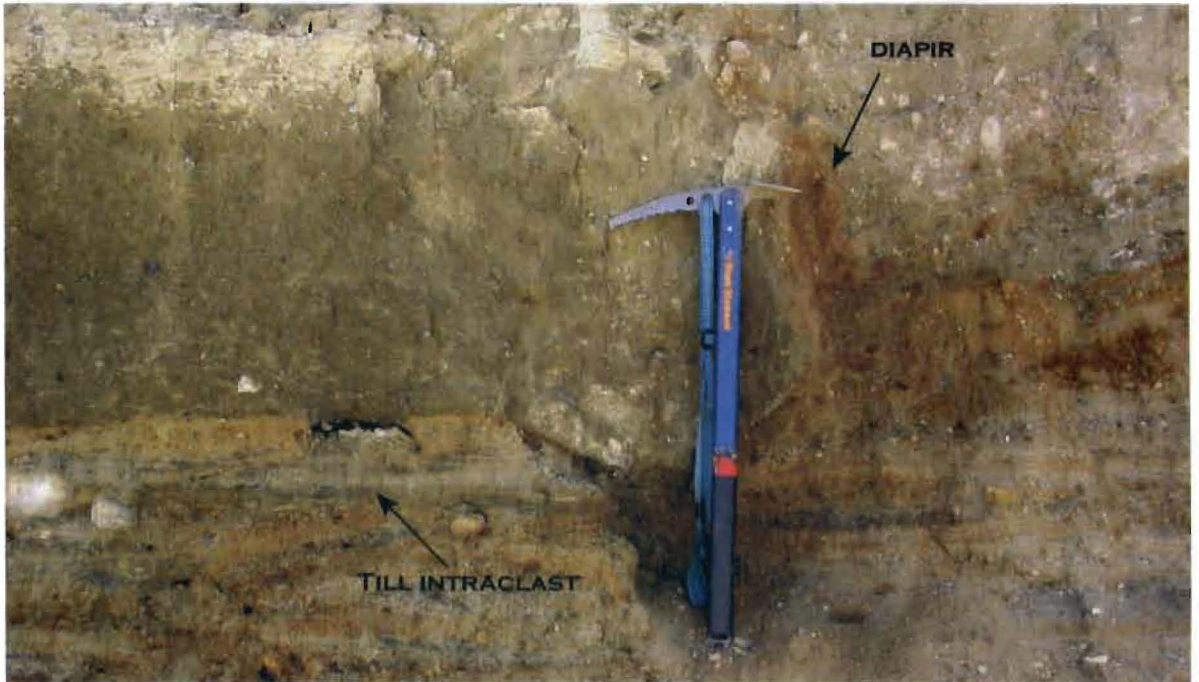


Figure 28. Diapir located to the right of the ice axe. Note the vertical clast orientation adjacent to the diapric structure. Contact disturbance is denoted by the till intraclast. Ice axe approximately 60 cm.

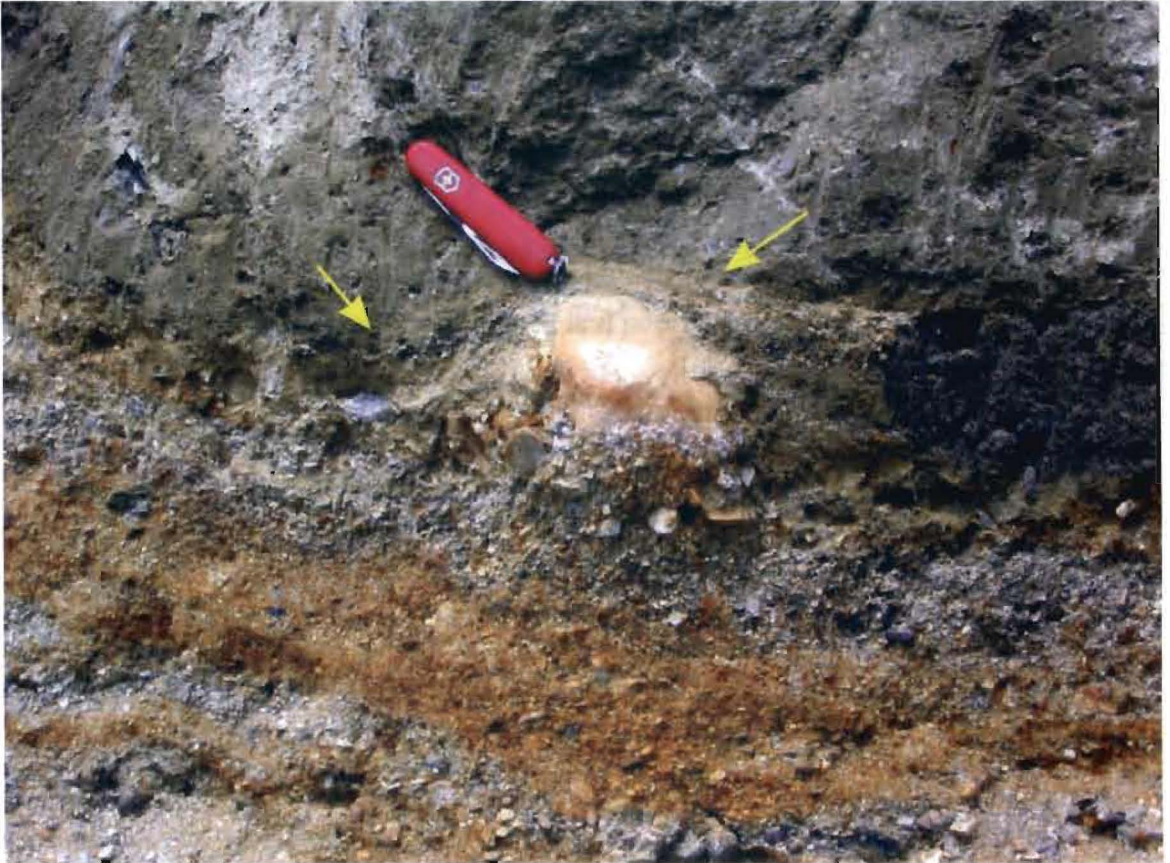


Figure 29. Photograph of clast at the till/outwash interface. Note the well-preserved tails above and below the clast (yellow arrows). Smearing along the contact is clearly shown. Swiss army knife approximately 8 cm.

Site 2: Sullys Hill

The glacial geomorphic expression of Sullys Hill is clearly displayed on a contour map (Fig. 30), which depicts an ice-marginal kame, at the head of the Big Coulee Spillway Valley. The site exposure is located on the southern flank of the kame (Fig. 31). The field exposure revealed a detailed succession of glaciofluvial sands and gravels interbedded with layers interpreted as gravity flow tills (Fig. 32). This glacial successions is approximately 5 m long and is folded into a synformal structure (Fig. 33). The glaciofluvial gravels are coarse grained and poorly sorted with both local and exotic lithologies. Striated and faceted clasts are common in both units (Fig. 34). The flow till consists of a sandy silt matrix with interlaminated bands of silty clay. These bands have been complexly deformed and faulted. Figure 35 displays a faulted interlaminated silty clay band within the gravity flow till. The resultant band was possibly faulted due to loading of the overlying higher density glaciofluvial materials (Rijsdijk, 2001, Aber et al., 1989). Figure 36 displays a well developed symmetrical fold of silty clay. Below the limbs of the symmetrical fold occurs the relict cavity or imprint of the boulder obstruction.

Till Clast Fabrics

Till fabric data from the DLM and Sullys Hill have been plotted and contoured on Schmidt equal-area projections. The Schmidt scatter plots and contoured versions are displayed in Fig. 37. Fabric modality criteria is based on Hicock et al. (1996), Table 3. The DLM contoured projection displayed a polymodal cluster arrangement. The contour envelopes are separated by about 90°. The clast plunge angles varied from 2°-60° and are dominantly spread out over the southern portion of the contoured projection.

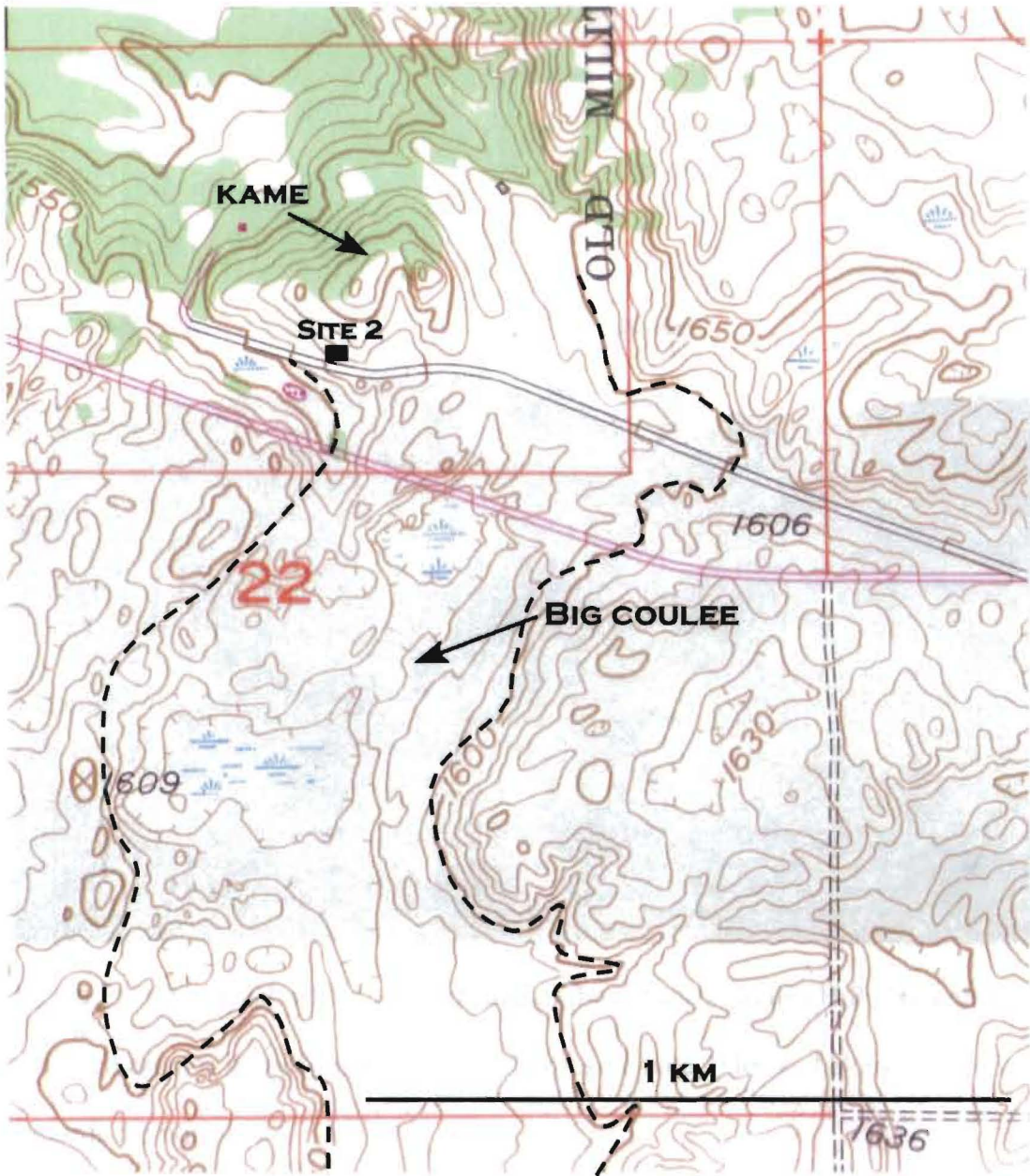


Figure 30. USGS 1:24,000 scale contour map depicting a portion of Sullys Hill and location of field exposure (site 2). Note the two conical peaks of the kame and the head of Big Coulee Spillway Valley. The black dotted-line represents an approximate outline of the Big Coulee Spillway Valley. Elevation in ft; contour interval = 10 ft. Contour map acquired from the North Dakota Geological Survey.

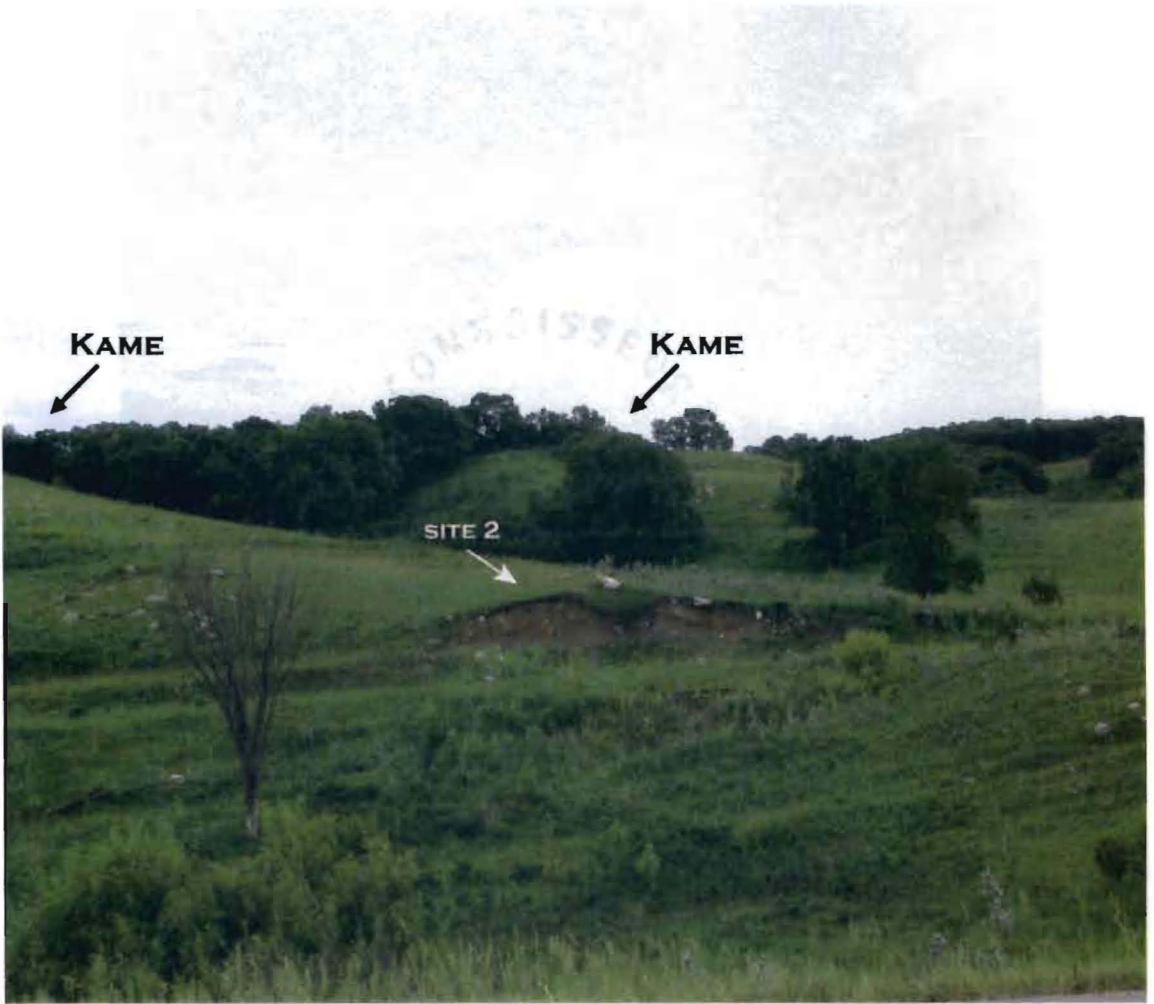


Figure 31. Photograph of the southern side of the kames on Sullys Hill. Note the scattered erratics in the foreground. Field exposure (site 2) located along the flank. View towards the northeast.



Figure 32. Sequence of gravity flow tills and glaciofluvial outwash on Sullys Hill. View toward the north. Ice axe approximately 60 cm.



Figure 33. Sequence of interbedded gravity flow tills and glaciofluvial outwash. Scale pole is 2 m long. View toward the north.



Figure 34. Photograph of striated and abraded surface. Clast derived from flow till at bottom of the sequence. View toward northeast. Knitting needle approximately 8.5 cm long in photograph.



Figure 35. Photograph depicts a normal fault below the arrow. Note change in flow till thickness near boulder obstruction. White dashed line represents the approximate fault trace. Swiss army knife approximately 8 cm. View toward the north.

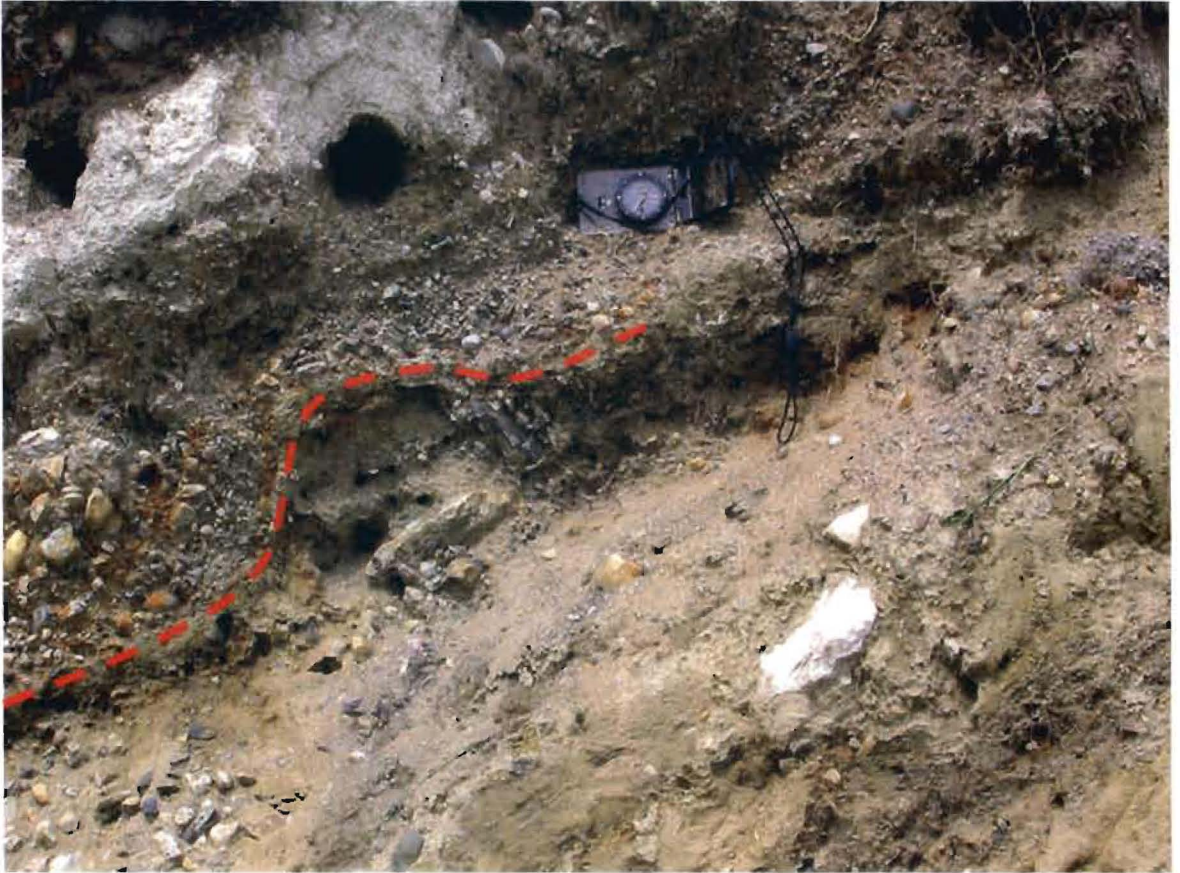
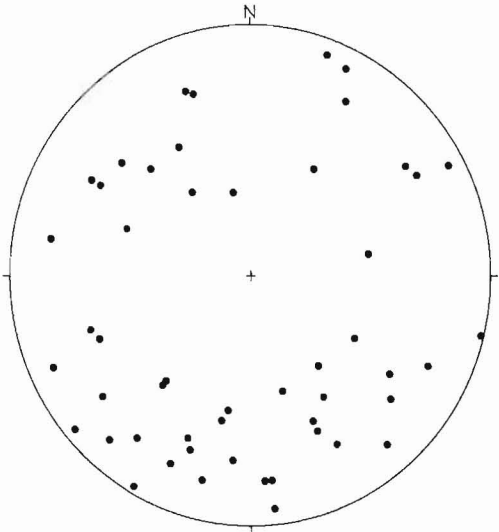
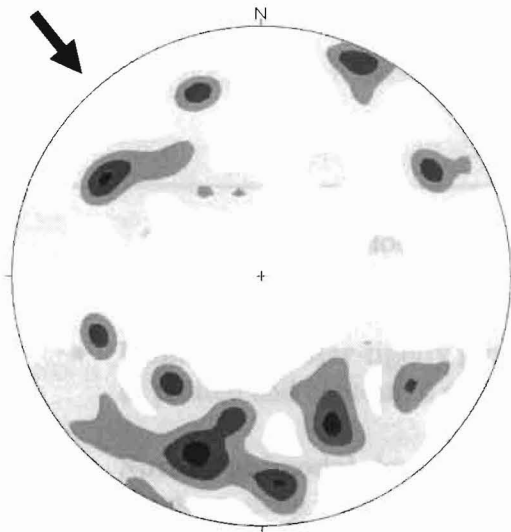


Figure 36. Photograph of symmetrical fold in the flow till (red dashed line). The compass is approximately 10 cm long. View toward the north.

ICE FLOW



SITE 1



SITE 2

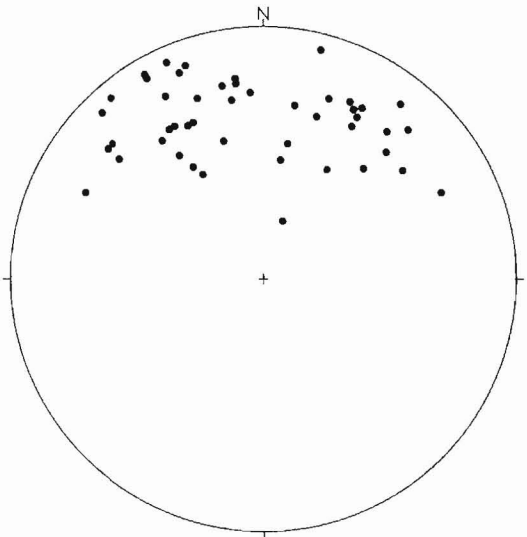
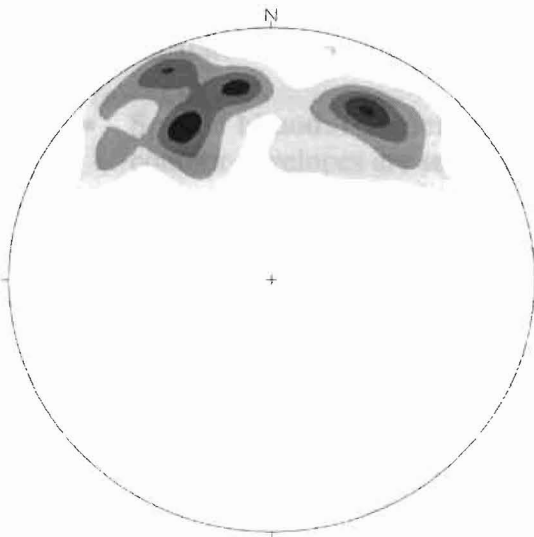


Figure 37. Schmidt equal-area, lower hemisphere projections of till stone long-axis fabrics. Both scatter plots (right) and contoured diagrams (left) are included for each fabric. Diagrams were produced by the software program RockWorks™. Note the data point clusters and various patterns.

Table 3. Fabric Modality Criteria based on (Hicock et al., 1996)

- **Unimodal cluster**-tightly grouped single concentration of long-axis points as plotted and contoured on a Schmidt equal-area net.
- **Spread unimodal**- loosely grouped but still a single concentration; no breaks or deep indents in the central parts of contour envelopes.
- **Bimodal clusters**- distinctly grouped concentrations and envelopes are separated at about 90°.
- **Spread bimodal**- loosely grouped concentrations separated by about 90°; contour envelopes are separated or are deeply indented in their central parts (nearly separated)
- **Polymodal to girdle-like**- three or more distinct concentrations to random distribution of points; contour envelopes are either broken up into several envelopes, are continuous around the perimeter, are continuous around a great circle, or are a combination of these patterns.

Most of the till clasts plunge in a southeast or southwest direction; however smaller groups plunging in opposite directions occur. The clast fabric data are compatible with stress from NW toward the SE, which conforms well to the alignment of the tear fault. This fabric may have also been affected by other subglacial events both prior to and after its formation. The resulting till fabric would likely be reoriented and modified with each superposed event. Till fabric modifications may take place penecontemporaneously with deposition (For example: subsequent flow during the melt-out process tends to reduce the overall fabric strength resulting in a polymodal distribution). Many till fabrics tend to be polymodal and therefore, may not plot where expected (Hicock et al., 1996).

The till fabric data of Sullys Hill is characterized by a bimodal fabric arrangement (Fig. 37). Several data concentrations occur in the northern portion of the contoured projection. Clast plunge angles varied from 6°- 70° and plunge toward the northeast or northwest. The clast orientation pattern generally reflects a northerly flow movement. The transport direction is typically associated with the orientation of the ancient depositional slope. The slope may have occurred in a cavity wall within or below the ice or on the surface of an existing glacial deposit (Boulton, 1971).

Microstructure Descriptions

Examination of thin-sections from sites 1 and 2 revealed similar microstructural results. Micromorphological descriptions follow the scheme introduced by van der Meer (1993, 1997). A glossary of micromorphological terms is provided in Table 4. The photomicrographs are also accompanied with interpretive sketches. Orientation of DLM samples (left to right) is NNE-SSE with an ice movement NW-SE. A detailed analysis

Table 4. Micromorphological terms (see van der Meer, 1987, 1993).
Glossary of terms modified from (Carr et al., 2000).

- **Plasmic fabric-** the arrangement of clay and silt-sized particles in a sample.
- **Domain-** a localized zone displaying a characteristic plasmic fabric.
- **Skelsepic-** preferred orientation of plasmic fabric around the surfaces of larger grains: indicates rolling of larger grains.
- **Lattisepic-** preferred orientation of plasmic fabric in two perpendicular orientations: commonly associated with skelsepic fabric.
- **Masepic-** preferred orientation of plasmic fabric in diffuse domains of parallel orientation: indicative of pervasive shearing.
- **Unistrial-** preferred orientation of plasmic fabric in discrete domains; indicative of discrete shears.
- **Silasepic-** randomly oriented domains of silt and clay size particles. Hardly discernable and few oriented domains. Associated with flow till microfabrics.
- **Galaxy/turbate structures-** circular alignments of grains around cores of consolidated sediment or larger grains; indicative of rotation.
- **Pressure shadows-** symmetric or asymmetric tails of material on the stoss and lee of large grains. Indicative of planar shearing (symmetric) or rotation (asymmetric).
- **Pebble type I-** arrangement of brecciated sediment such that it appears to form a series of rounded intraclasts delineated by packing voids.
- **Pebble type II-** soft sediment intraclasts of material similar in nature to the surrounding sample, but with a clearly defined discrete internal plasmic fabric.
- **Pebble type III-** soft sediment intraclasts of material different in nature to the surrounding sample: evidence of reworking of pre-existing sediments.

of microfibrils and microstructural features is presented below. Microstructural comparisons of site 1 and 2 are summarized in Table 5.

Site 1: DLM-Sample 10-06-01 and 10-06-02

In the field, the deposit appeared macroscopically homogeneous and structureless. Samples were collected a few centimeters above the till/outwash interface. At the micro-scale, no plasmic fabrics were observed at low magnifications. Weakly developed schistose plasmic fabrics only became discernable at 100x magnification (Fig. 38). The abundance of microstructures is apparent in spite of the presence of carbonate mud within the plasma (Khatwa et al., 2001). Fine-grained carbonates have been known to suppress the visibility of birefringent clay particles in thin-sections (van der Meer, 1987). Despite these factors, sharp localized domains of discrete shear lines, galaxy structures and asymmetric pressure shadows, as well as in situ crushed quartz grains indicate deposition and deformation in a high stress environment (Hiemstra and van der Meer, 1997).

The plasma represents the fine-grained area (clay to silt-sized particles) within the sediment sample. The larger particles or fragments are typically embedded within the plasma. The texture of the plasma has a dense and isotropic but grainy (fine silty) character. In addition, the grain-shape distribution displays evidence of edge rounding

Table 5. Comparison of microstructures formed during sediment flow and subglacial deformation. The occurrence of many microstructures suggests formation in disparate environments.

Microstructures	Gravity flow till Sullys Hill, ND	Subglacial till DLM, ND
Pressure shadows		X
Galaxy/turbate structures	X	X
Shears		X
Haloes	X	X
Till Pebble type II	X	X
Sigmoidal grains		X
Plasma Fabrics	X	X
Crushed grains	X	X
Dewatering and water-escape structures	X	X

NNE

SSE

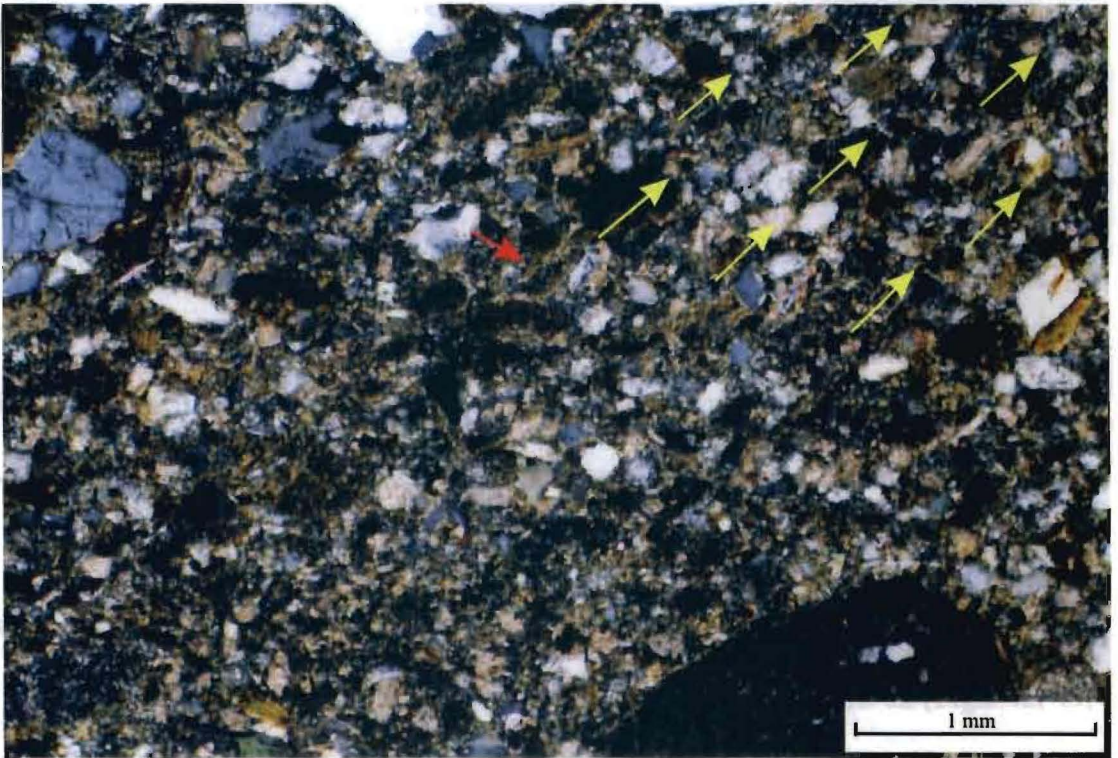


Figure 38. Weakly developed skelsepic plasmic fabric (oriented domains are parallel to surface of skeleton grains-red arrow) as a result of rotation in sample 10-02-01. Note the SSE oblique grain fabric depicted by yellow arrows. Scale bar indicates approximately 1 mm.

and abrasion, with smaller grains formed as “flakes” removed from larger clasts (Fig. 39) (Carr, 2001). Sample 10-02-01 (Fig. 40) displays a fractured and crushed quartz grain. This type of abrasion is the result of shear loading of grain contact surfaces (Hiemstra and van der Meer, 1997).

Rotational elements have been characterized in deforming till beds (van der Meer, 1993, 1997). Pebble type II structures have been observed (Fig. 41) in sample 10-06-02. This till pebble type is attributed to the marble-bed structure described by van der Meer (1993; et al. 1994). Pebble type II structures possess an internal plasmic fabric. This structure is believed to have formed under more plastic conditions than the pebble type I structure, which is devoid of an internal plasmic fabric. It must be assumed that the pebble type II structures formed in response to isolated rotational movements throughout the deforming layer.

Galaxy structures were detected in samples 10-06-01 and 10-06-02 (Figs. 42, 43, 44 and 45). These features consist of spirals of fine-grained particles that surround a core stone or stiff matrix. The tips of the fine-grained spirals generally extend out from the core stone. Typically, only the circular arrangement of the finer particles around a core stone or matrix is discerned in 2-D thin sections.

An indicator of rotational movement due to shearing is the pressure shadow (Figs. 46-50). Pressure shadows develop due to competency differences in the deforming till mass (Hart and Boulton, 1991). Typically, rigid particles within a less competent matrix encourage pressure shadow development. These shadows form in areas of lower pressure adjacent to a rigid body during progressive simple shear (Fig. 48).

NNE

SSE

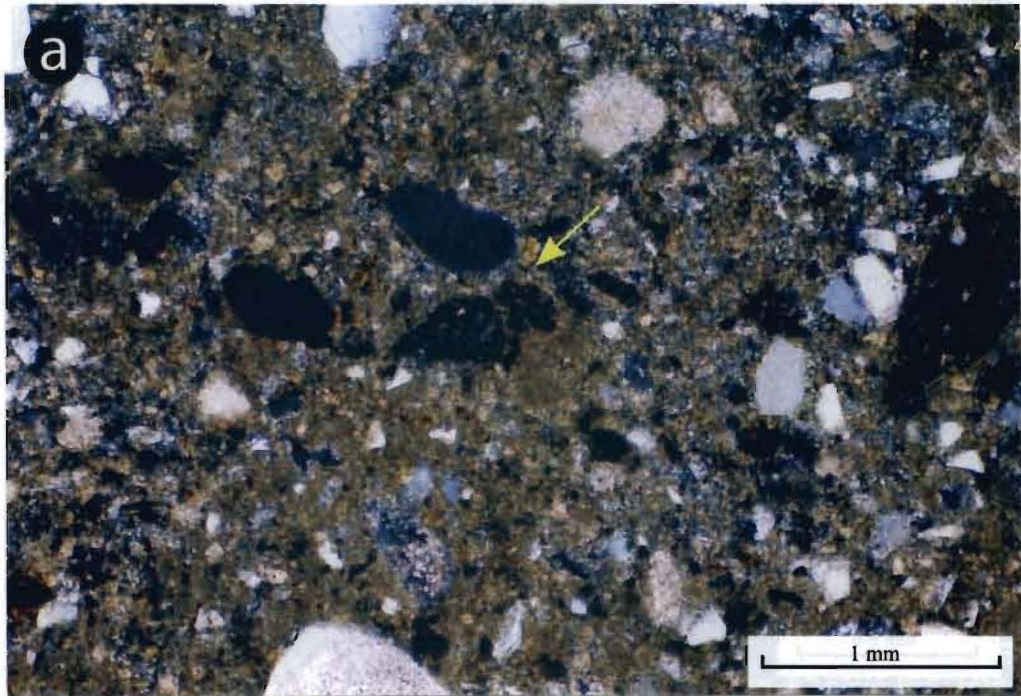


Figure 39 (a, b). Photomicrograph and accompanying sketch of sample 10-02-01. This sample depicts a sheared intraclast (till pebble). Note the juxtaposed grains and their alignment (yellow arrow). Scale bar indicates approximately 1 mm.

NNE

SSE

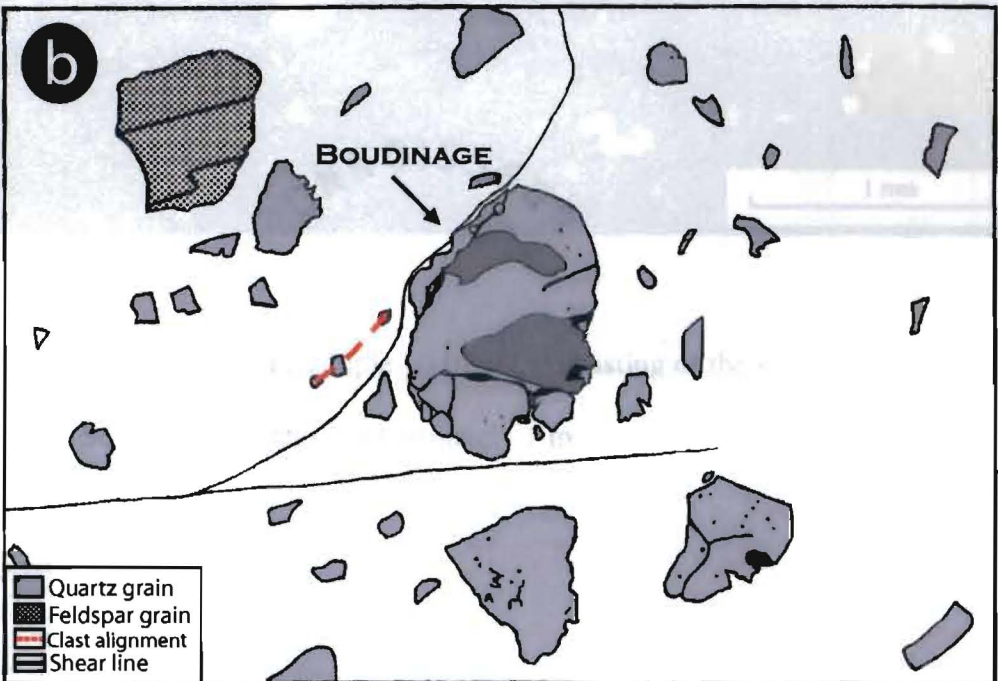
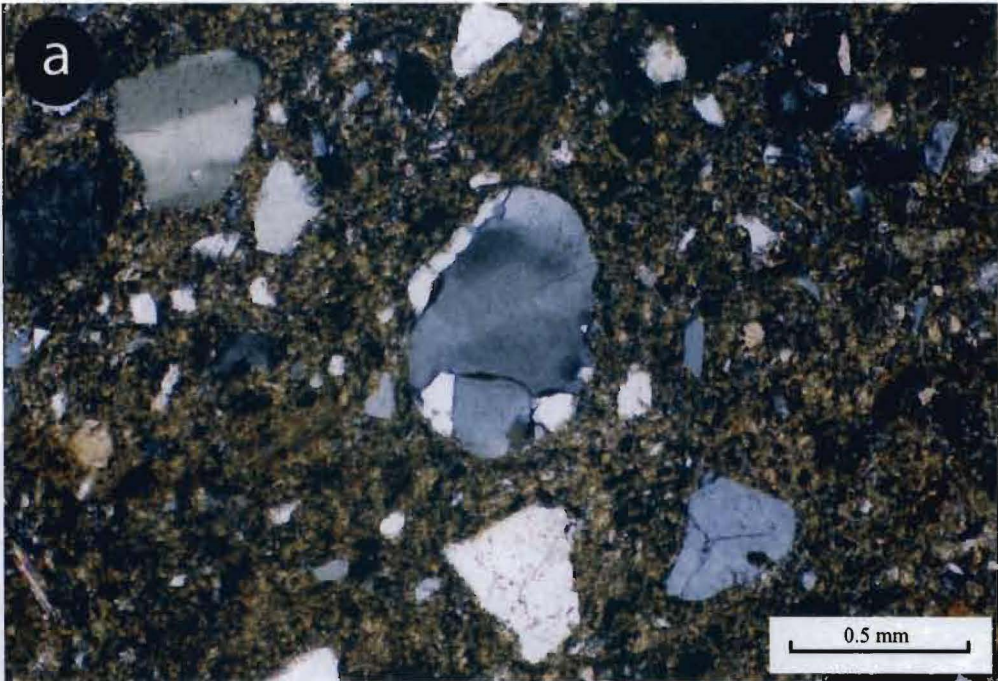


Figure 40 (a, b). Crushed quartz grain with boudinage. The boudinage in the upper part of the grain is ascribed to tangential grain-contact sliding.

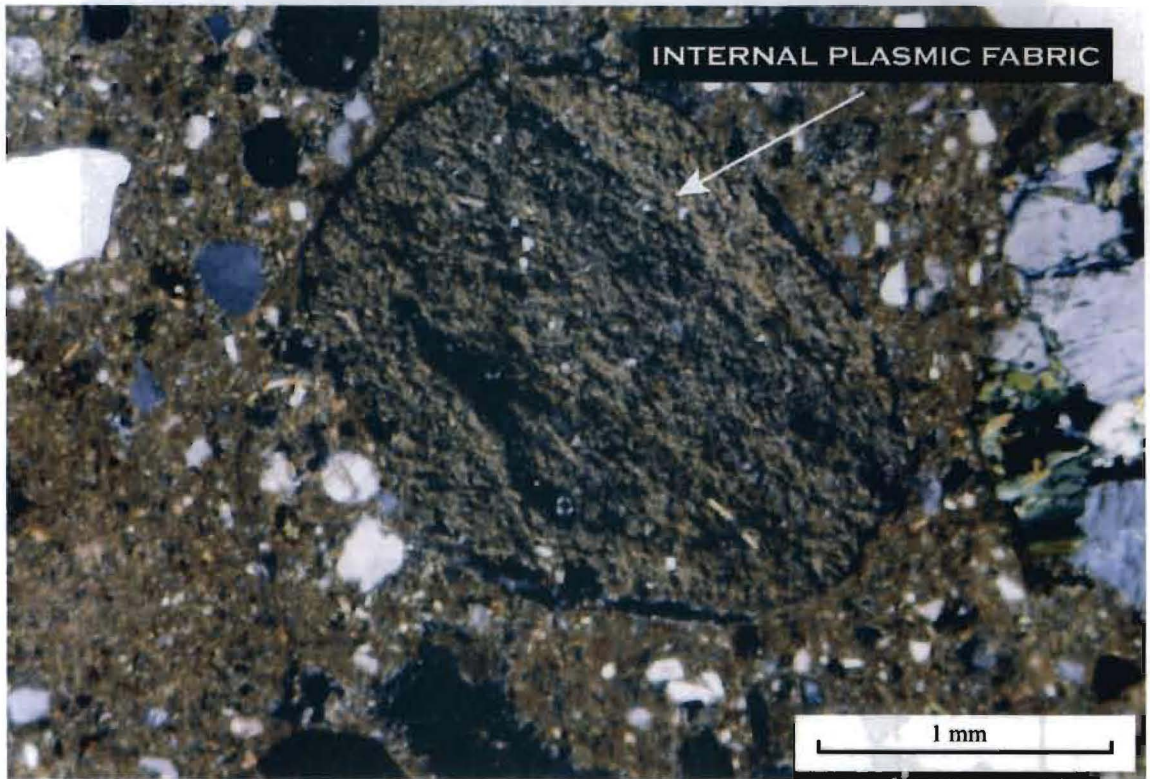


Figure 41. Pebble type II in sample 10-02-02, consisting of the same material as the host sediment. Scale bar indicates approximately 1 mm.

NNE

SSE

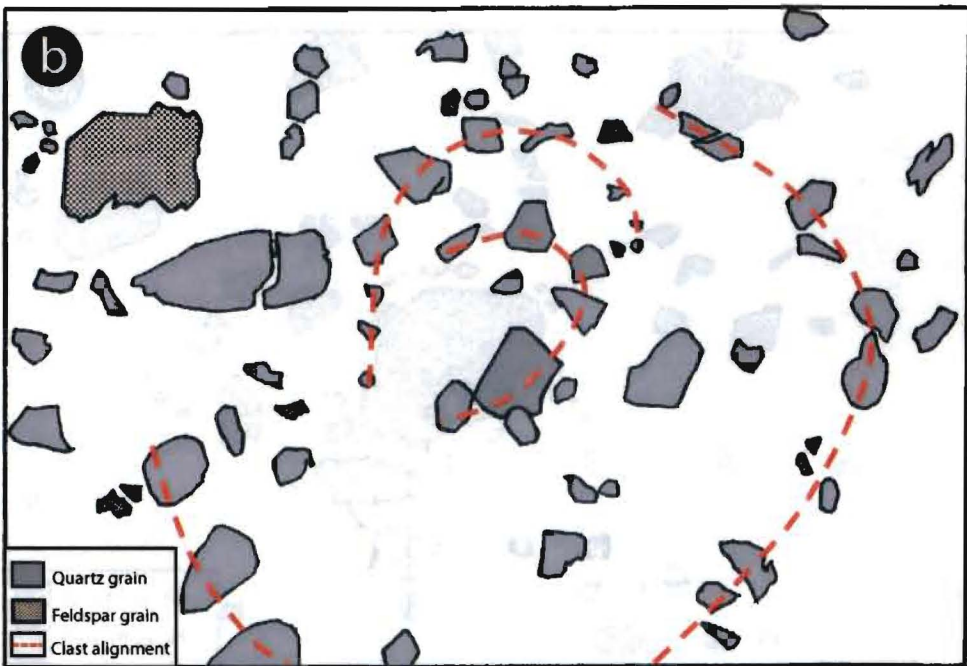
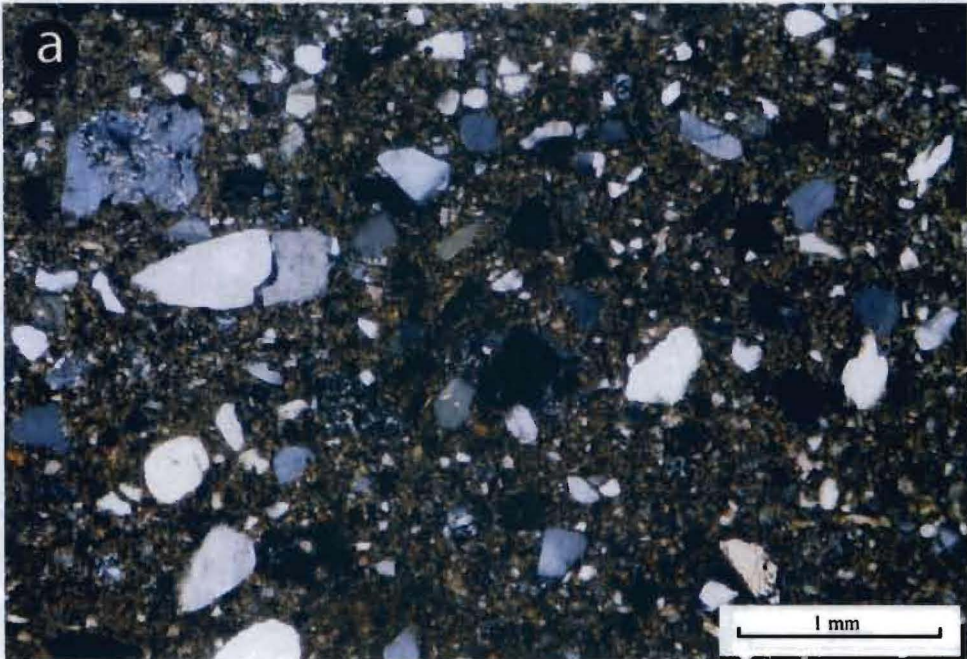


Figure 42 (a, b). Sample 10-02-01, depicts a galaxy structure with a stiff matrix acting as the core stone. Despite the galaxy structure, there is no plasmic fabric development. Only at larger magnifications a very weak skelsepic plasmic fabric becomes discernable. Scale bar indicates approximately 1 mm.

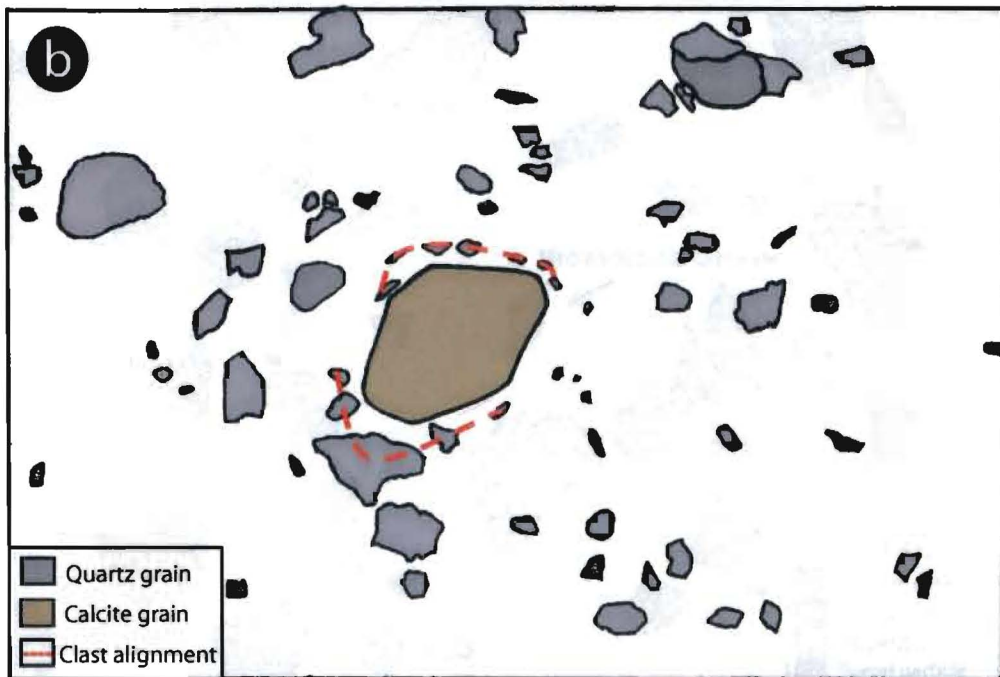
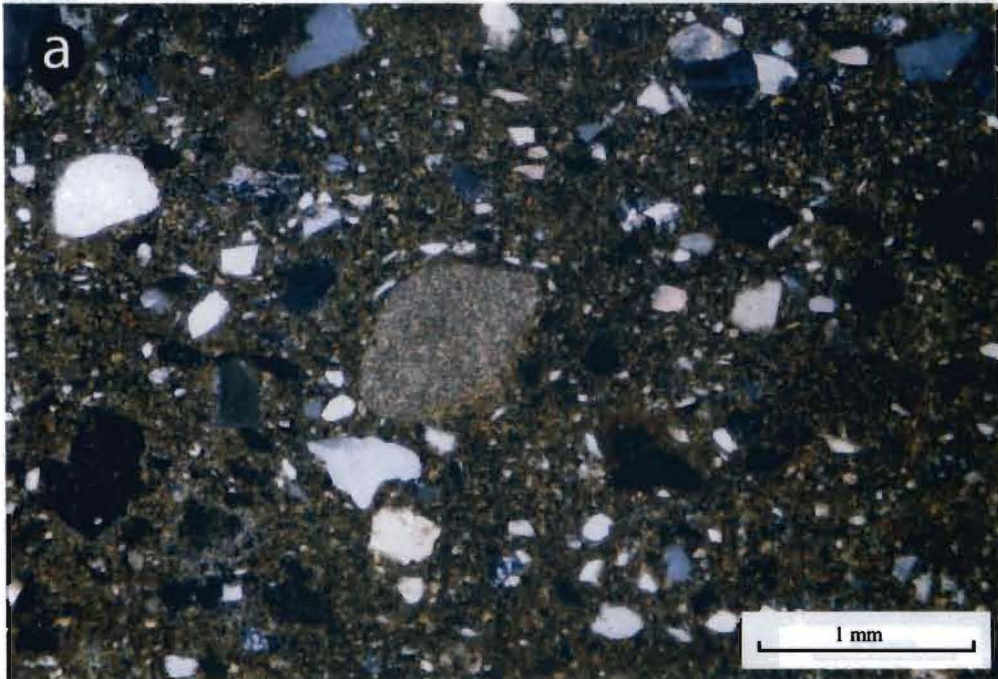


Figure 43 (a, b). Detail of sample of 10-02-02, demonstrates a galaxy structure with a carbonate grain acting as the core stone. Note the fine quartz grains encircling the carbonate grain.

NNE

SSE

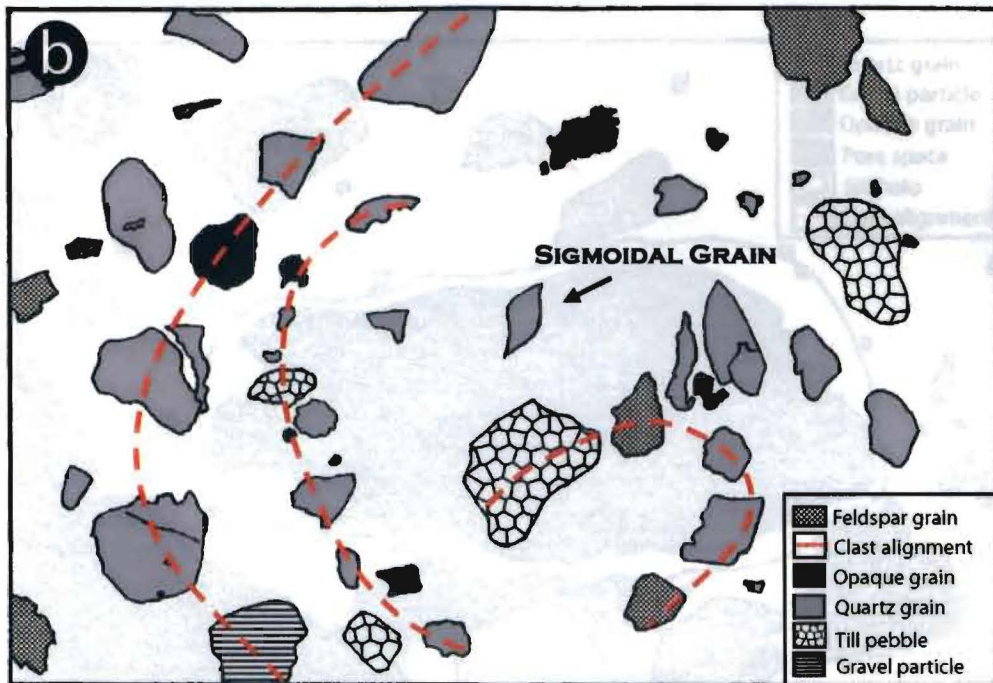
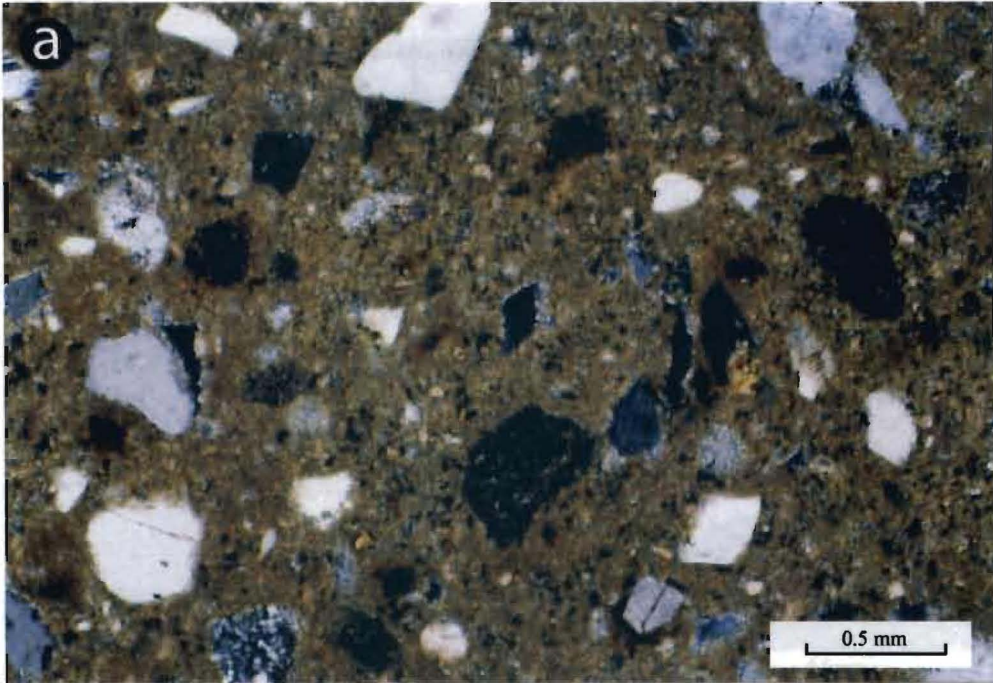


Figure 44. Detail of sample 10-02-01, depicts a well developed galaxy structure (red dashed lines). Note the sigmoidal shaped quartz grain in center of photomicrograph.

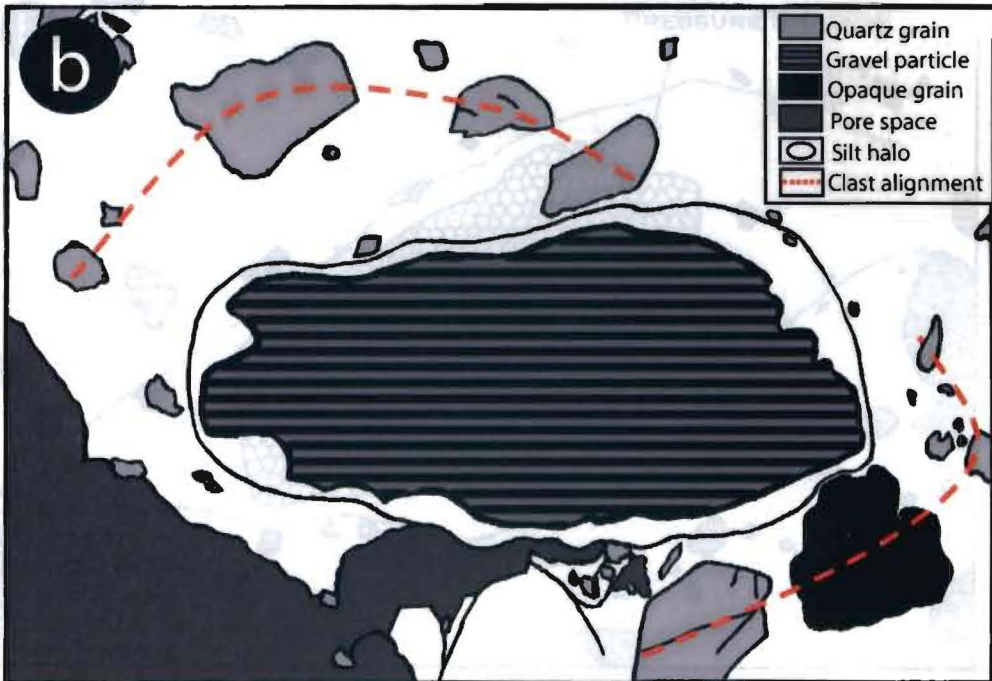
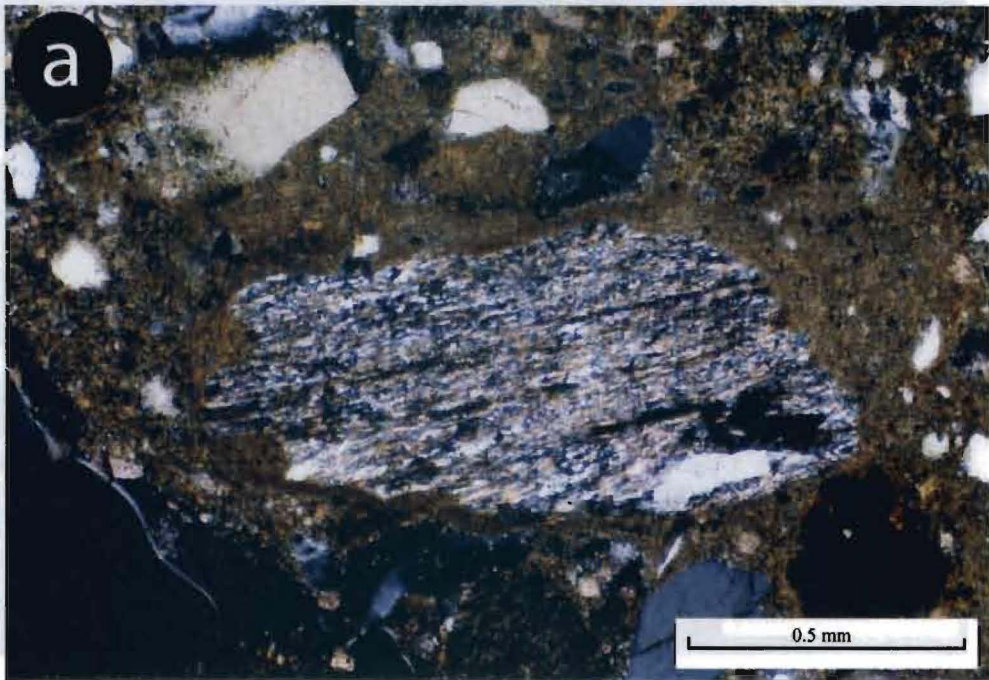


Figure 45 (a, b). Detail of sample 10-02-01, depicts a small gravel particle in its rounded casing of fines. The halo of fine grains exemplifies the scavenging process during rotational movement.

NNE

SSE

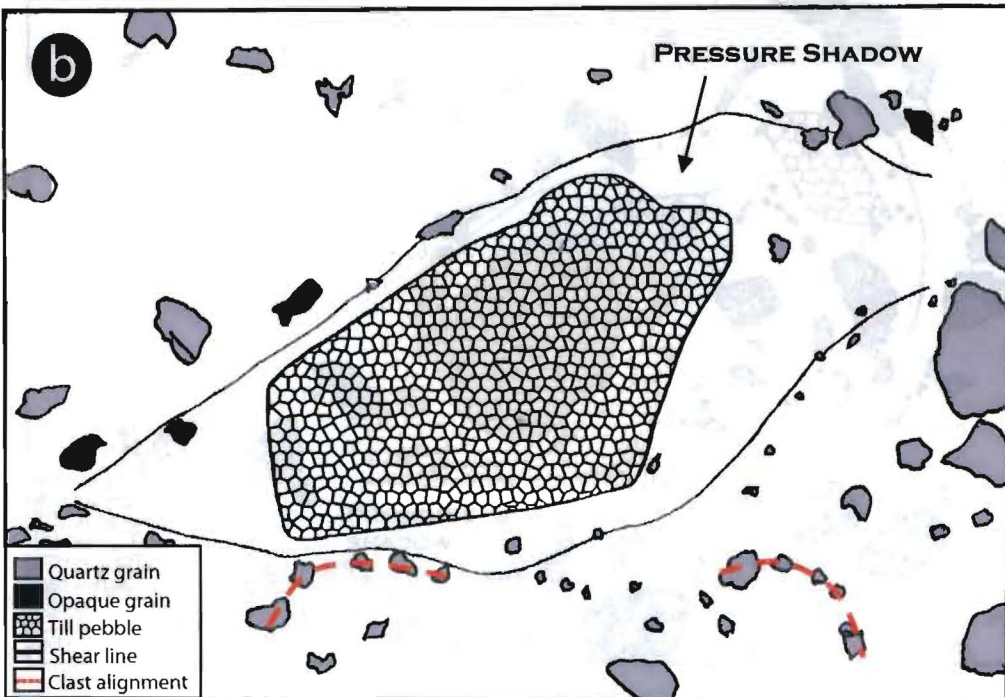
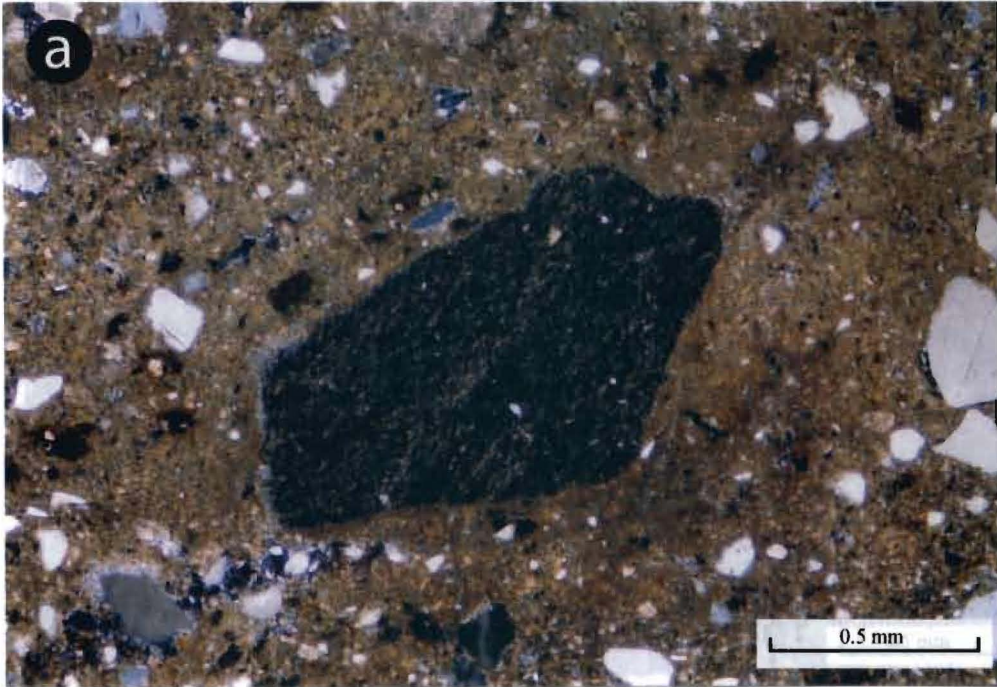


Figure 46 (a, b). Detail of sample 10-02-02, shows a faint asymmetric pressure shadow. Note the rotational structures (red dashed lines) and their occurrence to the shear lines.

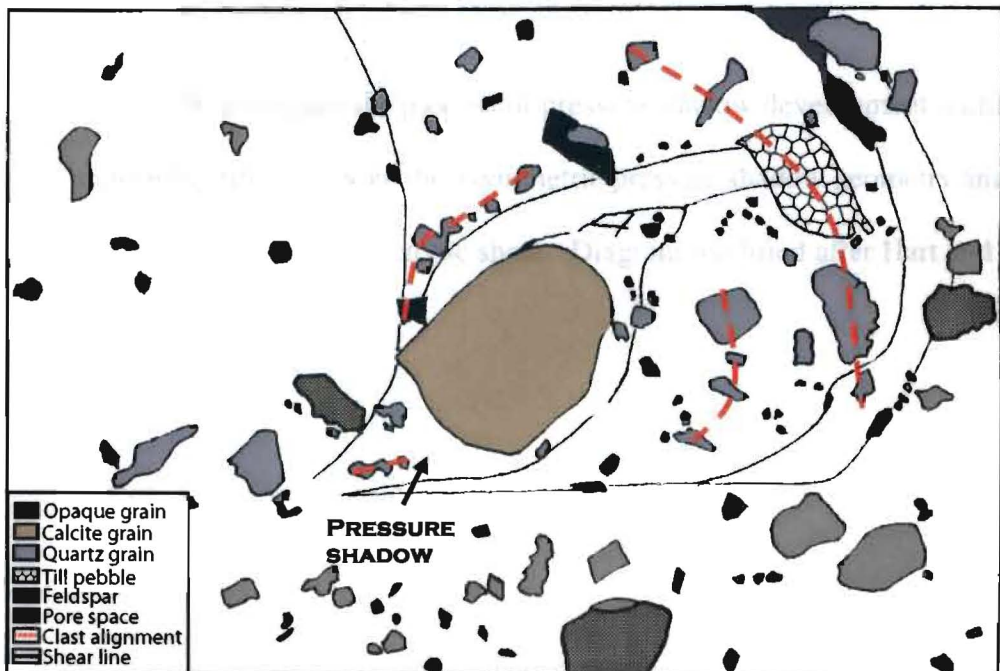
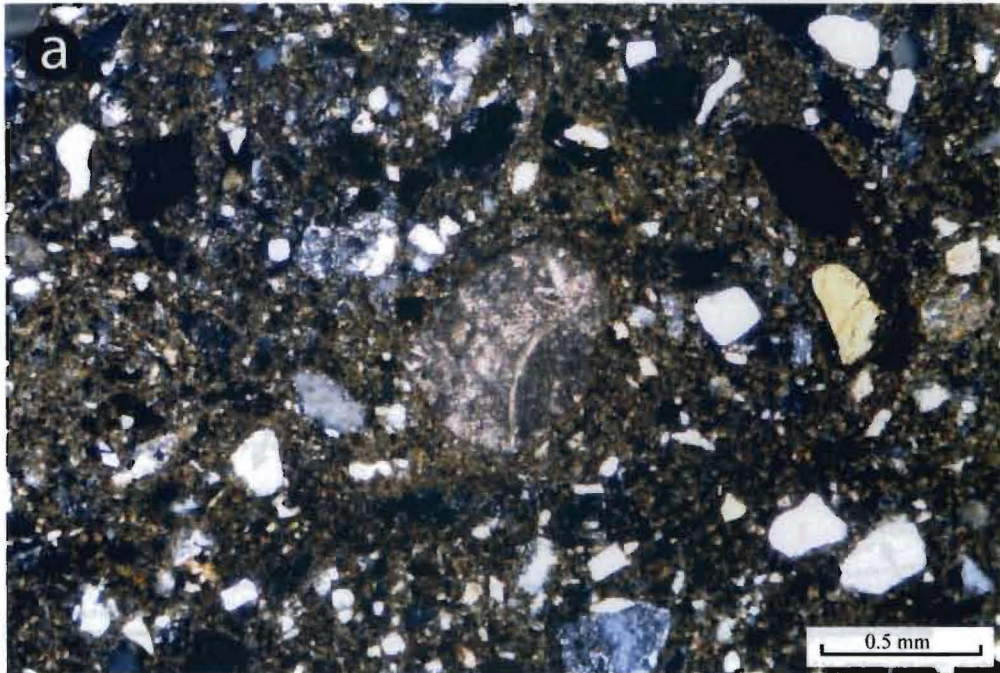


Figure 47 (a, b). Sample 10-06-02 from DLM, shows triangular extensions to a small carbonate grain. This structure is known as a pressure shadow and is clearly related to shear. Note the discrete shear lines and rotational structures.

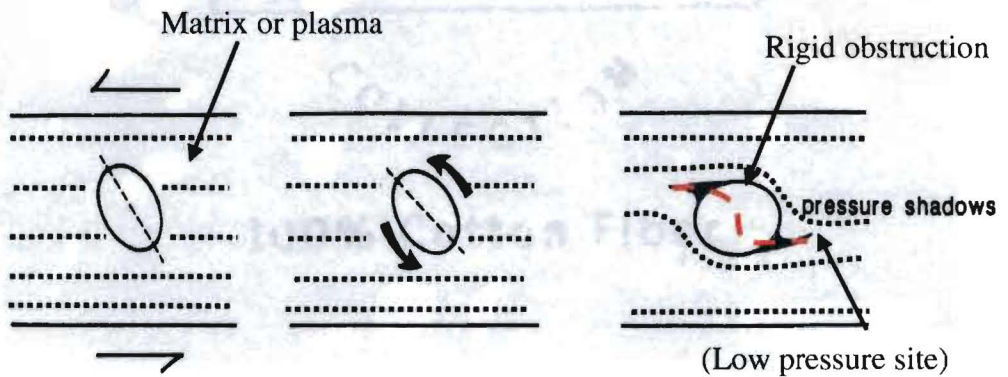


Figure 48. Illustrates the process of pressure shadow development within a deforming till bed. Note the asymmetric pressure shadow geometry and the rotational direction of tectonic shear. Diagram modified after Hart and Boulton (1991, Fig. 5).

NNE

SSE

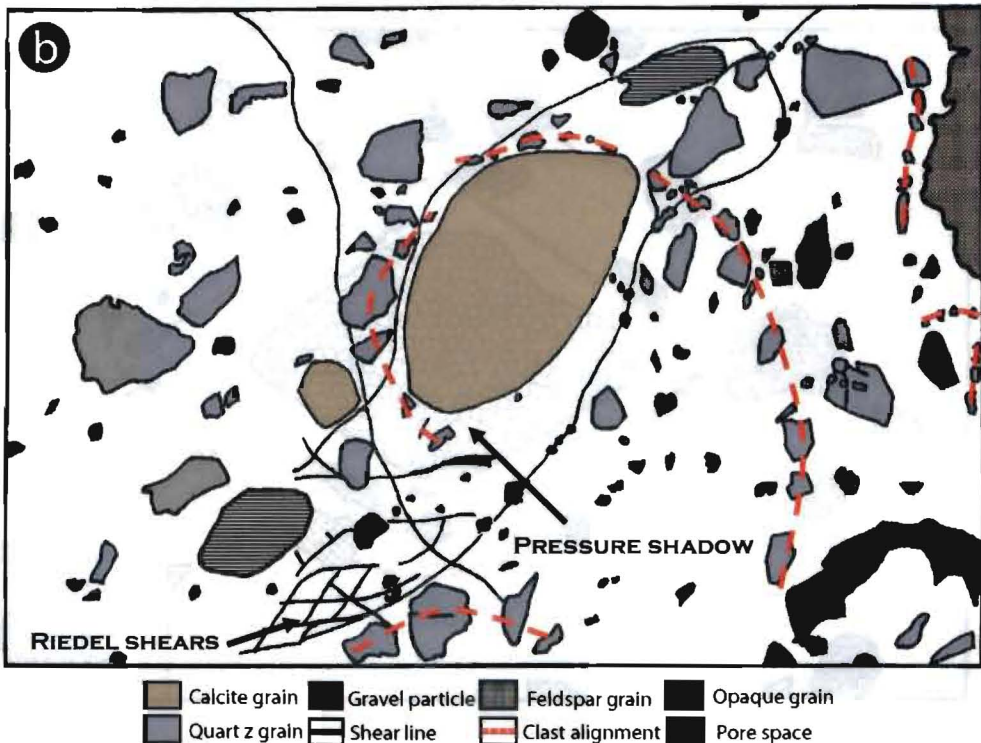
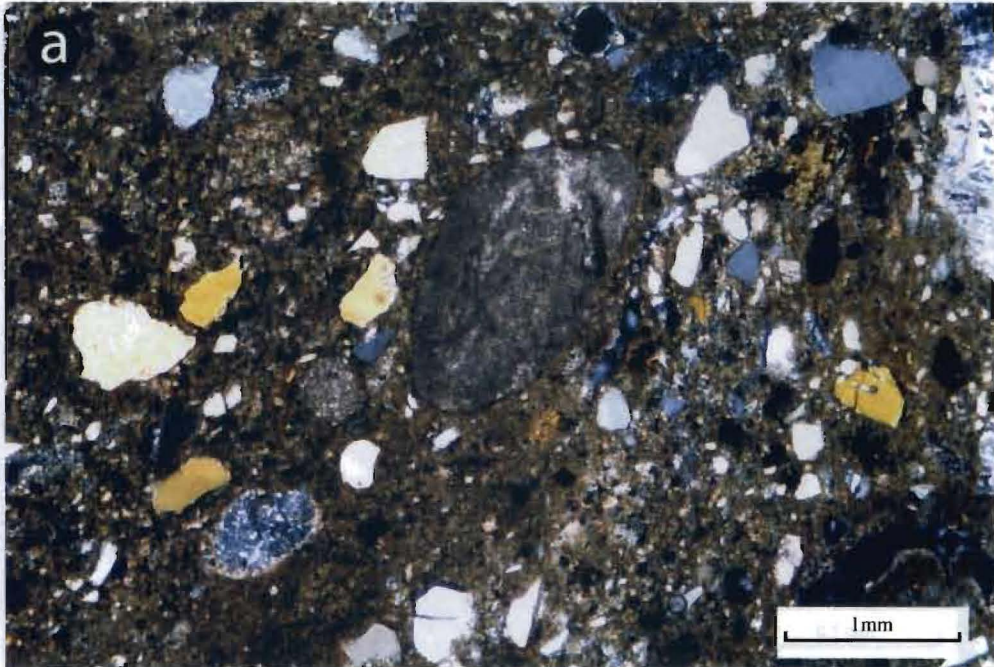


Figure 49 (a, b). Detail of sample 10-02-01, denotes a faint asymmetric pressure shadow. Note the presence of discrete shears (black lines) and galaxy structures (red dashed lines).

NNE

SSE

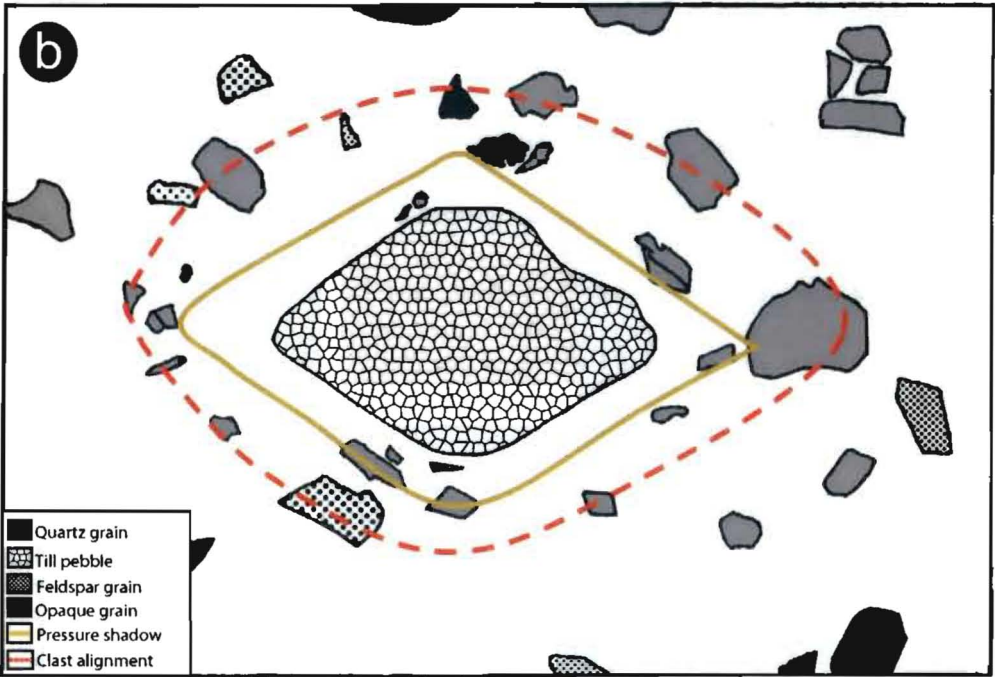
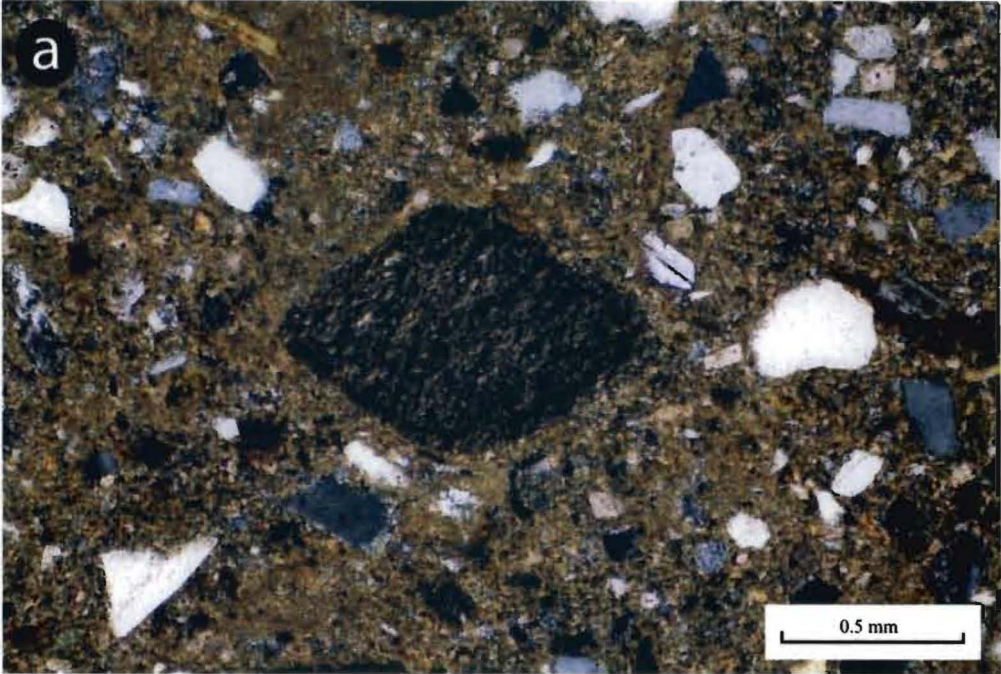


Figure 50. Detail of sample 10-02-01, displays a symmetrical pressure shadow (gold line). Note the galaxy structure (red dashed lines) around the core stone.

The orientation of the shadows or tails are utilized to interpret the relative movement within the till bed. In most of the observed cases the actual tails are not so clearly defined which leads to obscured results. Boudins have also been observed in sample 10-06-02 (Fig. 51). These form when a competent layer within a less competent matrix is stretched (Hart and Boulton, 1991). The less competent material (matrix) tends to stretch in a ductile fashion around the stronger more competent layers.

Planar movements have also been identified in the form of parallel discrete shears and sigmoidal shaped grains. Fig. 52 displays a sheared intraclast with a sigmoidal shaped geometry. This geometry exemplifies the mechanics of a shear zone, where the greatest principal stress (σ_1) becomes parallel to the shear zone boundaries. Evidence of discrete shear lines is exhibited in Figure 53.

Site 2: Sullys Hill-Samples 10-06-03, 10-06-04, 10-06-05, and 10-06-06

In the field the sediment flow deposit was underconsolidated and texturally heterogeneous. Samples 10-06-03 and 10-06-04 were collected on the eastern end of the synform at approximately 1.5 m depth and samples 10-06-05 and 10-06-06 were collected on the western edge at a depth of approximately 0.5 m. All the samples were characterized by a wide variety of grain sizes. However, the larger grains tend to be better rounded than the smaller grains (Fig. 54). Sample 10-06-03 consisted of an oblique grain fabric (Fig. 55). A weakly developed, skelsepic fabric was also evident in sample 10-06-03. The rest of the samples displayed a silasepic plasmic fabric. Many of the samples showed a high abundance of irregular pore spaces (Figs. 56, 57). All samples contained till pebble type II structures. In sample 10-06-04, illustrates the early

NNE

SSE

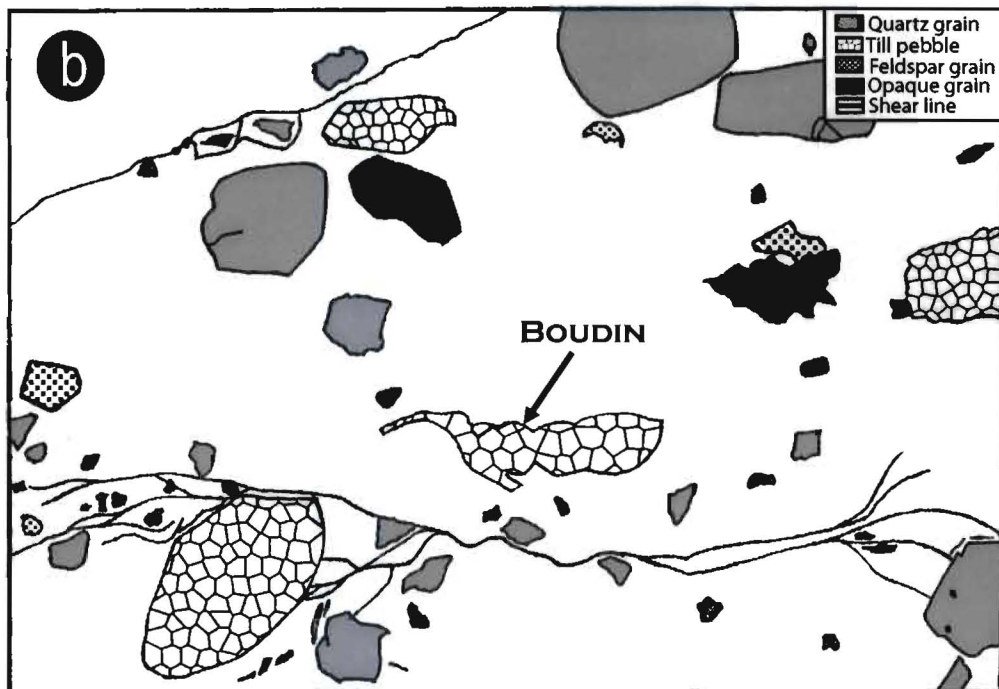
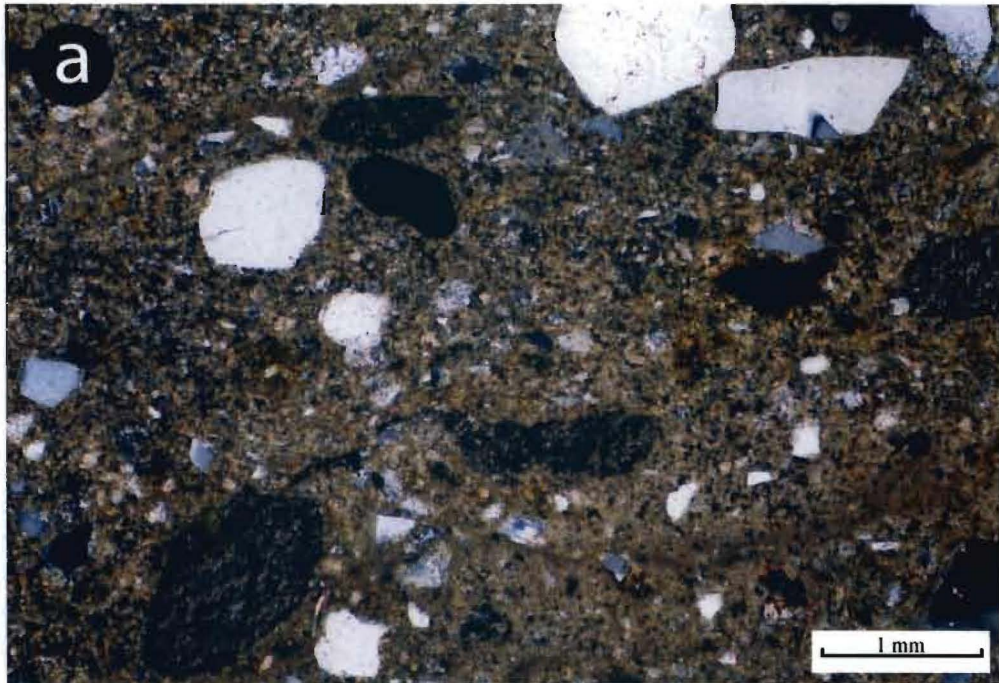


Figure 51 (a, b). Sample 10-06-02 demonstrates deformation by boudinage of an intraclast. Note the anastomosing shear zones in the upper left and lower right corners of the photomicrograph.

NNE

SSE

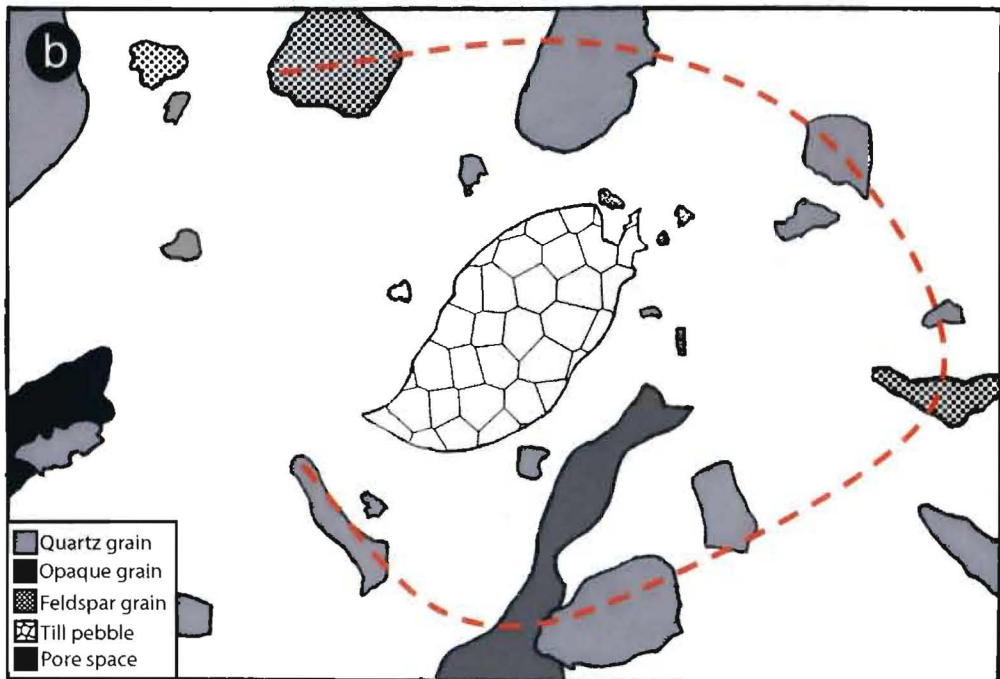
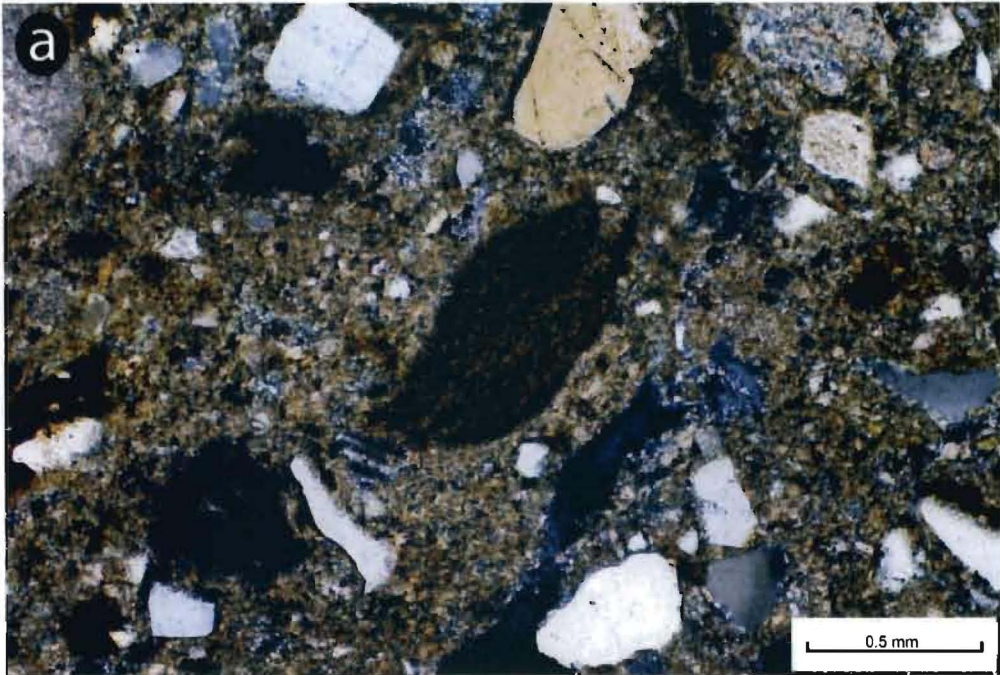


Figure 52 (a, b). Sample 10-02-01 displays a sheared intraclast. Note the distinct sigmoidal geometry and galaxy structure (red dashed line) surrounding the intraclast.

NNE

SSE

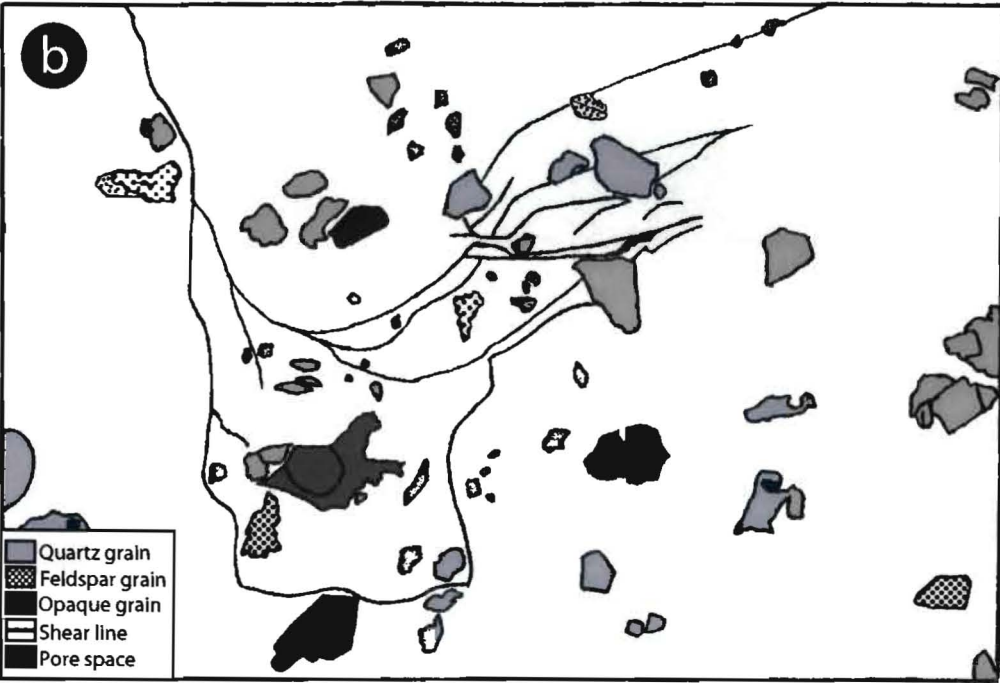
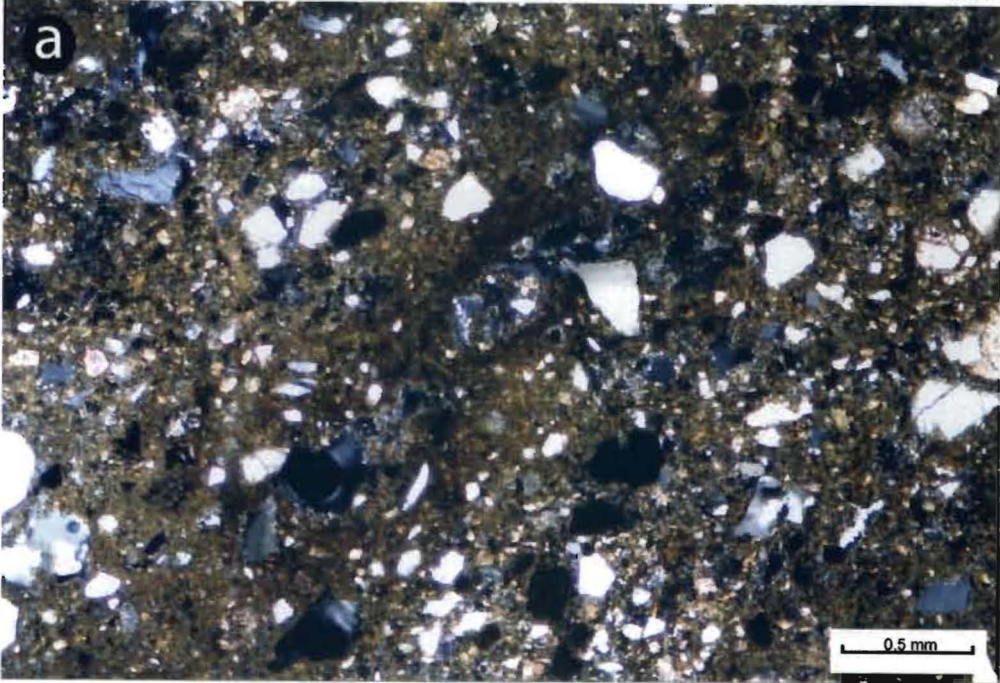


Figure 53 (a, b). Sample 10-02-01 shows a complex network of discrete shears.

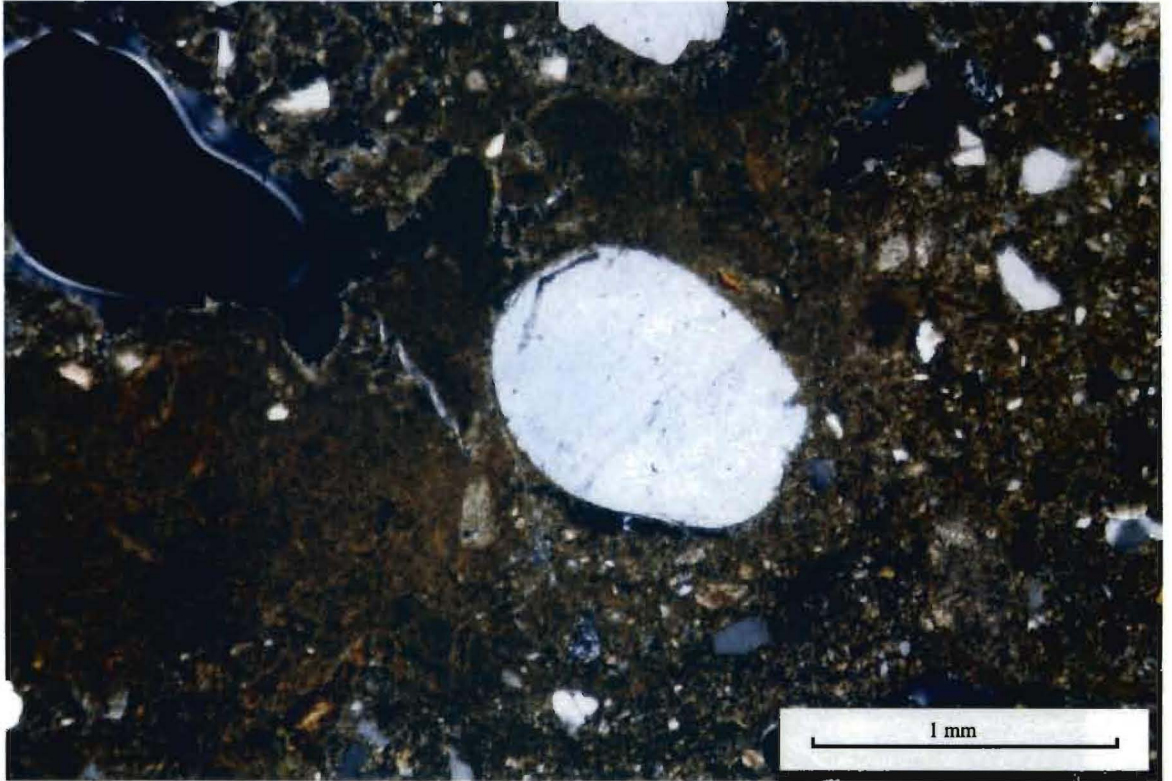


Figure 54. Detail of sample 10-06-06, depicts a well-rounded quartz grain reflecting minimal edge rounding. Note the subtle ring crack at the edge of the grain.

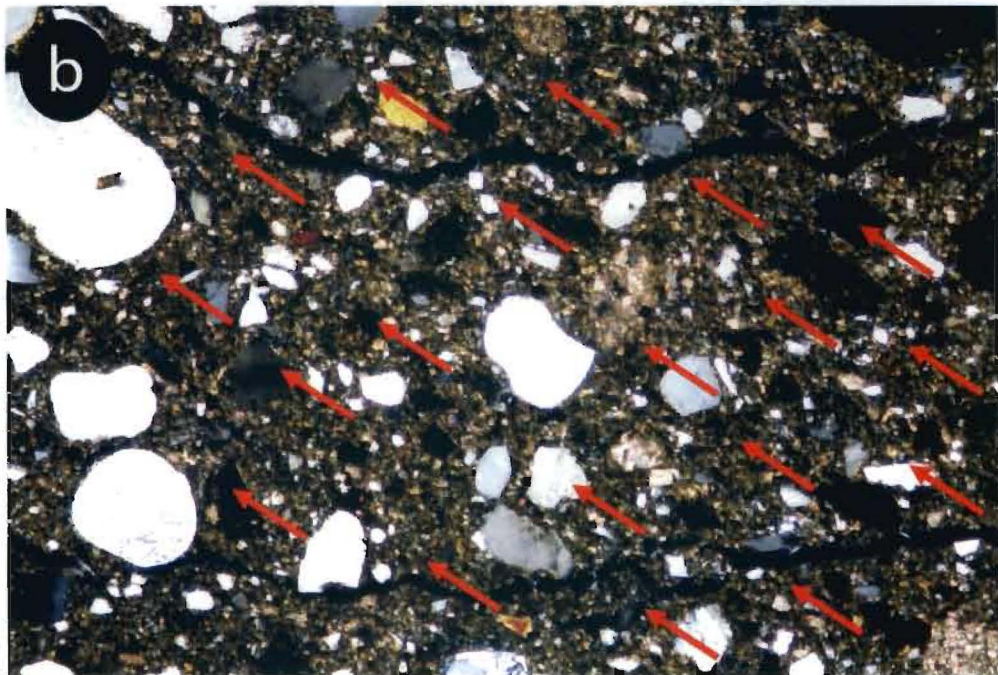
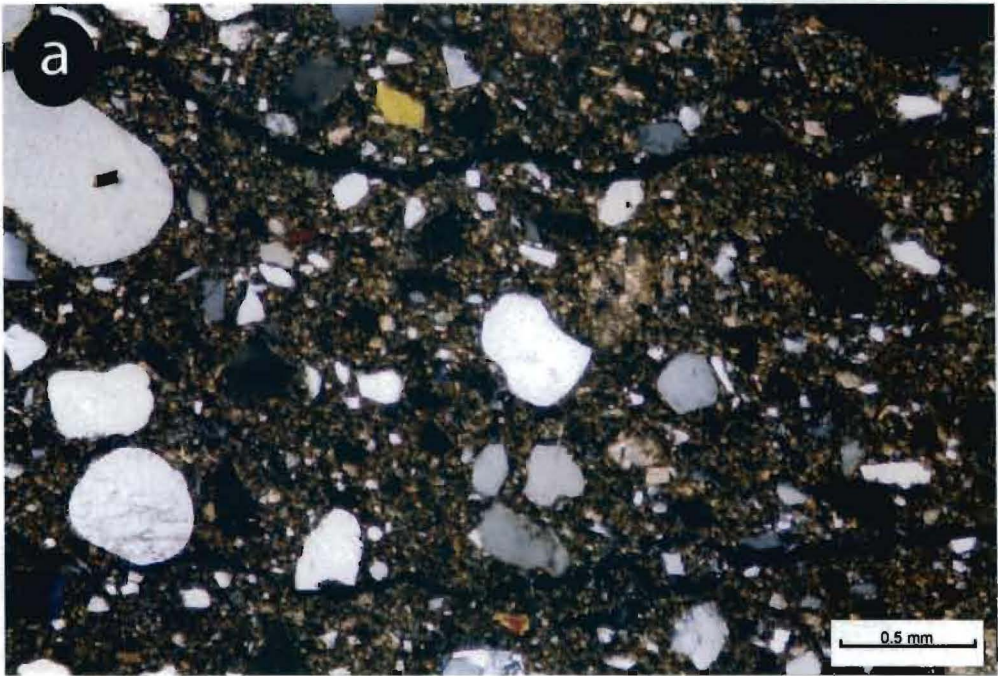


Figure 55 (a, b). Detail of sample 10-06-03, shows an oblique grain orientation and a weakly developed skelsepic plasmic fabric. Red arrows indicate direction of sediment flow.

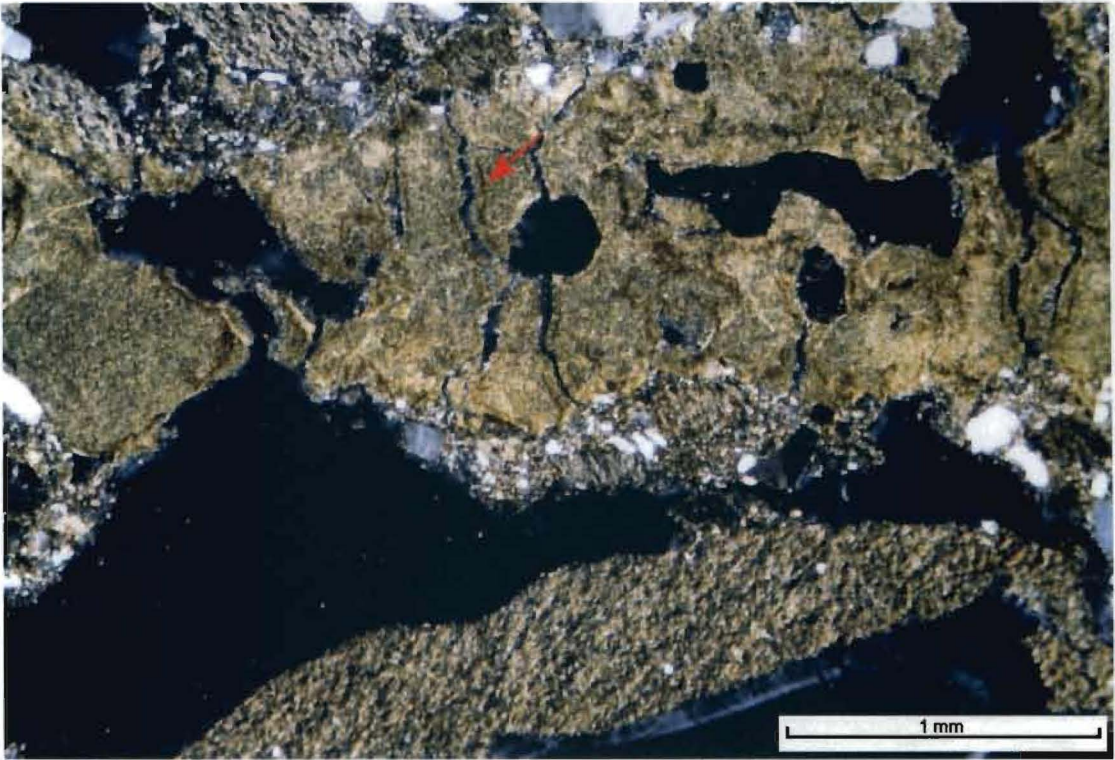


Figure 56. Detail of sample 10-06-04, depicts a network of pore spaces (black). Note the iron oxide banding along the sub-vertical pore spaces (location of red arrow).

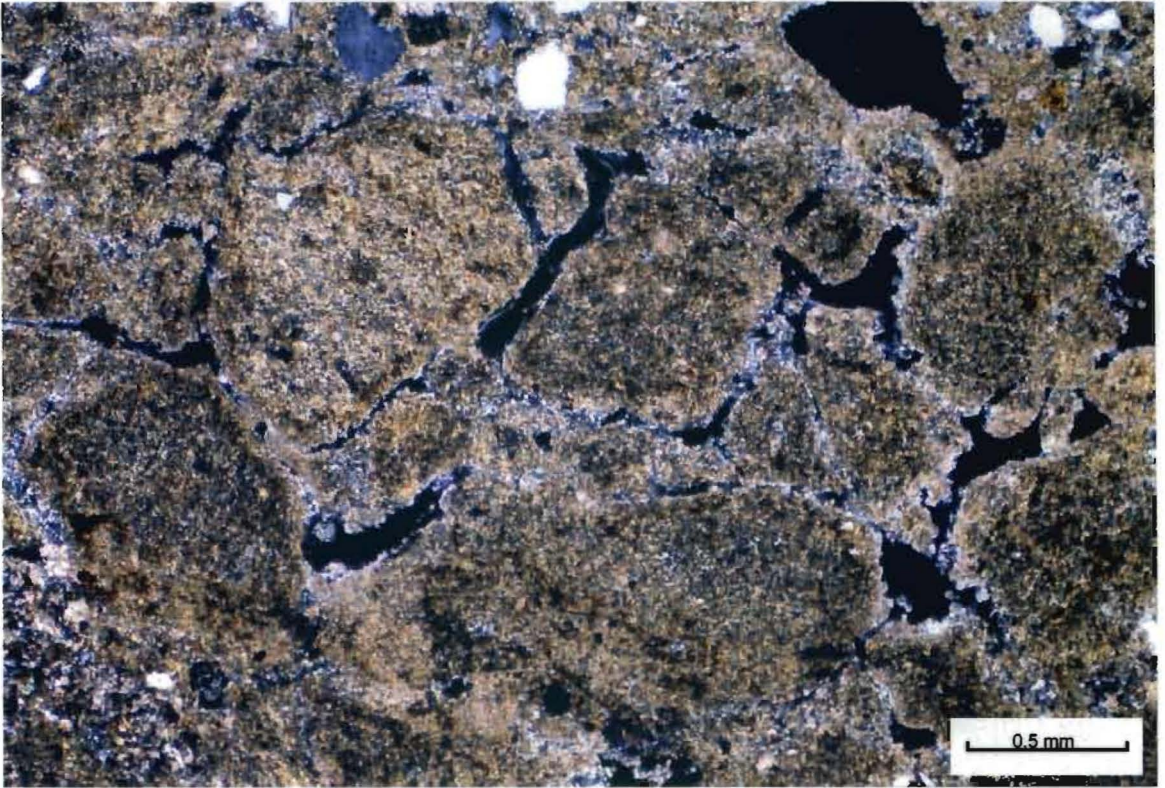


Figure 57. Detail of sample 10-06-04, shows bifurcating pores (black) and till pebble type I development.

stages of pebble type II development (Fig. 58). In addition, evidence of reworking of till pebbles can be seen in Figure 59. Rotational evidence has been discerned in most of the samples, and well developed galaxy structures were present in samples 10-06-06 and 10-06-05 (Figs. 60, and 61).

Computer Modeling and Remote Sensing

Glacial geomorphic observations were made by analyzing three-dimensional views of Devils Lake Mountain and Sullys Hill using ArcScene™ Geographic Information System (GIS) software. Color orthophoto quadrangles were draped over 30-meter digital elevation models. The 3-D views of DLM revealed a well-preserved glaciotectonic landscape (Figs. 62, 63). The DLM fault lineament was also examined (Fig. 64). An oblique view of Sullys Hill is depicted in Figures 65 and 66. The glacial landform assemblage of Sullys Hill consists of spillway valleys, kame deposits, kettle depressions and ice disintegration features. The imprint left on the landscape reflects considerable reworking of large volumes of glacial meltwater. The Big Coulee Spillway Valley south of the kame deposit in Fig. 66 illustrates the erosional impact of meltwater discharge. Blimp aerial photography and satellite imagery are presented in Figures 67 and 68.



Figure 58. Detail of sample 10-06-04, depicts the early stages of till pebble type II development. Note the subsurface accumulation of iron (red arrow) and the translocation of clay (black arrows). Clay concentrations occur along grain bridges and around pore spaces. Red dotted line indicates lithologic boundary.

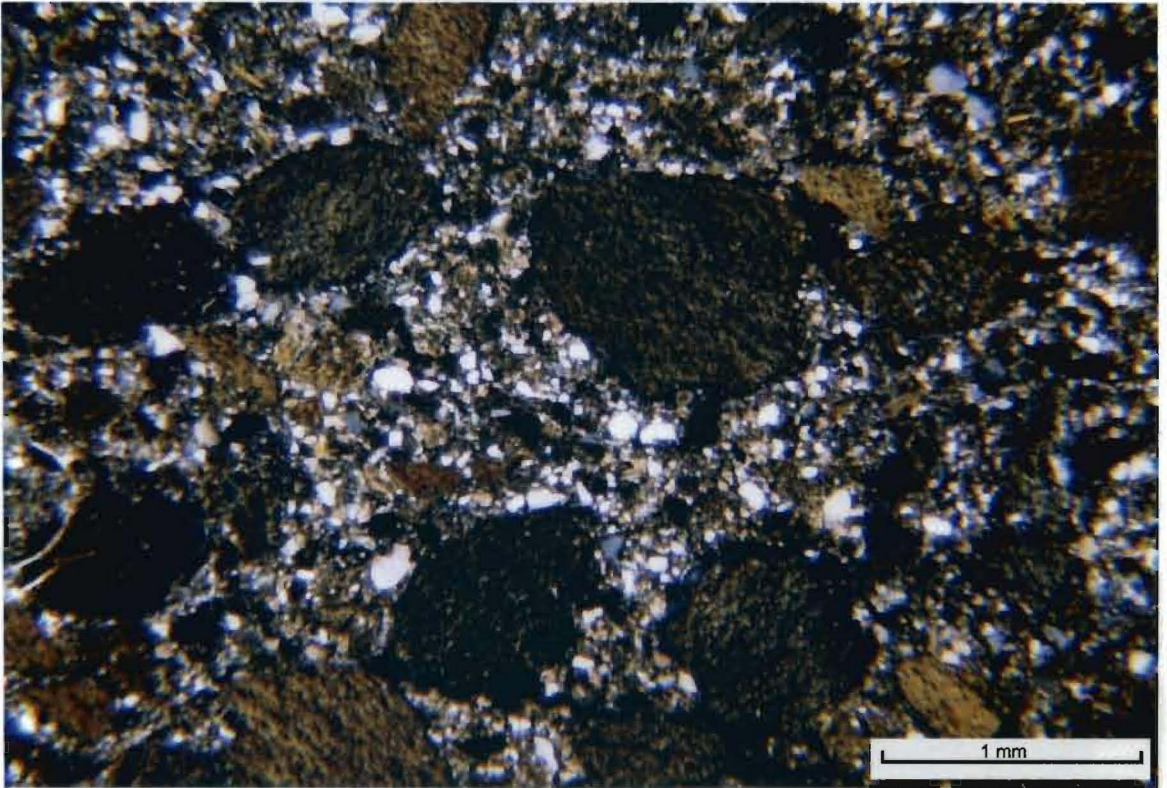


Figure 59. Detail of sample 10-06-05, denotes pebble type III incorporated within a different host sediment. Note the inhomogenous host sediment and well-developed internal plasmic fabrics of the till pebbles.

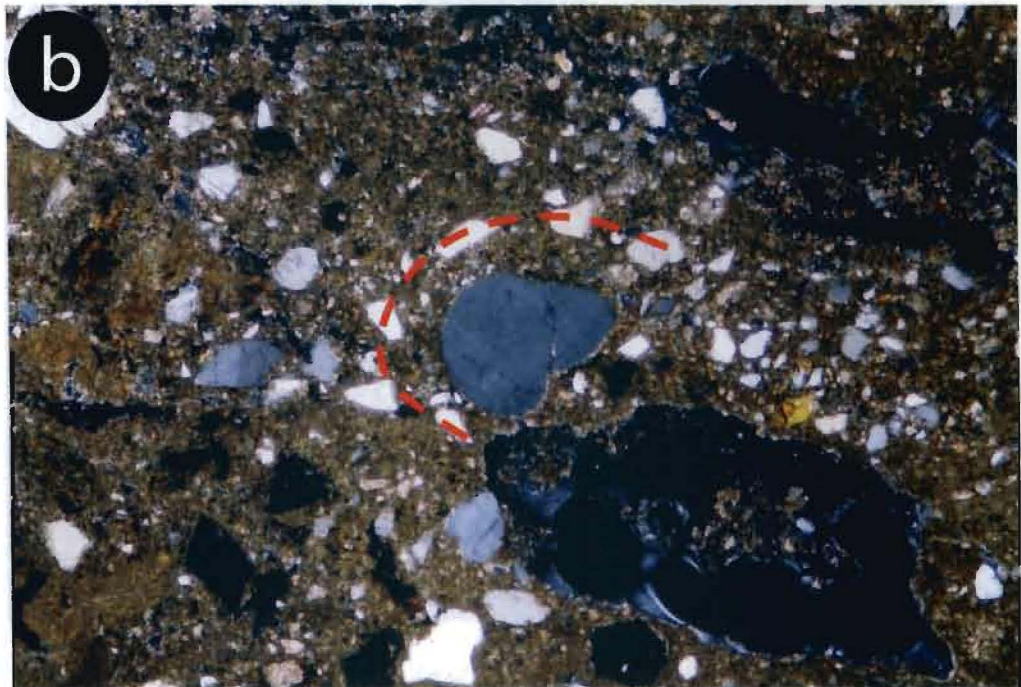
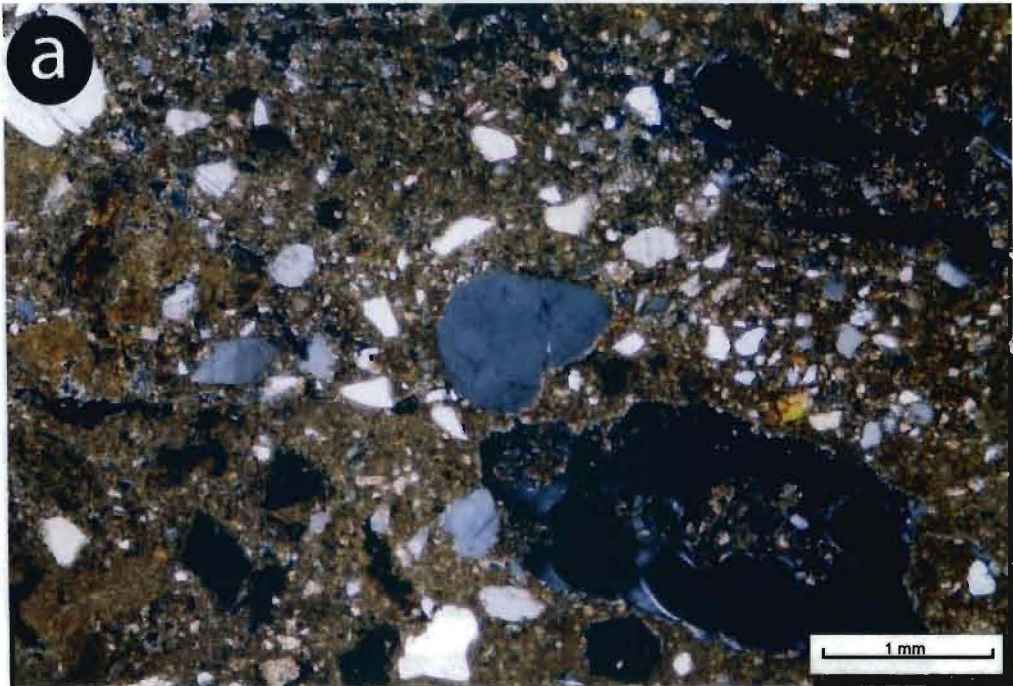


Figure 60 (a, b). A well pronounced galaxy structure (red dotted line) from sample 10-06-06. Note the subangular grains surrounding the well rounded core stone. Scale bar indicates approximately 1 mm.

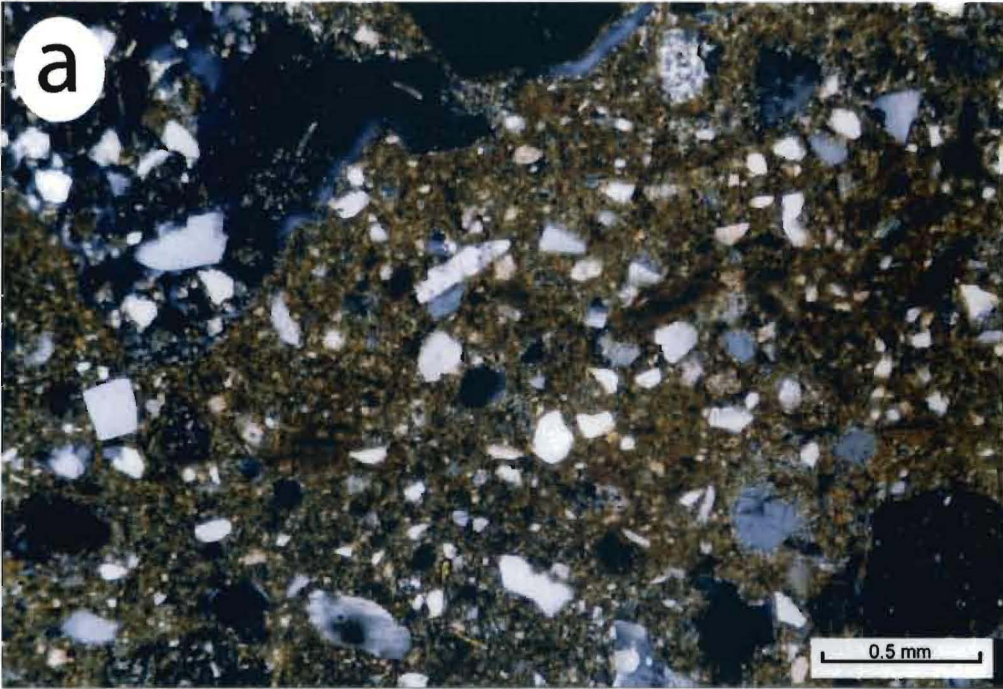


Figure 61 (a, b). Detail of sample 10-06-06, shows a rounded pattern of quartz grains surrounding several stiff matrices. Red arrows indicate location of plant fragments.

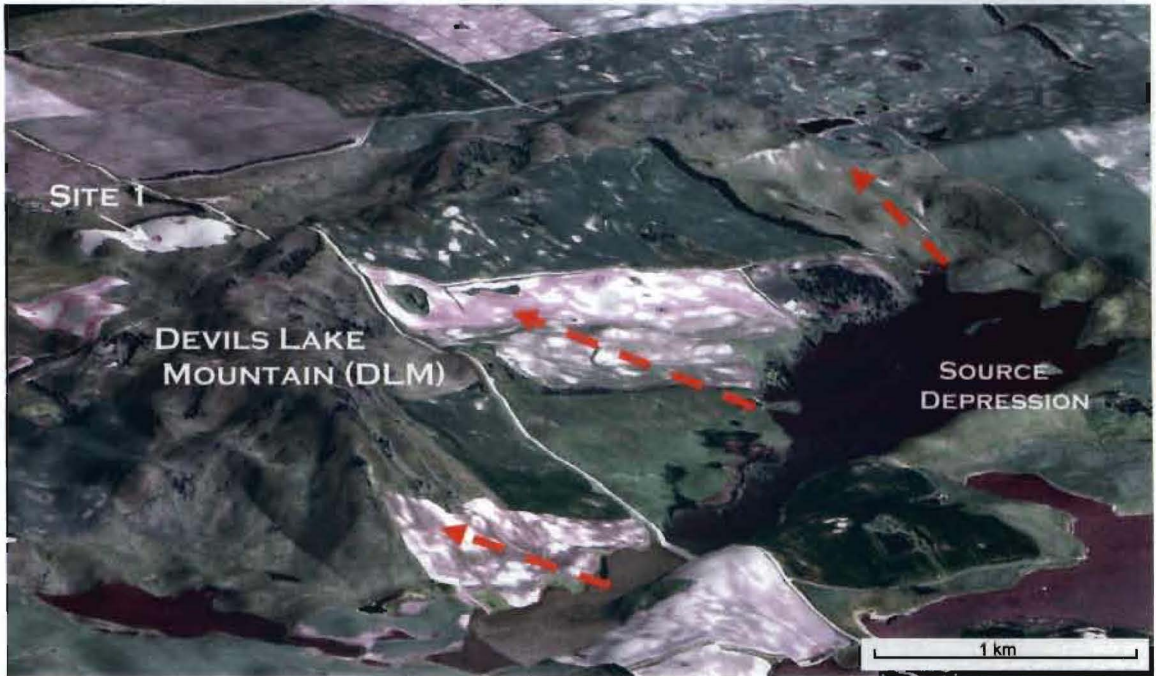


Figure 62. Oblique view of Devils Lake Mountain. Note the relative positions of source depression and ice-shoved mass. Arrows indicate a SSE ice-flow movement. View toward the SSW. Vertical exaggeration 7x. DEM acquired from the United States Geological Survey. Color orthophoto provided by North Dakota State Water Commission.

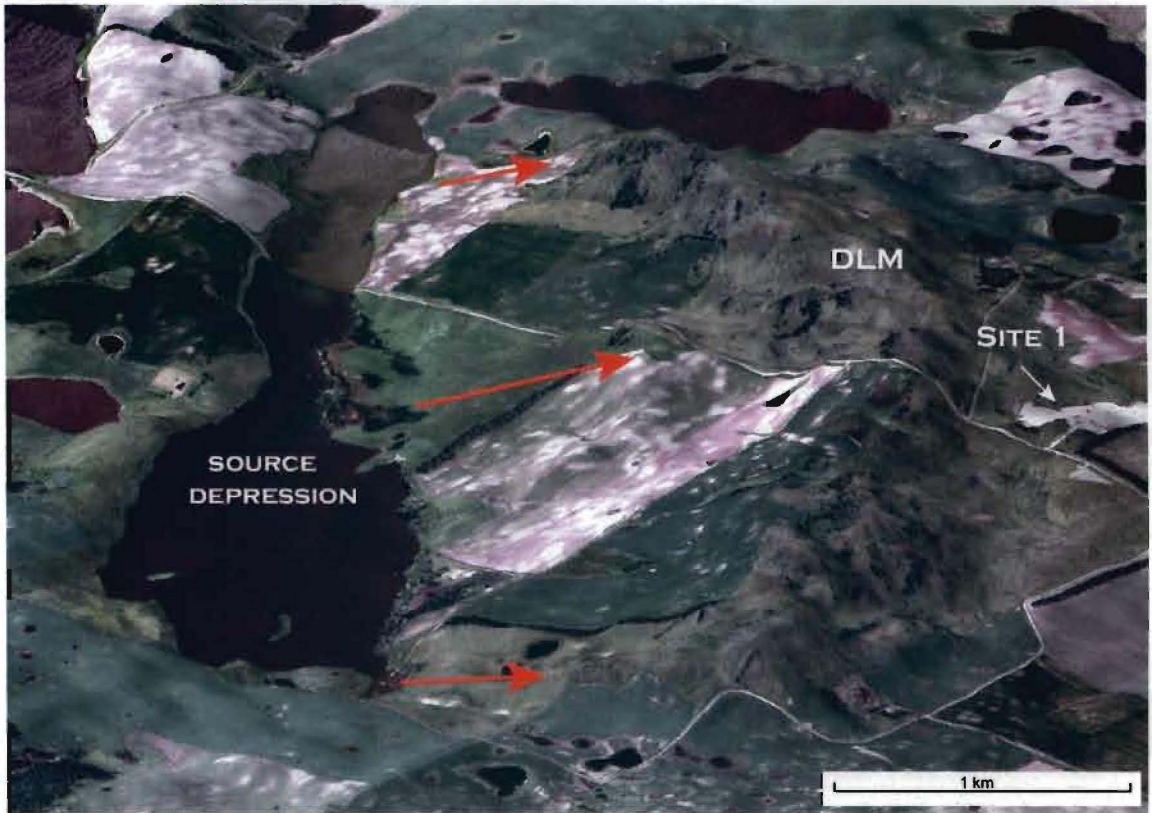


Figure 63. Oblique view of Devils Lake Mountain. Note the similarity in shape and size of the source depression and ice-shoved mass. Arrows indicate a SSE ice-flow movement. View toward the NNE. Vertical exaggeration 7x. DEM acquired from the United States Geological Survey. Color orthophoto provided by the North Dakota State Water Commission.

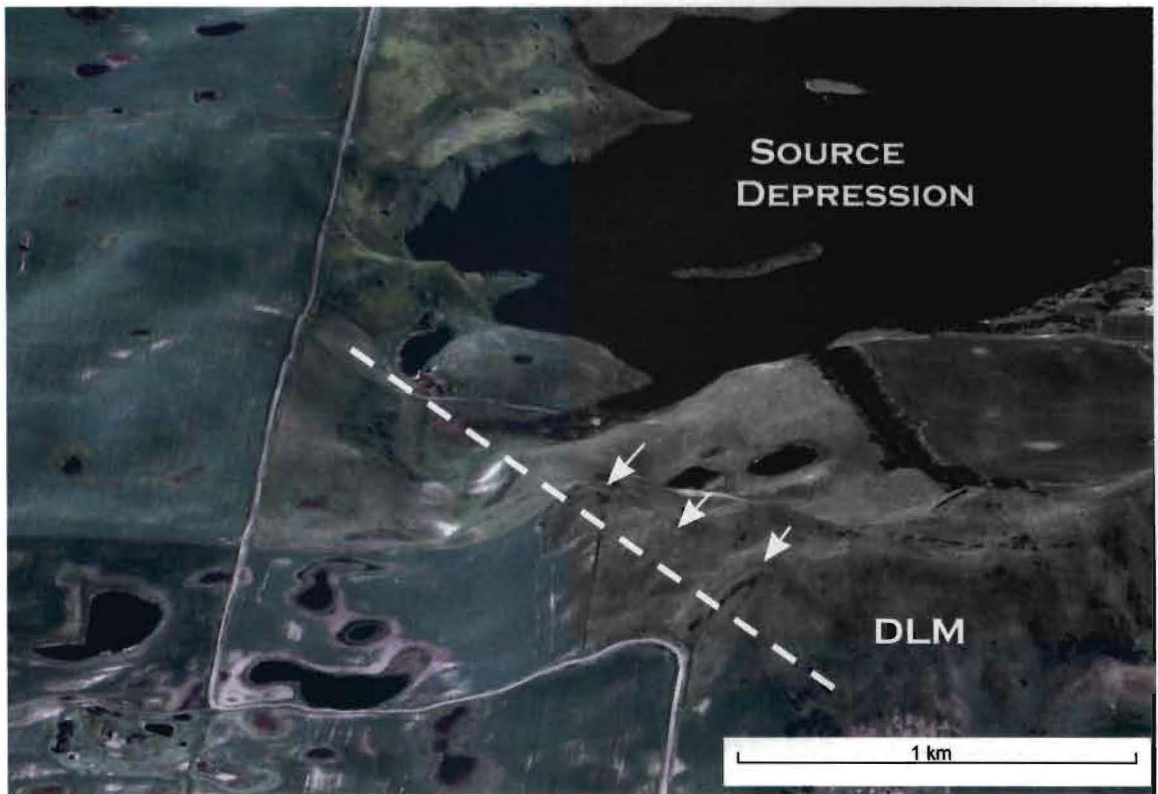


Figure 64. DLM fault lineament looking toward the NNW. Note the parallel alignment of the ice-shoved hill tops (white arrows). Vertical exaggeration 7x; see topographic map (Figure 28) for fault comparison. DEM acquired from the United States Geological Survey. Color orthophoto provided by the North Dakota State Water Commission.

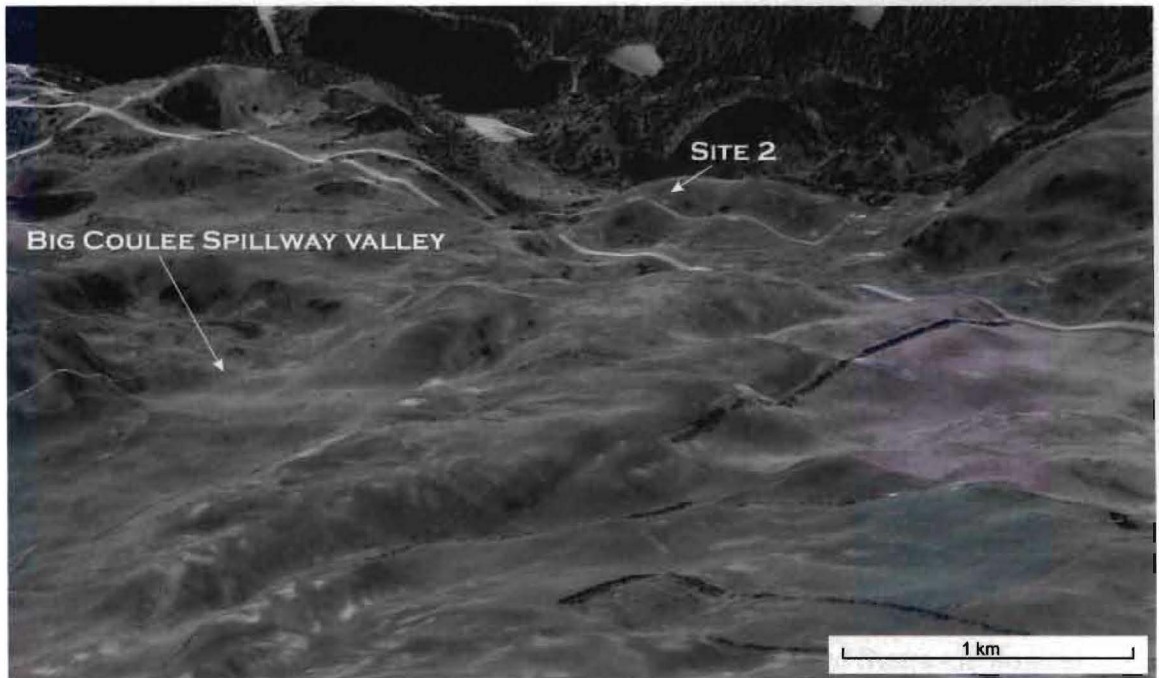


Figure 65. Site 2 denotes a kame deposit. Note the Big Coulee Spillway Valley toward the south. Vertical exaggeration 4x. View toward the NNW. DEM acquired from the United States Geological Survey. Color orthophoto provided by the North Dakota State Water Commission.



Figure 66. North side of the kame deposit. Note the concave spillway valley toward the south. Vertical exaggeration 4x. DEM acquired from the United States Geological Survey. Color orthophoto provided by the North Dakota State Water Commission.

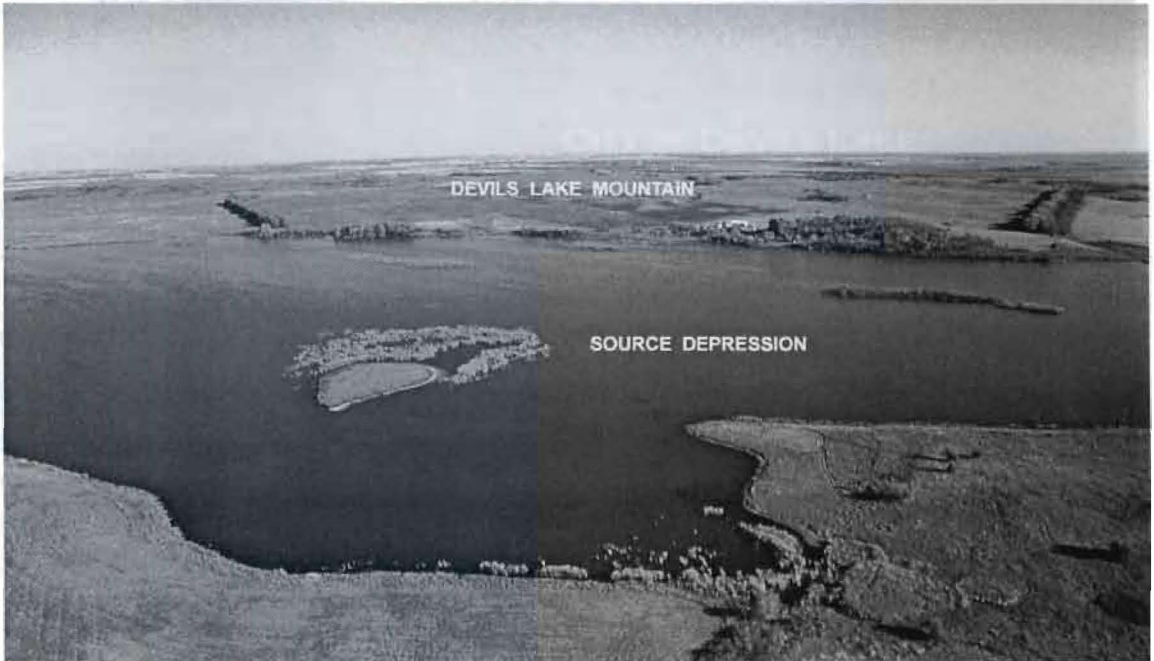


Figure 67. Devils Lake Mountain seen from the northwestern side. Photograph taken with the Canon EOS Rebel X SLR camera. Nearly all of the ice-shoved hill (background) and source depression (lake) are visible.

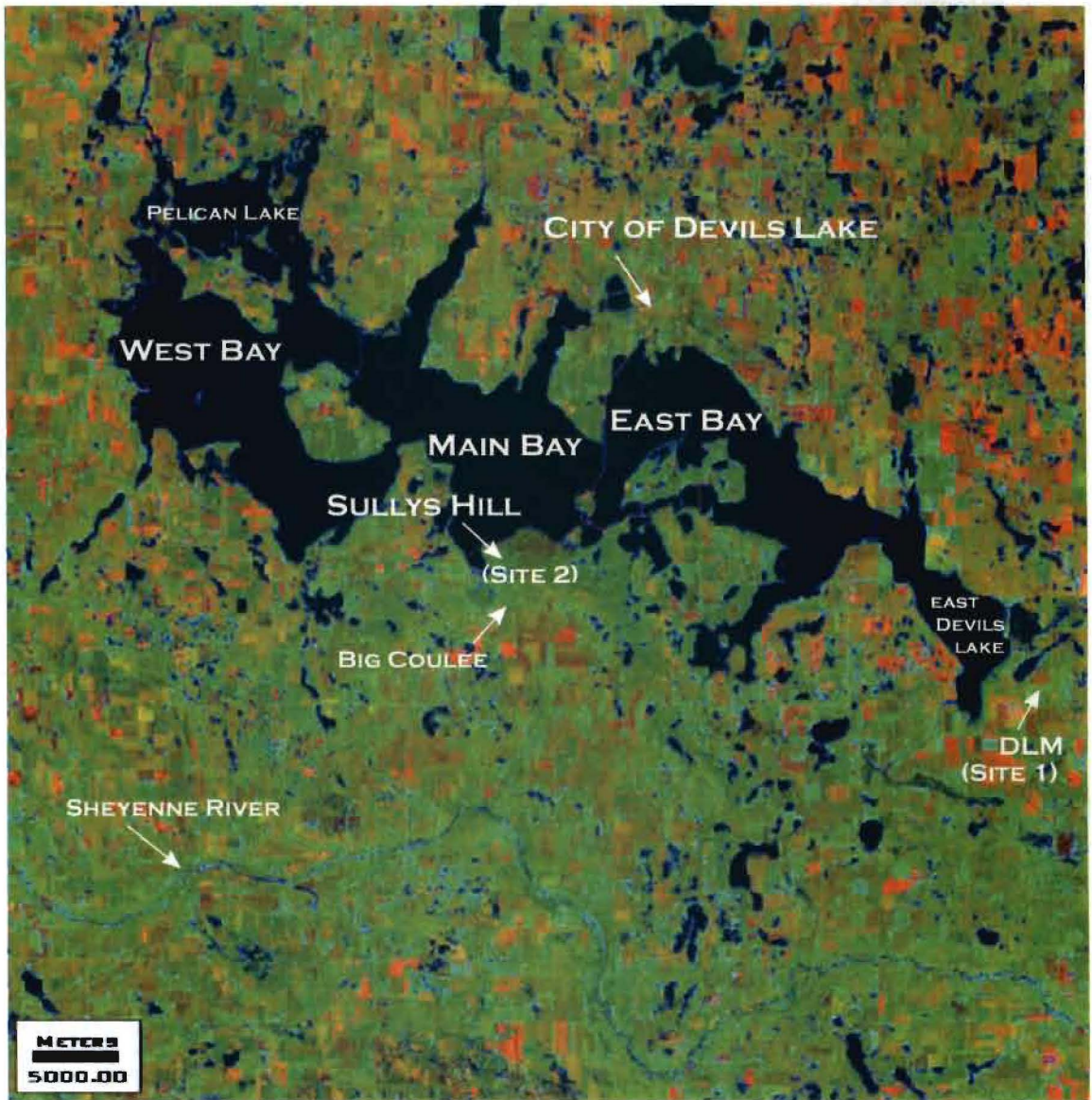


Figure 68. Landsat Thematic Mapper false-color composite of the Devils Lake vicinity, 8 Sept. 2000, Sobel edge detector with bands 247. Bands color coded to blue/green/red. Vegetation is depicted in green, and water in black.

Chapter 4. Interpretations

Microstructure Interpretations

Analysis of the Sullys Hill sediments in thin-section shows that microstructures are less abundant and diverse when compared with the DLM samples. The DLM samples have several microfeatures strongly indicative of either direct subglacial deposition or post-depositional modification during glacial overriding (Hiemstra, 2001). Distinctive sigmoidal geometries, pressure shadows and crushed quartz grains indicate that the sediment was deformed through discrete, parallel shear-displacements under high confining pressures. These features exemplify the diminishing velocity with depth in a deforming bed (van der Meer et al., 1994; Alley, 1991; Boulton and Hindmarsh, 1987). Van der Meer (1997) proposed that the deforming till bed consists of a series of rotating wheels, which spiral around less mobile cores. The contact between the wheels allows the particles to move from one wheel to other promoting a high degree of particle movement, especially in the vertical sense (Fig. 69). Many of these wheels of fine grains may be intercepted and captured by other rotating structures or from discrete shears. This model emphasizes the complex nature of particle movement within a deforming till bed. This process model is also supported by the theoretical work of Blake et al. (1992).

Hiemstra (2001) has observed the occurrence of rotational features (turbate or galaxy structures) within a few millimeters from localized shear planes. Apparently lateral displacements along the shear planes have generated these circular, rotational features. This has been identified in DLM sample 10-02-02 (Fig. 46). Hiemstra has interpreted this phenomenon as evidence of subglacial shearing.

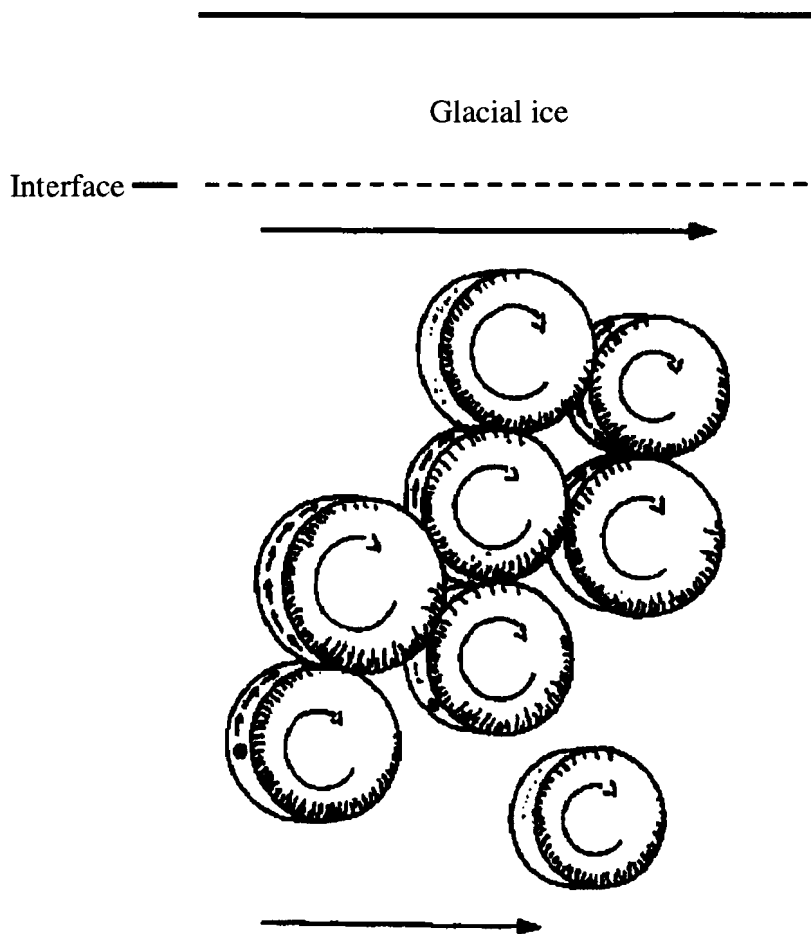


Figure 69. Particle mobility of a deforming till bed model proposed by van der Meer (1997). Arrows at top and bottom indicate the decrease in lateral velocity with depth. Modified after van der Meer (1997, Fig. 2).

It should be noted that even though the high carbonate content may have affected microstructural observations in the DLM samples, the samples still exhibited considerably more microstructures than the Sullys Hill samples. The DLM microstructures showed a SE transport direction.

The observed till fabrics may have been influenced by post-depositional periglacial activities. These processes such as non-incident freeze/thaw or wetting/drying actions may have modified the primary stress field derived from ice overridding. However, the grain geometries and crushed quartz grains suggest a deviatoric stress field of high magnitude. The glacial signature left on these samples points to a subglacial environment.

Microstructural data from the Sullys Hill samples revealed only circular deformation features, which suggests that rotational movements, not planar shear, was the dominant process during flowage and redeposition. The lack of sigmoidal shaped grains and minimal evidence of edge rounding and crushed quartz grains confirm that the sediment was not impeded by high confining pressures. The inhomogeneous texture and the presence of rotational features suggest a gravity flow origin. Specifically, these deposits are interpreted as having formed during the incomplete mixing of the source sediments under rotational movement (Lachniet et al., 2001). In addition, textural and microstructural observations indicate that the DLM samples are generally more continuous and better organized than the Sullys Hill samples.

Water-escape structures and evidence of clay and iron translocations have been observed in both the Sullys Hill and DLM samples. The abundant pore spaces and translocation features are far more prevalent in the Sullys Hill samples. These features

clearly indicate that the deposits were subjected to higher pore-water conditions during till redeposition. The complex network of pore spaces reflects that the water was not confined and able to expand in all directions during the dewatering process. The resultant microstructures are primary features which have formed during flow and redeposition. These features should be considered the result of sedimentary processes and not described in tectonic terms as would subglacial sediments. The Sullys Hill samples did not show any evidence subglacial modification.

Field Interpretations

Subglacial deforming bed processes have been identified within the DLM area. This has been verified by various macro-and microscopic features. Rotational and planar evidence has been clearly recognized in the basal zone of the deforming till bed. It has been suggested by Boulton (1979) and Hindmarsh (1987) and recently by Piotrowski et al. (2001) that rotational movement occurs along the till/bed interface due to the shear forces exerted by the glacier. As a result of this phenomenon, deformation gradients are produced within the till bed. This has been demonstrated to occur underneath Breidamerkurjökull and the Trapridge Glacier and many others (Table 6). Deformation profiles (Fig. 70) from modern systems have shown that strain and velocity distributions are greater immediately beneath the glacier and progressively decrease with depth (Boulton, 1979; Boulton and Hindmarsh, 1987; Hart and Boulton, 1991; Alley, 1991; Murray, 1997; Boulton and Dobbie, 1998, 2001; Truffer et al., 2001). This model of shear-strain distribution implies a more-or-less gradual transition between the deformation till and the underlying substratum. Observations of DLM confirm the

Glacier	Nature of deformation in subglacial sediment	Basal motion due to sediment deformation	Duration of observations (days)	Sediment discharge per 1 m transverse section per year	Ice thickness (m)	Other data and inferences	Source
Black Rapids glacier	Decollement at depth > 2 m	100% of basal motion 50–70% of total glacier motion	410	> 60–80 m ² a ⁻¹		Till 7.5 m thick	Truffer et al., 2000
Trapridge glacier	Strain distributed in topmost 0.3 m	25–45%	23	314 m ² a ⁻¹		Coarse-grained till	Blake, 1992
Columbia glacier	Deformation to depth of 0.65 m. Strain rate increases with depth		5	315 m ² a ⁻¹	950	Till carries 13 kPa of 100 kPa average basal shear stress	Humphrey et al., 1993
Breiðamerkurjökull	Net strain distributed to a depth of 0.38–0.45 m in till Net strain decreases with depth	67–85%	5.5	3.2–6.3 m ² a ⁻¹	8	Coarse-grained till	Boulton and Hindmarsh, 1987
Storglaciären, Sweden	Till deforming to a depth of 0.35 m	Approximately 26%	13	0.64 m ² a ⁻¹	95	Coarse-grained till supports 55 kPa shear stress. Till lies in rock basins. Rock knobs probably support much of the stress.	This paper
Ice Stream B, Antarctica	Till deforms to 5–6 m Till deforms to at least 2 m	17% or 31% Depth of deformation undetermined Probably 0.03 or 0.25 m			About 1000 1058 1027	Inferred from seismic velocities in substratum High porosity till (40%). Shear dilation inferred	Alley et al., 1986 Engelhardt et al., 1990 Engelhardt and Kamb, 1998

^aNote that the discharge measured over the period of the experiments has been calculated to the common base of a discharge per year as m³ a⁻¹ per metre of transverse section, or m² a⁻¹.

Table 6. Evidence of subglacial deformation from modern glacial systems. Acquired from Boulton and Dobbie (2001).

prediction of this model. Field observations also indicate that DLM was modified by overriding ice. This assumption has been verified by the discordant till layer southeast of DLM (site 1). Evidence suggests that DLM formed from proglacial thrusting (ice marginal compression) and was subsequently modified by subglacial processes.

The role of overpressurized aquifers and the presence of permafrost boundaries have been discussed by Bluemle and Clayton 1984. Evidence for permafrost conditions in the Devils Lake area is uncertain. However, many of these subglacial deformation features could have formed in permafrost conditions.

Deformation structures at Sullys Hill indicate a gravity-driven genesis. Sediment deformation was primarily triggered by stagnating glacial ice. Ductile structures in the flow till suggest that the sediment behaved in a fluid-like manner during till redeposition under thawed and saturated conditions.

Chapter 5. Conclusions

The following conclusions may be drawn from this preliminary study:

- A consistent directional trend has been verified in the DLM area based on:
 - (a) Till macrofabrics that consistently trend in a NW-SE direction;
 - (b) Both macro-and microscopic deformation structures within the till that are compatible with this direction;
 - (c) Fault lineament trends in the NW-SE direction;
 - (d) Orientation of source basin which indicates a paleo-ice flow direction from the NW-SE
- The same exposure and microstructural evidence on Sullys Hill confirm the following conjectures:
 - (a) Approximate extent of ice-margin during the Heidmal phase of the Late Wisconsinan Glaciation;
 - (b) Lack of pressure shadows and highly crushed grains verify flow till formation under low confining pressures;
 - (c) High abundance of pore spaces and water escape structures verify saturated water conditions

Observations presented in this study indicate that subglacial till appears as a hard, dense till with few lenses of sorted sediments. On the other hand, flow till has a loose incoherent character typically associated with glaciofluvial materials. Microstructural observations in this study indicate that subglacial till can be discerned by pressure

shadow artifacts and highly crushed grains. The study has also demonstrated that glacial micromorphology can be used to discriminate between subglacial and gravity-driven deformation processes.

Several authors have already shown the immense benefit that can be derived from the use of thin section research upon glacial sediments (Menzies, 2000; and Maltman 1992, van der Meer 1987, 1993). However, glacial micromorphology is most useful when undertaken with other pieces of separate and autonomous evidence, such as macroscopic descriptions of the exposures, clast fabrics and glacial stratigraphy (Lachniet et al., 2001, van der Wateren et al., 2000). In addition, caution must be taken when identifying glacial microstructures, largely because of replication of microstructures through different processes. Glacial micromorphology is an effective tool when adapted to glacial structural analyses. It is anticipated that glacial micromorphology will become more widely used within the fields of glacial geology and glaciology. However, further studies are needed in calibrating microstructural interpretations with deposits of known origin.

References Cited

- Aber, J.S., 1985, The character of glaciotectonism: *Geologie en Mijnbouw*, p. 389-395.
- Aber, J.S., 1988, Spectrum of constructional glaciotectonic landforms: Genetic classification of glacial deposits, Goldthwait and Matsch (eds.), Balkema, Rotterdam, p. 281-292.
- Aber, J. S., Croot, D.G., Fenton, M. M., 1989, *Glaciotectonic landforms and structures*. Kluwer, Dordrecht, 200 p.
- Aber, J.S., and Lundqvist, J., 1988, Glaciotectonic structures in central Sweden and their significance for glacial theory: *Geographie physique et Quaternaire*, v. 42, (n. 3), p. 315-323.
- Aber, J.S., Spellman, E.E., and Webster, M.P., 1997, Applications of Landsat imagery in the Great Plains: *Transactions of the Kansas Academy of Science*, v. 100, (n. 1-2), p. 47-60.
- Alley, R.B., 1991, Deforming-bed origin for southern Laurentide till sheets: *Journal of Glaciology*, v. 37, p. 67-76.
- Alley, R. B., 2000, Continuity comes first: recent progress in understanding subglacial deformation. In: Maltman, A. J., Hubbard, B. & Hambrey, M. J. (eds.), *Deformation of glacial materials*, Geological Society, Special Publications, London, v. 176, p. 171-179.
- Alley, R.B., D.D. Blankenship, C.R. Bentley, and S.T. Rooney, 1986, Deformation of till beneath Ice Stream B, West Antarctica: *Nature*, 322, p. 57-59.

- Banham, P.H., 1977, Glaciotectonics in till stratigraphy: *Boreas*, v. 6, p. 101-105.
- Benn, D.I., and Evans, D.J.A., 1996, The interpretation and classification of subglacially-deformed materials: *Quaternary Science Reviews*, v. 15, p. 23-52.
- Benn, I.D., and Evans D.J.A., 1998, *Glaciers and Glaciation*. John Wiley and Sons, Inc., New York, 760 p.
- Blake E., Clarke G.K.C., and Gérin C.M., 1992, Tools for examining subglacial bed deformation: *Journal of Glaciology*, v. 38, p. 388-396.
- Bluemle, J.P., 1966, Ice-thrust Bedrock in Northwest Cavalier County, North Dakota: *Proceedings of the North Dakota Academy of Science*, v. XX, p. 112-118.
- Bluemle, J.P., 1970, Anomalous hills and associated depressions in central North Dakota: *Geological Society America, Abstracts with Programs*, v. 2, p. 325-326.
- Bluemle, J.P., 1974, *Guide to the geology of North-Central North Dakota*: Prepared by the North Dakota Geological Survey in Cooperation with the Department of Public Instruction, Educational Series 7, 41 p.
- Bluemle, J.P., 1979, Glacial thrusting as a landform mechanism in North Dakota: *North Dakota Geological Survey Newsletter*. v. 6, (no. 2), p. 18.
- Bluemle, J.P., Clayton, L., 1984, Large-scale glacial thrusting and related processes in North Dakota: *Boreas*, v. 13, p. 279-299.
- Bluemle, J.P., 2000, *The Face of North Dakota, Third Edition*: North Dakota Geological Survey, Educational Series 26, 205 p.

- Boulton, G.S., 1971, Till genesis and fabric in Svalbard, Spitsbergen: Till/a Symposium, Ohio State University Press, Columbus, p. 41-72.
- Boulton, G.S., 1979, Stability of temperate ice caps and ice sheets resting on beds of deformable sediment: *Journal of Glaciology*, v. 24, p. 29-43.
- Boulton, G.S., 1996, The origin of till sequences by subglacial sediment deformation beneath mid-latitude ice sheets: *Annals of Glaciology*, v. 22, p. 75-84.
- Boulton, G.S., Dent D.L., and Morris E.M., 1974, Subglacial shearing and crushing, and the role of water pressure in tills from south-east Iceland: *Geografiska annaler. Series A, Physical Geography*, v. 56a, p. 135-145.
- Boulton, G.S., and Dobbie K.E., 1998, Slow flow of granular aggregates: the deformation of sediments beneath glaciers: *Philosophical Transactions of Royal Society of London*, v. 356, p. 2713-2745.
- Boulton, G.S., and Dobbie K.E., 2001, Sediment deformation beneath glaciers and its coupling to the subglacial hydraulic system: *Quaternary International*, v. 86, p. 3-28.
- Boulton, G.S., and Hindmarsh R.C.A., 1987, Sediment deformation beneath glaciers: rheology and geological consequences: *Journal of Geophysical Research*, v. 92, (no. B9), p. 9059-9082.
- Brewer, R., and Sleeman, J.R., 1960, Soil structure and fabric. Their definition and description: *Journal of Soil Science*, v. 11, p. 172-185.

- Brodzikowski, K., and Loon, A.J. van, 1985, Inventory of deformational structures as a tool for unraveling the Quaternary geology of glaciated areas, *Boreas*, v. 14, p. 175-188.
- Carr S.J., 2001, Micromorphological criteria for subglacial and glacial marine sediments: evidence from a contemporary tidewater glacier, Spitsbergen: *Quaternary International* v. 86, p. 71-79.
- Carr S.J., Hafliðason H., and Sejrup, H.P., 2000, Micromorphological evidence supporting Late Weichselian glaciation of Northern North Sea: *Boreas*, v. 29, p. 315-328.
- Clarke, G.K.C., 1987, Subglacial till: a physical framework for its properties and processes: *Journal of Geophysical Research*, v. 92, (no. B9), p. 9023-9036.
- Clarke, P.U., 1994, Unstable behavior of the Laurentide ice sheet over deforming sediment and its implication for climate change: *Quaternary Research*, v. 41, p. 19-25.
- Clayton, L., and Moran, S.R., 1974, A glacial-process-form model. In Coates, D.R. (ed.), *Glacial geomorphology*, p. 203-243. SUNY-Binghamton Publications in Geomorphology, Binghamton, New York.
- Clayton, L., Moran, S.R., and Bluemle, J.P., 1980, Explanatory text to accompany the Geologic Map of North Dakota. North Dakota Geological Survey, Report of Investigation No. 69.
- Colgan, P.M., Mickelson, D.M., and Culter, P.M., 2003, Ice-marginal terrestrial landsystems: Southern Laurentide ice sheet margin: In Evans, D.J.A., Editor, *Glacial Landsystems*, Arnold London, p. 111-142.

- Davis, G.H., and Reynold, S.J., 1996, Structural geology of rocks and regions, Second Edition, John Wiley and Sons, Inc., New York, 776 p.
- Dreimanis, A., 1983, Penecontemporaneous partial disaggregation and/or resedimentation during the formation and deposition of subglacial till: *Acta Geològica Hispànica*, v. 18, p. 153-160.
- Dreimanis, A., 1989, Tills: Their genetic terminology and classification: In R.P. Goldthwait and C.L. Matsch (eds.), Genetic classification of glacial deposits, Rotterdam. Balkema, p. 17-83.
- Dreimanis, A., 1990, Formation, deposition, and identification of subglacial and supraglacial tills: In R. Kujansuu and M. Saaranisto (eds.): *Glacial Indicator Tracing*. Rotterdam: A.A. Balkema, p. 35-60.
- Dreimanis, A., and Lundqvist J., 1984, What should be called Till?, *Striae*, v. 20, p. 5-10.
- Dreimanis, A. and Schüchter C., 1985, Field criteria for the recognition of till or tillite, *Palaeogeography, Palaeoclimatology, Palaeoecology*, v. 51, p. 7-14.
- Elson, J.A., 1961, The geology of tills: In. E. Penner and J. Butler (eds.), *Proceed. 14th Canada Soil Mechanics Conference*, National Research Council of Canada, Associate Committee on Soil and Snow Mechanics. Technical Memorandum, v. 69, p. 5-36.
- Elson, J.A., 1989, Comment on glacitectonite, deformation till, and comminution till: In R.P. Goldthwait and C.L. Matsch (eds.), Genetic classification of glacial deposits, Rotterdam. Balkema, p. 85-88.
- Evan, D.J.A., 2003, *Glaciers*, *Progress in Physical Geography*, v. 27, p. 261-274.

Flint, R.F., 1971, *Glacial and Quaternary geology*, John Wiley and Sons, Inc.
New York, 906 p.

FitzPatrick, E.A., 1984, *Micromorphology of soils*, Chapman and Hall, London,
433 p.

Gale, S.J., and Hoare, P.G., 1991, *Quaternary Sediments*, John Wiley and Sons,
Inc., New York, 323 p.

Glen, J.W., Donner, J.J. and West, R.G., 1957, On the mechanism by which
stones in till become orientated: *American Journal of Science*, v. 255, p.
194-205.

Goldthwait, R.P., and Matsch, C.L., 1989, *Genetic Classification of Glacigenic
Deposits*: Rotterdam, A.A. Balkema, 304 p.

Hambrey, M.J., 1994, *Glacial environments*, Vancouver UBS Press, 296 p.

Hart, J.K., and Boulton G.S., 1991, The interrelation of glaciotectonic and
glaciodepositional processes within the glacial environment: *Quaternary
Science Reviews*, v. 10, p. 335-350.

Hicock, S.R., 1992, Lobal interactions and rheologic superposition in subglacial
till near Bradtville, Ontario, Canada, *Boreas*, v. 21, p. 73-88.

Hicock, S.R., Goff, J.R., Lian, O.B., and Little, E.C., 1996, On the interpretation
of subglacial till fabric: *Journal of Sedimentary Research*, v. 66, (no. 5), p.
928-934.

Hiemstra, J.F., 2001, Microscopic analyses of Quaternary glacigenic sediments of
Marguerite Bay, Antarctic Peninsula: *Arctic, Antarctic, and Alpine
Research*, v. 33, (no. 3), p. 258-265.

- Hiemstra, J.F., and Meer, J.J.M. van der, 1997, Pore-water controlled grain fracturing as an indicator for subglacial shearing in tills: *Journal of Glaciology*, v. 43, p. 446-454.
- Hindmarsh, R., 1997, Deforming beds: Viscous and plastic scales of deformation: *Quaternary Science Reviews*, v. 16, p. 1039-1056.
- Hobbs, H.S., and Bluemle, J.P., 1987, Geology of Ramsey County, North Dakota: North Dakota Geological Survey, Bulletin 71, Pt.1, North Dakota State Water Commission, 69 p.
- Khatwa, A., and Tulaczyk, S., 2001, Microstructural interpretations of modern and Pleistocene subglacially deformed sediments: the relative role of parent material and subglacial processes: *Journal of Quaternary Science*, v. 16 (no. 6), p. 507-517.
- Lachniet, M.S., Larson, G.J., Lawson, D.E., Evenson, D.E., and Alley, R.B., 2001, Microstructures of sediment flow deposits and subglacial sediments: a comparison: *Boreas*, v. 30, p. 254-262.
- Lawson, D.E., 1979, Sedimentological analysis of the western terminus region of Matanuska Glacier, Alaska, United States Cold Regions Research and Engineering Lab (CRREL) Report, p. 9-79.
- Lawson, D.E., 1981, Sedimentological characteristics and classification of depositional processes and deposits in the glacial environment, US CRREL Report, p. 27-81.

- Maltman, A.J., Hubbard, B., and Hambrey, M.J., 2000, Deformation of Glacial Materials, Geological Society Special Publication No. 176, Geological Society of London, 352 p.
- Manz, L., 2002, Glaciotectonics at Falkirk, North Dakota Geologic Survey Newsletter, v. 29, (no.2), p. 3.
- McCarroll, D. and Rijdsdijk, K.F., 2003, Deformation styles as key for interpreting glacial depositional environments: *Journal of Quaternary Science*, v. 18, (no. 6), p. 473-489.
- Meer, J.J.M. van der, 1985, Micromorphology of glacial sediments as a tool in distinguishing genetic varieties of till: INQUA Till Symposium, Geological Survey of Finland, Special Paper 3, p. 77-89.
- Meer, J.J.M. van der, 1990, Micromorphology of some North Sea till samples, a pilot study: *Journal of Quaternary Science*, v. 5, (no. 2), p. 95-101.
- Meer, J.J.M. van der, 1993, Microscopic evidence of subglacial deformation: *Quaternary Science Reviews*, v. 12, p. 553-587.
- Meer, J.J.M. van der, 1996, Micromorphology, In Menzies, J., (eds.), 1996, *Past Glacial Environments-Sediments, Forms and Techniques*. Oxford: Butterworth-Heineman, 598 p.
- Meer, J.J.M. van der, 1997, Particle and aggregate mobility in till: Microscopic evidence of subglacial processes, *Quaternary Science Reviews*, v. 16, p. 827-831.
- Meer, J.J.M. van der, Mücher, J.H., and Höfle, H. Ch., 1992, Micromorphological observations on till samples from the Shackleton

- Range and North Victoria Land, Antarctica: *Polarforschung*, v. 62, (no. 1), p. 57-65.
- Meer, J.J.M. van der, Muecher, H.J. and Höfle, H. Ch., 1994, Observations in some thin-sections of Antarctica glacial deposits: *Polarforschung*, v. 62, p. 57-65.
- Meer, J.J.M. van der, Rappol, M., Semeijn, J.N., 1983, Micromorphological and preliminary X-ray observations on a basal till from Lunteren, The Netherlands: *Acta Geologica Hispanica*, v. 18, p. 199-205.
- Menzies, J., 1981, Freezing fronts and their possible influence upon processes of subglacial erosion and deposition: *Annals of Glaciology*, v. 2, p. 52-56.
- Menzies, J., 2000, Micromorphological analyses of microfabrics and microstructures indicative of deformation processes in glacial sediments. In: Maltman, A. J., Hubbard, B. & Hambrey, M. J. (eds.), *Deformation of glacial materials*, Geological Society, Special Publications, London, v. 176, p. 245-257.
- Menzies, J., and Maltman, A.J., 1992, Microstructures in diamictons-evidence of subglacial bed conditions: *Geomorphology*, v. 6, p. 27-40.
- Menzies, J., Zaniewski, K., and Dreger, D., 1997, Evidence, from microstructures, of deformable bed conditions within drumlins, Chimney Bluffs, New York State: *Sedimentary Geology*, v. 111, p. 161-175.
- Mickelson, D.M., and Colgan, P.M., 2003, The southern Laurentide Ice Sheet. In: A.R., Gillespie, Porter, S.C., and Atwater, B.F., *The Quaternary Period in*

- the United States, *Developments in Quaternary Science*, 1 (ed.) Rose, J., p. 1-16.
- Moran, S.R., Clayton, L. and Hooke, R.L., 1980, Glacier-bed landforms of the prairie region of North America: *Journal of Glaciology*, v. 25, (no. 93), p. 457- 476.
- Murray, T., 1997, Assessing the paradigm shift: Deformable glacier beds: *Quaternary Science Reviews*, v. 16, p. 995-1016.
- Passchier, C.W., Trouw, R.A.J., *Microtectonics*, Springer-Verlag Telos, 298 p.
- Piotrowski, J.A., Mickelson, D.M., Tulaczyk, S., Krzyszkowski, D., and Junge, F.W., 2001, Were deforming subglacial beds beneath past ice sheets really widespread?: *Quaternary International* v. 86, p. 139-150.
- Rijsdijk, K.F., 2001, Density-driven deformation structures in glacially consolidated diamicts: Examples from Traeth Y MWNT, Cardiganshire, Wales, U.K., *Journal of Sedimentary Research*, v. 71, (no. 1), p. 122-135.
- Slater, G., 1926, Glacial tectonics as reflected in disturbed drift deposits: *Geologists' Association Proceedings*, v. 37, p. 392-400.
- Sugden, D.E., and John, B.S., 1976, *Glaciers and landscape, a geomorphologic approach*. London: Edward Arnold, 376 p.
- Truffer, M., Echelmeyer, K.A., and Harrison, W.D., 2001, Implications of till deformation on glacier dynamics: *The Journal of Glaciology*, v. 47, p. 123-134.

Wateren, F.M., van der, 1995, Processes of Glaciotectonism: In Menzies, J., (ed.), 1995, Past Glacial Environments- Processes, Dynamics and Sediments. Oxford: Butterworth-Heinemann, p. 309-335.

Wateren, F.M., van der, Kluiving, S.J., and Bartek, L.R., 2000, Kinematic indicators of subglacial shearing. In: Maltman, A. J., Hubbard, B. & Hambrey, M. J. (eds.), Deformation of glacial materials, Geological Society, Special Publications, London, v. 176, p. 260-278.

I, William Russell Jacobson Jr., hereby submit this thesis/report to Emporia State University as partial fulfillment of the requirements for an advanced degree. I agree that the Library of the University may make it available to use in accordance with its regulations governing materials of this type. I further agree that quoting, photocopying, or other reproduction of this document is allowed for private study, scholarship (including teaching) and research purposes of a nonprofit nature. No copying which involves potential financial gain will be allowed without written permission of the author.

WILLIAM RUSSELL Jacobson Jr.
Signature of Author

12/16/04
Date

Glaciotectonic Analysis of Devils Lake, North Dakota
Title of Thesis

Ray Cooper
Signature of Graduate Office Staff

12 - 22 - 04
Date Received

2
2

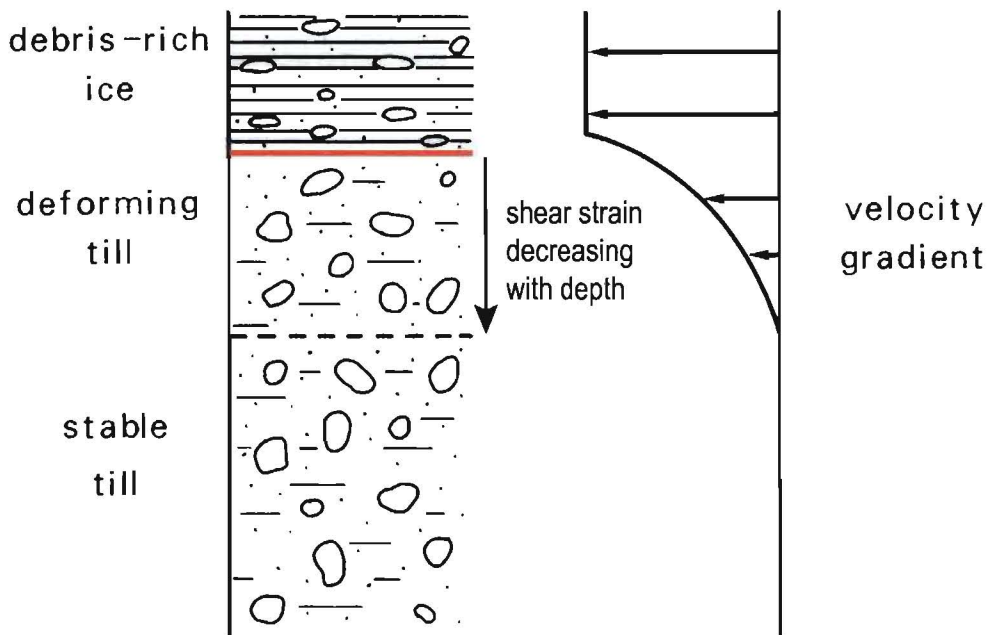


Figure 70. Generalized deformation profile from Breidamerkerjökull, Iceland. Velocity vectors parallel to ice flow. Greatest amount of deformation and displacement took place in the upper part of the deforming till. Approximately 0.5 m of displacement after 10 days. Modified from Boulton (1979).